

# Nonparametric Density Estimation via Variance-Reduced Sketching

Yifan Peng<sup>1</sup>, Yuehaw Khoo<sup>\*2</sup>, and Daren Wang<sup>3</sup>

<sup>1</sup>Committee on Computational and Applied Mathematics, University of Chicago

<sup>2</sup>Department of Statistics, University of Chicago

<sup>3</sup>Department of Statistics, University of Notre Dame

## Abstract

Nonparametric density models are of great interest in various scientific and engineering disciplines. Classical density kernel methods, while numerically robust and statistically sound in low-dimensional settings, become inadequate even in moderate higher-dimensional settings due to the curse of dimensionality. In this paper, we introduce a new framework called Variance-Reduced Sketching (VRS), specifically designed to estimate multivariable density functions with a reduced curse of dimensionality. Our framework conceptualizes multivariable functions as infinite-size matrices, and facilitates a new sketching technique motivated by numerical linear algebra literature to reduce the variance in density estimation problems. We demonstrate the robust numerical performance of VRS through a series of simulated experiments and real-world data applications. Notably, VRS shows remarkable improvement over existing neural network estimators and classical kernel methods in numerous density models. Additionally, we offer theoretical justifications for VRS to support its ability to deliver nonparametric density estimation with a reduced curse of dimensionality.

**Keywords**— Density estimation, Matrix sketching, Tensor sketching, Range estimation, High-dimensional function approximation

## 1 Introduction

Nonparametric density estimation has extensive applications across diverse fields, including biostatistics (Chen (2017)), machine learning (Sriperumbudur and Steinwart (2012) and Liu et al. (2023)), engineering (Chaudhuri et al. (2014)), and economics (Zambom and Dias (2013)). In this context, the goal is to estimate the underlying density function based on a collection of independently and identically distributed data. Classical density estimation methods such as histograms (Scott (1979) and Scott (1985)) and kernel density estimators (Parzen (1962) and Davis et al. (2011)), known for their numerical robustness and statistical stability in lower-dimensional settings, often suffer from the curse of dimensionality even in moderate higher-dimensional spaces. Mixture models (Dempster

---

\*Corresponding author

(1977) and Escobar and West (1995)) offer a potential solution for higher-dimensional problems, but these methods are lacking the flexibility to extend in the nonparametric settings. Additionally, adaptive methods (Liu et al. (2007) and Liu et al. (2023)) have been developed to address higher-dimensional challenges. Recently, deep generative modeling has emerged as a popular technique to approximate high-dimensional densities from given samples, especially in the context of images. This category includes generative adversarial networks (GAN) (Goodfellow et al. (2020); Liu et al. (2021)), normalizing flows (Dinh et al. (2014); Rezende and Mohamed (2015); Dinh et al. (2016)), and autoregressive models (Germain et al. (2015); Uria et al. (2016); Papamakarios et al. (2017); Huang et al. (2018)). Despite their remarkable performance, particularly with high-resolution images, statistical guarantees for these neural network methods continue to be a challenge. In this paper, we aim to develop a new framework specifically designed to estimate multivariate nonparametric density functions. Within this framework, we conceptualize multivariate density functions as matrices or tensors and extend matrix/tensor approximation algorithm to this nonparametric setting, in order to reduce the curse of dimensionality in higher dimensions.

## 1.1 Contributions

Motivated by Hur et al. (2023), we propose a new matrix/tensor-based sketching framework for estimating multivariate density functions in nonparametric models, referred to as *Variance-Reduced Sketching* (VRS). To illustrate the advantages of VRS, consider the setting of estimating an  $\alpha$ -times differentiable density function in  $d$  dimensions. In terms of squared  $\mathbf{L}_2$  norm, the error rate of the classical kernel density estimator (KDE) with sample size  $N$  is of order

$$\mathcal{O}\left(\frac{1}{N^{2\alpha/(2\alpha+d)}}\right), \quad (1)$$

while the VRS estimator can achieve error rates of order<sup>1</sup>

$$\mathcal{O}\left(\frac{1}{N^{2\alpha/(2\alpha+1)}} + \frac{\prod_{j=1}^d r_j}{N}\right). \quad (2)$$

Here,  $\{r_j\}_{j=1}^d$  are the ranks of the true density function, and the precise definition can be found in Assumption 3. Note that when  $\{r_j\}_{j=1}^d$  are bounded constants, the error rate in (2) reduces to  $\mathcal{O}\left(\frac{1}{N^{2\alpha/(2\alpha+1)}}\right)$ , which is a nonparametric error rate in one dimension, significantly better than (1), especially when  $d$  is large. In Figure 1, we conduct a simulation study to numerically compare deep neural network estimators, classical kernel density estimators, and VRS. Additional empirical studies are provided in Section 5. Extensive numerical evidence suggests that VRS significantly outperforms various deep neural network estimators and KDE by a considerable margin.

The promising performance of VRS comes from its ability to reduce the problem of multivariate density estimation to the problem of estimating low-rank matrices/tensors in space of functions. For example, we can think of a two-variable density function as an infinite-size matrix. When estimating this two-variable density using classical kernel methods, it typically exhibits a two-dimensional error rate. In contrast, VRS reduces the matrix estimation problem to an estimation problem of its range. Since the range

---

<sup>1</sup>Assuming the minimal singular values are all constants, the error bound in (2) matches Theorem 2.

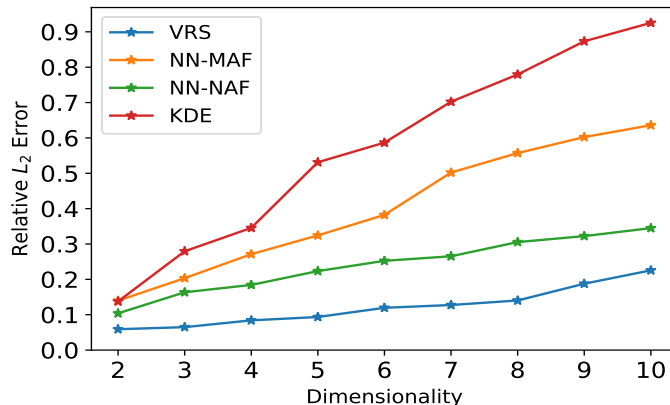


Figure 1: Density estimation with data sampled from the Ginzburg-Landau density in (37). The  $x$ -axis represents dimensionality, varying from 2 to 10. The performance of different estimators is evaluated using  $L_2$ -errors. Additional details are provided in **Simulation III** of Section 5.

of the density function is a single-variable function when the rank is low, we achieve a single-variable estimation error rate. Such philosophy can be generalized to density estimation in arbitrary dimensions. To estimate the range, VRS employs a new sketching strategy, wherein the empirical density function is sketched with a set of carefully chosen sketch functions, as illustrated in Figure 2. These sketch functions are selected to retain the range of the density while reducing the variance of the range estimation from any multidimensional scaling to 1-dimensional scaling, hence the name Variance-Reduced Sketching.

Our VRS sketching approach allows us to achieve the error bound demonstrated in (2), contrasting with the error bound of KDE in (1), which suffers from the curse of dimensionality. Our VRS framework is fundamentally different from the randomized sketching algorithm for finite-dimensional matrices previously studied in Halko et al. (2011), as randomly chosen sketching does not address the curse of dimensionality in multivariable density estimation models. Additionally, the statistical guarantees for VRS are derived from a computationally tractable algorithm. This contrasts with deep learning methods, where generalization errors highly depend on the architecture of the neural network estimators, and the statistical analysis of generalization errors of neural network estimators is not necessarily related to optimization errors achieved by computationally tractable optimizers.

## 1.2 Related literature

Matrix approximation algorithms, such as singular value decomposition and QR decomposition, play a crucial role in computational mathematics and statistics. A notable advancement in this area is the emergence of randomized low-rank approximation algorithms. These algorithms excel in reducing time and space complexity substantially without sacrificing too much numerical accuracy. Seminal contributions to this area are outlined in works such as Liberty et al. (2007) and Halko et al. (2011). Additionally, review papers like Woodruff et al. (2014), Drineas and Mahoney (2016), Martinsson (2019), and Martinsson and Tropp (2020) have provided comprehensive summaries of

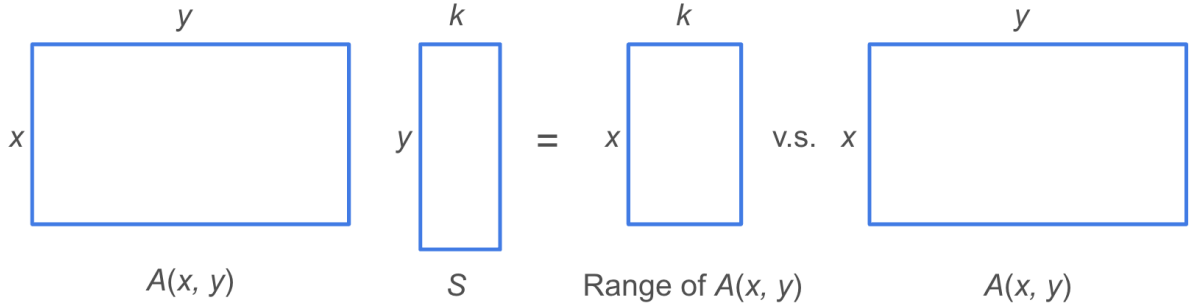


Figure 2: The sketched function  $AS$  by VRS retains the range in the variable  $x$  of  $A(x, y)$ . The complexity of estimating the range of  $A$  using  $AS$  is much lower than the complexity of directly estimating  $A$ .

these randomized approaches, along with their theoretical stability guarantees. Randomized low-rank approximation algorithms typically start by estimating the range of a large low-rank matrix  $A \in \mathbb{R}^{n \times n}$  by forming a reduced-size sketch. This is achieved by right multiplying  $A$  with a random matrix  $S \in \mathbb{R}^{n \times k}$ , where  $k \ll n$ . The random matrix  $S$  is selected to ensure that the range of  $AS$  remains a close approximation of the range of  $A$ , even when the column size of  $AS$  is significantly reduced from  $A$ . As such, the random matrix  $S$  is referred to as randomized linear embedding or sketching matrix by [Tropp et al. \(2017b\)](#) and [Nakatsukasa and Tropp \(2021\)](#). The sketching approach reduces the cost in singular value decomposition from  $O(n^3)$  to  $O(n^2)$ , where  $O(n^2)$  represents the complexity of matrix multiplication.

Recently, a series of studies have extended the matrix sketching technique to range estimation for high-order tensor structures, such as the Tucker structure ([Che and Wei \(2019\)](#); [Sun et al. \(2020\)](#); [Minster et al. \(2020\)](#)) and the tensor train structure ([Al Daas et al. \(2023\)](#); [Kressner et al. \(2023\)](#); [Shi et al. \(2023\)](#)). These studies developed specialized structures for sketching to reduce computational complexity while maintaining high levels of numerical accuracy in handling high-order tensors.

Previous work has also explored randomized sketching techniques in specific estimation problems. For instance, [Mahoney et al. \(2011\)](#) and [Raskutti and Mahoney \(2016\)](#) utilized randomized sketching to solve unconstrained least squares problems. [Williams and Seeger \(2000\)](#), [Rahimi and Recht \(2007\)](#), [Kumar et al. \(2012\)](#) and [Tropp et al. \(2017a\)](#) improved Nyström method with randomized sketching techniques. Similarly, [Alaoui and Mahoney \(2015\)](#), [Wang et al. \(2017\)](#), and [Yang et al. \(2017\)](#) applied randomized sketching to kernel matrices in kernel ridge regression to reduce computational complexity. While these studies mark significant progress in the literature, they usually require extensive observation of the estimated function prior to employing the randomized sketching technique, in order to maintain acceptable accuracy. This step would be significantly expensive for the higher-dimensional setting. Notably, [Hur et al. \(2023\)](#) and subsequent studies [Tang et al. \(2022\)](#); [Ren et al. \(2023\)](#); [Peng et al. \(2023\)](#); [Chen and Khoo \(2023\)](#); [Tang and Ying \(2023\)](#) addressed the issues by taking the variance of data generation process into the creation of sketching for high-dimensional tensor estimation. This sketching technique allows for the direct estimation of the range of a tensor with reduced sample complexity, rather than directly estimating the full tensor.

### 1.3 Organization

Our manuscript is organized as follows. In Section 2, we detail the procedure for implementing the range estimation through sketching and study the corresponding error analysis. In Section 3, we extend our study to density function estimation based the range estimators developed in Section 2, and provide the corresponding statistical error analysis with a reduced curse of dimensionality. Additionally, we extend our method to image PCA denoising in Section 4. In Section 5, we present comprehensive numerical results to demonstrate the superior numerical performance of our method. Finally, Section 6 summarizes our conclusions.

### 1.4 Notations

We use  $\mathbb{N}$  to denote the natural numbers  $\{1, 2, 3, \dots\}$  and  $\mathbb{R}$  to denote all the real numbers. We say that  $X_n = O_{\mathbb{P}}(a_n)$  if for any given  $\epsilon > 0$ , there exists a  $K_\epsilon > 0$  such that  $\limsup_{n \rightarrow \infty} \mathbb{P}(|X_n/a_n| \geq K_\epsilon) < \epsilon$ . For real numbers  $\{a_n\}_{n=1}$ ,  $\{b_n\}_{n=1}$  and  $\{c_n\}_{n=1}$ , we denote  $a_n = O(b_n)$  if  $\lim_{n \rightarrow \infty} a_n/b_n < \infty$  and  $a_n = o(c_n)$  if  $\lim_{n \rightarrow \infty} a_n/c_n = 0$ . Let  $[0, 1]$  denote the unit interval in  $\mathbb{R}$ . For positive integer  $d$ , denote the  $d$ -dimensional unit cube as  $[0, 1]^d$ .

Let  $\{f_i\}_{i=1}^n$  be a collection of elements in the Hilbert space  $\mathcal{H}$ . Then

$$\text{Span}\{f_i\}_{i=1}^n = \{b_1 f_1 + \dots + b_n f_n : \{b_i\}_{i=1}^n \subset \mathbb{R}\}. \quad (3)$$

Note that  $\text{Span}\{f_i\}_{i=1}^n$  is a linear subspace of  $\mathcal{H}$ . For a generic measurable set  $\Omega \subset \mathbb{R}^d$ , denote  $\mathbf{L}_2(\Omega) = \{f : \Omega \rightarrow \mathbb{R} : \|f\|_{\mathbf{L}_2(\Omega)}^2 = \int_{\Omega} f^2(z) dz < \infty\}$ . For any  $f, g \in \mathbf{L}_2(\Omega)$ , let the inner product between  $f$  and  $g$  be

$$\langle f, g \rangle = \int_{\Omega} f(z)g(z)dz.$$

We say that  $\{\phi_k\}_{k=1}^{\infty}$  is a collection of orthonormal functions in  $\mathbf{L}_2(\Omega)$  if  $\langle \phi_k, \phi_l \rangle = 1$  if  $k = l$ , and 0 if  $k \neq l$ . Let  $Z \in \Omega$  and  $\mathbb{I}_Z$  be the indicator function at the point  $Z$ . We define

$$\langle \mathbb{I}_{\{Z\}}, f \rangle = f(Z).$$

If  $\{\phi_k\}_{k=1}^{\infty}$  spans  $\mathbf{L}_2(\Omega)$ , then  $\{\phi_k\}_{k=1}^{\infty}$  is a collection of orthonormal basis functions in  $\mathbf{L}_2(\Omega)$ . In what follows, we briefly introduce the notations for Sobolev spaces. Let  $\Omega \subset \mathbb{R}^d$  be any measurable set. For multi-index  $\beta = (\beta_1, \dots, \beta_d) \in \mathbb{N}^d$ , and  $f(z_1, \dots, z_d) : \Omega \rightarrow \mathbb{R}$ , define the  $\beta$ -derivative of  $f$  as  $D^\beta f = \partial_1^{\beta_1} \dots \partial_d^{\beta_d} f$ . Then

$$W_2^\alpha(\Omega) := \{f \in \mathbf{L}_2(\Omega) : D^\beta f \in \mathbf{L}_2(\Omega) \text{ for all } |\beta| \leq \alpha\},$$

where  $|\beta| = \beta_1 + \dots + \beta_d$  and  $\alpha$  represents the total order of derivatives. The Sobolev norm of  $f \in W_2^\alpha$  is  $\|f\|_{W_2^\alpha(\Omega)}^2 = \sum_{0 \leq |\beta| \leq \alpha} \|D^\beta f\|_{\mathbf{L}_2(\Omega)}^2$ .

### 1.5 Background: linear algebra in tensorized function spaces

We briefly introduce linear algebra in tensorized function spaces, which is the necessary to develop our Variance-Reduced Sketching (VRS) framework for nonparametric density estimation.

## Multivariable functions as tensors

Given positive integers  $\{s_j\}_{j=1}^d \in \mathbb{N}$ , let  $\Omega_j \subset \mathbb{R}^{s_j}$ . Let  $A(z_1, \dots, z_d) : \Omega_1 \times \Omega_2 \cdots \times \Omega_d \rightarrow \mathbb{R}$  be a generic multivariable function and  $u_j(z_j) \in \mathbf{L}_2(\Omega_j)$  for  $j = 1, \dots, d$ . Denote

$$A[u_1, \dots, u_d] = \int_{\Omega_1} \cdots \int_{\Omega_d} A(z_1, \dots, z_d) u_1(z_1) \cdots u_d(z_d) dz_1 \cdots dz_d. \quad (4)$$

Define the Frobenius norm of  $A$  as

$$\|A\|_F^2 = \sum_{k_1, \dots, k_d=1}^{\infty} A^2[\phi_{1,k_1}, \dots, \phi_{d,k_d}], \quad (5)$$

where  $\{\phi_{j,k_j}\}_{k_j=1}^{\infty}$  are any orthonormal basis functions of  $\mathbf{L}_2(\Omega_j)$ . Note that in (5),  $\|A\|_F$  is independent of the choices of basis functions  $\{\phi_{j,k_j}\}_{k_j=1}^{\infty}$  in  $\mathbf{L}_2(\Omega_j)$  for  $j = 1, \dots, d$ . The operator norm of  $A$  is defined as

$$\|A\|_{\text{op}} = \sup_{\|u_j\|_{\mathbf{L}_2(\Omega_j)} \leq 1, j=1, \dots, d} A[u_1, \dots, u_d]. \quad (6)$$

We say that  $A$  is a tensor in tensor product space  $\mathbf{L}_2(\Omega_1) \otimes \mathbf{L}_2(\Omega_2) \otimes \cdots \otimes \mathbf{L}_2(\Omega_d)$  if there exist scalars  $\{b_{k_1, \dots, k_d}\}_{k_1, \dots, k_d=1}^{\infty} \subset \mathbb{R}$  and functions  $\{f_{j,k_j}\}_{k_j=1}^{\infty} \subset \mathbf{L}_2(\Omega_j)$  for each  $j = 1, \dots, d$  such that

$$A(z_1, \dots, z_d) = \sum_{k_1, \dots, k_d=1}^{\infty} b_{k_1, \dots, k_d} f_{1,k_1}(z_1) \cdots f_{d,k_d}(z_d) \quad (7)$$

and that  $\|A\|_F < \infty$ . From classical functional analysis, we have that

$$\mathbf{L}_2(\Omega_1) \otimes \mathbf{L}_2(\Omega_2) \cdots \otimes \mathbf{L}_2(\Omega_d) = \mathbf{L}_2(\Omega_1 \times \Omega_2 \cdots \times \Omega_d) \quad \text{and} \quad \|A\|_{\mathbf{L}_2(\Omega_1 \times \cdots \times \Omega_d)} = \|A\|_F. \quad (8)$$

## Projection operators in function spaces

Let  $\mathcal{U} = \text{span}\{\phi_1, \dots, \phi_m\} \subset \mathbf{L}_2(\Omega)$ , where  $m \in \mathbb{N}$  and  $\{\phi_\mu\}_{\mu=1}^m$  are any orthonormal functions. Then  $\mathcal{U}$  is an  $m$ -dimensional linear subspace of  $\mathbf{L}_2(\Omega)$  and we denote  $\dim(\mathcal{U}) = m$ . Let  $\mathcal{P}_{\mathcal{U}}$  be the projection operator onto the subspace  $\mathcal{U}$ . Therefore for any  $f \in \mathbf{L}_2(\Omega)$ , the projection of  $f$  on  $\mathcal{U}$  is

$$\mathcal{P}_{\mathcal{U}}(f) = \sum_{\mu=1}^m \langle f, \phi_\mu \rangle \phi_\mu. \quad (9)$$

Note that we always have  $\|\mathcal{P}_{\mathcal{U}}\|_{\text{op}} \leq 1$  for any projection operator  $\mathcal{P}_{\mathcal{U}}$ .

For  $j = 1, \dots, d$ , let  $\{\phi_{j,\mu_j}\}_{\mu_j=1}^{\infty}$  be any orthonormal functions of  $\mathbf{L}_2(\Omega_j)$  and  $\mathcal{U}_j = \text{span}\{\phi_{j,\mu_j}\}_{\mu_j=1}^{m_j}$ , where  $m_j \in \mathbb{N}$ . With the expansion in (7), define the tensor  $A \times_1 \mathcal{P}_{\mathcal{U}_1} \cdots \times_d \mathcal{P}_{\mathcal{U}_d}$  as

$$(A \times_1 \mathcal{P}_{\mathcal{U}_1} \cdots \times_d \mathcal{P}_{\mathcal{U}_d})(z_1, \dots, z_d) = \sum_{k_1, \dots, k_d=1}^{\infty} b_{k_1, \dots, k_d} \mathcal{P}_{\mathcal{U}_1}(f_{1,k_1})(z_1) \cdots \mathcal{P}_{\mathcal{U}_d}(f_{d,k_d})(z_d). \quad (10)$$

We have  $\|A \times_1 \mathcal{P}_{\mathcal{U}_1} \cdots \times_d \mathcal{P}_{\mathcal{U}_d}\|_F \leq \|A\|_F \|\mathcal{P}_{\mathcal{U}_1}\|_{\text{op}} \cdots \|\mathcal{P}_{\mathcal{U}_d}\|_{\text{op}} = \|A\|_F < \infty$  by Lemma 16 and the fact that  $\|\mathcal{P}_{\mathcal{U}_d}\|_{\text{op}} \leq 1$ . It follows that  $A \times_1 \mathcal{P}_{\mathcal{U}_1} \cdots \times_d \mathcal{P}_{\mathcal{U}_d}$  is a tensor in  $\mathbf{L}_2(\Omega_1) \otimes \mathbf{L}_2(\Omega_2) \otimes \cdots \otimes \mathbf{L}_2(\Omega_d)$  and therefore can be viewed as a function in  $\mathbf{L}_2(\Omega_1 \times \Omega_2 \cdots \times \Omega_d)$ .

More generally given  $k \leq d$ , let  $x = (z_1, \dots, z_k) \in \Omega_1 \times \cdots \times \Omega_k$  and  $y = (z_{k+1}, \dots, z_d) \in \Omega_{k+1} \times \cdots \times \Omega_d$ . We can view  $A(z_1, \dots, z_d) = A(x, y)$  as a function in  $\mathbf{L}_2(\Omega_1 \times \cdots \times \Omega_k) \otimes \mathbf{L}_2(\Omega_{k+1} \times \cdots \times \Omega_d)$ . For  $j = 1, \dots, k$ , let  $\mathcal{U}_j \subset \mathbf{L}_2(\Omega_j)$  be any subspace. Suppose  $\mathcal{U}_x \subset \mathbf{L}_2(\Omega_1 \times \cdots \times \Omega_k)$  is such that

$$\mathcal{U}_x = \mathcal{U}_1 \otimes \cdots \otimes \mathcal{U}_k = \text{Span}\{f_1(z_1) \cdots f_k(z_k), f_j(z_j) \in \mathcal{U}_j \text{ for all } 1 \leq j \leq k\}.$$

Then we have  $A \times_x \mathcal{P}_{\mathcal{U}_x} = A \times_1 \mathcal{P}_{\mathcal{U}_1} \cdots \times_k \mathcal{P}_{\mathcal{U}_k}$ , as shown in Lemma 18.

## 2 Density range estimation by sketching

Let  $d_1$  and  $d_2$  be arbitrary positive integers, and let  $\Omega_1 \subset \mathbb{R}^{d_1}$  and  $\Omega_2 \subset \mathbb{R}^{d_2}$  be two measurable sets. Let  $A^*(x, y) : \Omega_1 \times \Omega_2 \rightarrow \mathbb{R}$  be the unknown density function, and  $\{Z_i\}_{i=1}^N \subset \Omega_1 \times \Omega_2$  be the observed data sampled from  $A^*$ . Denote  $\hat{A}$  the empirical measure formed by  $\{Z_i\}_{i=1}^N$ . More precisely,

$$\hat{A} = \frac{1}{N} \sum_{i=1}^N \mathbb{I}_{\{Z_i\}}. \quad (11)$$

In this section, we introduce a sketching algorithm to estimate  $\text{Range}_x(A^*)$  based on  $\hat{A}$  with a reduced curse of dimensionality, where

$$\text{Range}_x(A^*) = \left\{ f(x) : f(x) = \int_{\Omega_2} A^*(x, y) g(y) dy \text{ for any } g(y) \in \mathbf{L}_2(\Omega_2) \right\}. \quad (12)$$

To this end, let  $\mathcal{M}$  be a linear subspace of  $\mathbf{L}_2(\Omega_1)$  that acts as an estimation subspace and  $\mathcal{L}$  be a linear subspace of  $\mathbf{L}_2(\Omega_2)$  that acts as a sketching subspace. More details on how to choose  $\mathcal{M}$  and  $\mathcal{L}$  are deferred to Remark 1. Our procedure is composed of the following three stages.

- Sketching stage. Let  $\{w_\eta\}_{\eta=1}^{\dim(\mathcal{L})}$  be the orthonormal basis functions of  $\mathcal{L}$ . We apply the projection operator  $\mathcal{P}_{\mathcal{L}}$  to  $\hat{A}$  by computing

$$\left\{ \int_{\Omega_2} \hat{A}(x, y) w_\eta(y) dy \right\}_{\eta=1}^{\dim(\mathcal{L})}. \quad (13)$$

Note that for each  $\eta = 1, \dots, \dim(\mathcal{L})$ ,  $\int_{\Omega_2} \hat{A}(x, y) w_\eta(y) dy$  is a function solely depending on  $x$ . This stage is aiming at reducing the curse of dimensionality associated to variable  $y$ .

- Estimation stage. We estimate the functions  $\left\{ \int_{\Omega_2} \hat{A}(x, y) w_\eta(y) dy \right\}_{\eta=1}^{\dim(\mathcal{L})}$  by utilizing the estimation space  $\mathcal{M}$ . Specifically, for each  $\eta = 1, \dots, \dim(\mathcal{L})$ , we approximate  $\int_{\Omega_2} \hat{A}(x, y) w_\eta(y) dy$  by

$$\tilde{f}_\eta(x) = \arg \min_{f \in \mathcal{M}} \left\| \int_{\Omega_2} \hat{A}(x, y) w_\eta(y) dy - f(x) \right\|_{\mathbf{L}_2(\Omega_1)}^2. \quad (14)$$

- Orthogonalization stage. Let

$$\tilde{A}(x, y) = \sum_{\eta=1}^{\dim(\mathcal{L})} \tilde{f}_\eta(x) w_\eta(y). \quad (15)$$

Compute the leading singular functions in the variable  $x$  of  $\tilde{A}(x, y)$  to estimate the  $\text{Range}_x(A^*)$ .

We formally summarize our procedure in Algorithm 1.

---

**Algorithm 1** Density range Estimation via Variance-Reduced Sketching

---

**INPUT:** Estimator  $\hat{A}(x, y) : \Omega_1 \times \Omega_2 \rightarrow \mathbb{R}$ , parameter  $r \in \mathbb{Z}^+$ , linear subspaces  $\mathcal{M} \subset \mathbf{L}_2(\Omega_1)$  and  $\mathcal{L} \subset \mathbf{L}_2(\Omega_2)$ .

- 1: Compute  $\left\{ \int_{\Omega_2} \hat{A}(x, y) w_\eta(y) dy \right\}_{\eta=1}^{\dim(\mathcal{L})}$ , the projection of  $\hat{A}$  onto  $\{w_\eta(y)\}_{\eta=1}^{\dim(\mathcal{L})}$ , the basis functions of  $\mathcal{L}$ .
- 2: Compute the estimated functions  $\{\tilde{f}_\eta(x)\}_{\eta=1}^{\dim(\mathcal{L})}$  in  $\mathcal{M}$  by (14).
- 3: Compute the leading  $r$  singular functions in the variable  $x$  of  $\tilde{A}(x, y) = \sum_{\eta=1}^{\dim(\mathcal{L})} \tilde{f}_\eta(x) w_\eta(y)$  and denote them as  $\{\hat{\Phi}_\rho(x)\}_{\rho=1}^r$ .

**OUTPUT:**  $\{\hat{\Phi}_\rho(x)\}_{\rho=1}^r$ .

---

Suppose the estimation space  $\mathcal{M}$  is spanned by the orthonormal basis functions  $\{v_\mu(x)\}_{\mu=1}^{\dim(\mathcal{M})}$ . In what follows, we provide an explicit expression of  $\tilde{A}(x, y)$  in (15) based on the  $\hat{A}(x, y)$ .

In the sketching stage, computing (13) is equivalent to compute  $\hat{A} \times_y \mathcal{P}_{\mathcal{L}}$ , as

$$\hat{A} \times_y \mathcal{P}_{\mathcal{L}} = \sum_{\eta=1}^{\dim(\mathcal{L})} \left( \int_{\Omega_2} \hat{A}(x, y) w_\eta(y) dy \right) w_\eta(y).$$

In the estimation stage, we have the following explicit expression for (14) by Lemma 20:

$$\hat{f}_\eta(x) = \sum_{\mu=1}^{\dim(\mathcal{M})} \hat{A}[v_\mu, w_\eta] v_\mu(x),$$

where  $\hat{A}[v_\mu, w_\eta] = \iint \hat{A}(x, y) v_\mu(x) w_\eta(y) dx dy$ . Therefore,  $\tilde{A}(x, y)$  in (15) can be rewritten as

$$\tilde{A}(x, y) = \sum_{\mu=1}^{\dim(\mathcal{M})} \sum_{\eta=1}^{\dim(\mathcal{L})} \hat{A}[v_\mu, w_\eta] v_\mu(x) w_\eta(y). \quad (16)$$

By Lemma 19,  $\hat{A} \times_x \mathcal{P}_{\mathcal{M}} \times_y \mathcal{P}_{\mathcal{L}}$  has the exact same expression as  $\tilde{A}$ . Therefore, we establish the identification

$$\tilde{A} = \hat{A} \times_x \mathcal{P}_{\mathcal{M}} \times_y \mathcal{P}_{\mathcal{L}}. \quad (17)$$

In Algorithm 3 of the appendix, we provide further implementation details on how to compute the leading  $r$  singular functions in the variable  $x$  of  $\hat{A} \times_x \mathcal{P}_{\mathcal{M}} \times_y \mathcal{P}_{\mathcal{L}}$  using singular value decomposition. Let  $\mathcal{P}_x^*$  be the projection operator onto the  $\text{Range}_x(A^*)$ , and let  $\hat{\mathcal{P}}_x$  be the projection operator onto the space spanned by  $\{\hat{\Phi}_\rho(x)\}_{\rho=1}^r$ , the output of Algorithm 1. In Section 2.1, we show that the range estimator in Algorithm 1 is consistent by providing theoretical quantification on the difference between  $\mathcal{P}_x^*$  and  $\hat{\mathcal{P}}_x$ .

## 2.1 Error analysis of Algorithm 1

We start with introducing necessary conditions to establish the consistency of our range estimators.

**Assumption 1.** *Suppose  $\Omega_1 \subset \mathbb{R}^{d_1}$  and  $\Omega_2 \subset \mathbb{R}^{d_2}$  be two measurable sets. Let  $A^*(x, y) : \Omega_1 \times \Omega_2 \rightarrow \mathbb{R}$  be a generic population function with  $\|A^*\|_{\mathbf{L}_2(\Omega_1 \times \Omega_2)} < \infty$ .*

$$A^*(x, y) = \sum_{\rho=1}^r \sigma_\rho \Phi_\rho^*(x) \Psi_\rho^*(y),$$

where  $r \in \mathbb{N}$ ,  $\sigma_1 \geq \sigma_2 \geq \dots \geq \sigma_r > 0$ , and  $\{\Phi_\rho^*(x)\}_{\rho=1}^r$  and  $\{\Psi_\rho^*(y)\}_{\rho=1}^r$  are orthonormal basis functions in  $\mathbf{L}_2(\Omega_1)$  and  $\mathbf{L}_2(\Omega_2)$  respectively.

Assumption 1 postulates that the density  $A^*$  is a finite-rank function. Finite-rank conditions are commonly observed in the literature. In Example 1 and Example 2 of Appendix A, we illustrate that both additive models and mean-field models satisfy Assumption 1. Additionally in Example 3, we demonstrate that all multivariable differentiable functions can be effectively approximated by finite-rank functions.

The following assumption quantifies the bias between  $A^*$  and its projection.

**Assumption 2.** *Let  $\mathcal{M} \subset \mathbf{L}_2(\Omega_1)$  and  $\mathcal{L} \subset \mathbf{L}_2(\Omega_2)$  be two linear subspaces such that  $\dim(\mathcal{M}) = m^{d_1}$  and  $\dim(\mathcal{L}) = \ell^{d_2}$ , where  $m, \ell \in \mathbb{N}$ . For  $\alpha \geq 1$ , suppose that*

$$\|A^* - A^* \times_x \mathcal{P}_\mathcal{M} \times_y \mathcal{P}_\mathcal{L}\|_{\mathbf{L}_2(\Omega_1 \times \Omega_2)}^2 = O(m^{-2\alpha} + \ell^{-2\alpha}), \quad (18)$$

$$\|A^* - A^* \times_y \mathcal{P}_\mathcal{L}\|_{\mathbf{L}_2(\Omega_1 \times \Omega_2)}^2 = O(\ell^{-2\alpha}), \quad \text{and} \quad (19)$$

$$\|A^* \times_y \mathcal{P}_\mathcal{L} - A^* \times_x \mathcal{P}_\mathcal{M} \times_y \mathcal{P}_\mathcal{L}\|_{\mathbf{L}_2(\Omega_1 \times \Omega_2)}^2 = O(m^{-2\alpha}). \quad (20)$$

**Remark 1.** *When  $\Omega_1 = [0, 1]^{d_1}$  and  $\Omega_2 = [0, 1]^{d_2}$ , Assumption 2 directly follows from approximation theories in Sobolev spaces. Indeed in the Appendix B, under the assumption that  $\|A^*\|_{W_2^\alpha([0, 1]^{d_1+d_2})} < \infty$ , we justify Assumption 2 when  $\mathcal{M}$  and  $\mathcal{L}$  are derived from three different popular nonparametric approaches: the reproducing kernel Hilbert spaces in Lemma 2, the Legendre polynomial system in Lemma 5, and the spline basis in Lemma 7.*

Note that by the identification in (17),  $\tilde{A} = \hat{A} \times_x \mathcal{P}_\mathcal{M} \times_y \mathcal{P}_\mathcal{L}$ . The following theorem shows that  $\text{Range}_x(A^*)$  can be well-approximated by the leading singular functions in  $x$  of  $\hat{A} \times_x \mathcal{P}_\mathcal{M} \times_y \mathcal{P}_\mathcal{L}$ .

**Theorem 1.** *Suppose Assumption 1 and 2 hold. For a sufficiently large constant  $C$ , suppose that*

$$\sigma_r > C \max \left\{ \ell^{-\alpha}, m^{-\alpha}, \sqrt{\frac{m^{d_1} + \ell^{d_2}}{N}} \right\}. \quad (21)$$

Let  $\mathcal{P}_x^*$  be the projection operator onto the  $\text{Range}_x(A^*)$ , and let  $\hat{\mathcal{P}}_x$  be the projection operator onto the space spanned by the leading  $r$  singular functions in the variable  $x$  of  $\hat{A} \times_x \mathcal{P}_\mathcal{M} \times_y \mathcal{P}_\mathcal{L}$ . Then

$$\|\hat{\mathcal{P}}_x - \mathcal{P}_x^*\|_{\text{op}}^2 = O_{\mathbb{P}} \left\{ \sigma_r^{-2} \left( \frac{m^{d_1} + \ell^{d_2}}{N} + m^{-2\alpha} \right) \right\}. \quad (22)$$

The proof of Theorem 1 can be found in Appendix C.1. It follows that if  $m \asymp N^{1/(2\alpha+d_1)}$ ,  $\ell = C_L \sigma_r^{-1/\alpha}$  for a sufficiently large constant  $C_L$ , and sample size  $N \geq C_\sigma \max\{\sigma_r^{-2-d_1/\alpha}, \sigma_r^{-2-d_2/\alpha}\}$  for a sufficiently large constant  $C_\sigma$ , then Theorem 1 implies that

$$\|\widehat{\mathcal{P}}_x - \mathcal{P}_x^*\|_{\text{op}}^2 = \text{O}_{\mathbb{P}} \left\{ \frac{\sigma_r^{-2}}{N^{2\alpha/(2\alpha+d_1)}} + \frac{\sigma_r^{-2-d_2/\alpha}}{N} \right\}. \quad (23)$$

To interpret our result in Theorem 1, consider a simplified scenario where the minimal spectral value  $\sigma_r$  is a positive constant. Then (23) further reduces to

$$\|\widehat{\mathcal{P}}_x - \mathcal{P}_x^*\|_{\text{op}}^2 = \text{O}_{\mathbb{P}} \left\{ \frac{1}{N^{2\alpha/(2\alpha+d_1)}} \right\},$$

which matches the optimal nonparametric density estimation rate in  $W_2^\alpha(\mathbb{R}^{d_1})$ . This indicates that our method is able to estimate  $\text{Range}_x(A^*)$  without the curse of dimensionality introduced by the variable  $y \in \mathbb{R}^{d_2}$ . Utilizing the estimator of  $\mathcal{P}_x^*$ , we can further estimate the population function  $A^*$  with a reduced curse of dimensionality as detailed in Section 3.

### 3 Density estimation by sketching

In this section, we study multivariable density estimation by utilizing the range estimator outlined in Algorithm 1. Let  $\mathcal{O}$  be a measurable subset of  $\mathbb{R}$  and  $A^*(z_1, \dots, z_d) : \mathcal{O}^d \rightarrow \mathbb{R}$  be the unknown population function. In this section, we propose a tensor-based algorithm to estimate function  $A^*$  with a reduced curse of dimensionality.

**Remark 2.** *In density estimation, it is sufficient to assume  $\mathcal{O} = [0, 1]$ . This is a common assumption widely used in the nonparametric statistics literature. Indeed, if the density function has compact support, through necessary scaling, we can assume the support is a subset of  $\mathcal{O}^d = [0, 1]^d$ .*

We begin by stating the necessary assumptions for our tensor-based estimator of  $A^*$ .

**Assumption 3.** *For  $j = 1, \dots, d$ , it holds that*

$$A^*(z_1, \dots, z_d) = \sum_{\rho=1}^{r_j} \sigma_{j,\rho} \Phi_{j,\rho}^*(z_j) \Psi_{j,\rho}^*(z_1, \dots, z_{j-1}, z_{j+1}, \dots, z_d)$$

where  $r_j \in \mathbb{N}$ ,  $\sigma_{j,1} \geq \sigma_{j,2} \geq \dots \geq \sigma_{j,r_j} > 0$ , and  $\{\Phi_{j,\rho}^*\}_{\rho=1}^{r_j}$  and  $\{\Psi_{j,\rho}^*\}_{\rho=1}^{r_j}$  are orthonormal functions in  $\mathbf{L}_2(\mathcal{O})$  and  $\mathbf{L}_2(\mathcal{O}^{d-1})$  respectively. Furthermore,  $\|A^*\|_{\mathbf{L}_2(\mathcal{O}^d)} < \infty$ .

Assumption 3 is a direct extension of Assumption 1, and all of Example 1, 2, and 3 in the appendix continue to hold for Assumption 3. Throughout this section, for  $j \in \{1, \dots, d\}$ , denote the operator  $\mathcal{P}_j^*$  as the projection operator onto  $\text{Range}_j(A^*) = \text{Span}\{\Phi_{j,\rho}^*(z_j)\}_{\rho=1}^{r_j}$ . More precisely,  $\mathcal{P}_j^* = \sum_{\rho=1}^{r_j} \Phi_{j,\rho}^* \otimes \Phi_{j,\rho}^* \in \mathbf{L}_2(\mathcal{O}) \otimes \mathbf{L}_2(\mathcal{O})$ .

In what follows, we formally introduce our algorithm to estimate the density function  $A^*$ . Let  $\{\phi_k^S\}_{k=1}^\infty \subset \mathbf{L}_2(\mathcal{O})$  be a collection of orthonormal basis functions. For  $j \in$

$\{1, \dots, d\}$ , let  $m \in \mathbb{N}, \ell_j \in \mathbb{N}$  and denote

$$\mathcal{M}_j = \text{span} \left\{ \phi_\mu^{\mathbb{S}}(z_j) \right\}_{\mu=1}^m \quad \text{and} \quad (24)$$

$$\mathcal{L}_j = \text{span} \left\{ \phi_{\eta_1}^{\mathbb{S}}(z_1) \cdots \phi_{\eta_{j-1}}^{\mathbb{S}}(z_{j-1}) \phi_{\eta_{j+1}}^{\mathbb{S}}(z_{j+1}) \cdots \phi_{\eta_d}^{\mathbb{S}}(z_d) \right\}_{\eta_1, \dots, \eta_{j-1}, \eta_{j+1}, \dots, \eta_d=1}^{\ell_j}. \quad (25)$$

**Remark 3.** *The collection of orthonormal basis functions  $\{\phi_k^{\mathbb{S}}\}_{k=1}^\infty \subset \mathbf{L}_2(\mathcal{O})$  can be derived through various nonparametric estimation methods. In the appendix, we present three examples of  $\{\phi_k^{\mathbb{S}}\}_{k=1}^\infty$ , including reproducing kernel Hilbert space basis functions (Appendix B.1), Legendre polynomial basis functions (Appendix B.2), and spline basis functions (Appendix B.3) to illustrate the potential choices.*

In Algorithm 2, we formally summarize our tensor-based estimator of  $A^*$ , which utilizes the range estimator developed in Section 2.1.

---

**Algorithm 2** Multivariable Density Estimation via Variance-Reduced Sketching

---

**INPUT:** Empirical measure  $\widehat{A}$  as in (11), parameters  $\{r_j\}_{j=1}^d \subset \mathbb{Z}^+$ , linear subspaces  $\{\mathcal{M}_j\}_{j=1}^d$  as in (24) and  $\{\mathcal{L}_j\}_{j=1}^d$  as in (25).

- 1: **for**  $j \in \{1, \dots, d\}$  **do**
- 2:   Input  $\{\widehat{A}, r_j, \mathcal{M}_j, \mathcal{L}_j\}$  to Algorithm 1 to estimate  $\text{Range}_j(A^*)$  and output leading  $r_j$  singular
- 3:   functions  $\{\widehat{\Phi}_{j,\rho_j}\}_{\rho_j=1}^{r_j}$ . Compute projection operator  $\widehat{\mathcal{P}}_j = \sum_{\rho_j=1}^{r_j} \widehat{\Phi}_{j,\rho_j} \otimes \widehat{\Phi}_{j,\rho_j}$ .
- 4: **end for**
- 5: Compute coefficient tensor  $B \in \mathbb{R}^{r_1 \times \dots \times r_d}$ :

$$B_{\rho_1, \dots, \rho_d} = \widehat{A}[\widehat{\Phi}_{1,\rho_1}, \dots, \widehat{\Phi}_{d,\rho_d}], \text{ for all } \rho_1 \in \{1, \dots, r_1\}, \dots, \rho_d \in \{1, \dots, r_d\}.$$

- 6: Compute estimated multivariable function

$$\left( \widehat{A} \times_1 \widehat{\mathcal{P}}_1 \cdots \times_d \widehat{\mathcal{P}}_d \right) (z_1, \dots, z_d) = \sum_{\rho_1=1}^{r_1} \cdots \sum_{\rho_d=1}^{r_d} \left( B_{\rho_1, \dots, \rho_d} \widehat{\Phi}_{1,\rho_1}(z_1) \cdots \widehat{\Phi}_{d,\rho_d}(z_d) \right).$$

**OUTPUT:** The estimate density function  $\widehat{A} \times_1 \widehat{\mathcal{P}}_1 \cdots \times_d \widehat{\mathcal{P}}_d$ .

---

In Section 5.1, we provide an in-depth discussion on how to choose the tuning parameters  $m, \{\ell_j\}_{j=1}^d$  and  $\{r_j\}_{j=1}^d$  in a data-driven way. The time complexity of Algorithm 2 is

$$\mathcal{O} \left( Nm \sum_{j=1}^d \ell_j^{d-1} + m^2 \sum_{j=1}^d \ell_j^{d-1} + Nm \sum_{j=1}^d r_j + N \prod_{j=1}^d r_j \right). \quad (26)$$

In (26), the first term is the cost of computing  $\{\widehat{A} \times_x \mathcal{P}_{\mathcal{M}_j} \times_y \mathcal{P}_{\mathcal{L}_j}\}_{j=1}^d$ , the second term corresponds to the cost of singular value decomposition of  $\{\widehat{A} \times_x \mathcal{P}_{\mathcal{M}_j} \times_y \mathcal{P}_{\mathcal{L}_j}\}_{j=1}^d$ , the third term represents the cost of computing  $\{\widehat{\mathcal{P}}_j\}_{j=1}^d$ , and the last term reflects the cost of computing  $\widehat{A} \times_1 \widehat{\mathcal{P}}_1 \cdots \times_d \widehat{\mathcal{P}}_d$  given  $\{\widehat{\mathcal{P}}_j\}_{j=1}^d$ . In the following theorem, we show that the difference between  $\widehat{A} \times_1 \widehat{\mathcal{P}}_1 \cdots \times_d \widehat{\mathcal{P}}_d$  and  $A^*$  is well-controlled.

**Theorem 2.** Suppose that  $\{Z_i\}_{i=1}^N \subset \mathcal{O}^d$  are independently sampled from a density  $A^* : \mathcal{O}^d \rightarrow \mathbb{R}^+$  satisfying  $\|A^*\|_{W_2^\alpha(\mathcal{O}^d)} < \infty$  with  $\alpha \geq 1$  and  $\|A^*\|_\infty < \infty$ .

Suppose in addition that  $A^*$  satisfies Assumption 3, and that  $\{\mathcal{M}_j, \mathcal{L}_j\}_{j=1}^d$  are in the form of (24) and (25), where  $\{\phi_k^{\mathcal{S}}\}_{k=1}^\infty \subset \mathbf{L}_2(\mathcal{O})$  are derived from reproducing kernel Hilbert spaces, the Legendre polynomial basis, or spline basis functions.

Let  $\widehat{A}$  in (11),  $\{r_j\}_{j=1}^d$ , and  $\{\mathcal{M}_j, \mathcal{L}_j\}_{j=1}^d$  be the input of Algorithm 2, and  $\widehat{A} \times_1 \widehat{\mathcal{P}}_1 \cdots \times_d \widehat{\mathcal{P}}_d$  be the corresponding output. Denote  $\sigma_{\min} = \min_{j=1, \dots, d} \{\sigma_{j, r_j}\}$  and suppose for a sufficiently large constant  $C_{\text{snr}}$ ,

$$N^{2\alpha/(2\alpha+1)} > C_{\text{snr}} \max \left\{ \prod_{j=1}^d r_j, \frac{1}{\sigma_{\min}^{(d-1)/\alpha+2}}, \frac{1}{\sigma_{\min}^{2\alpha/(\alpha-1/2)}} \right\}.$$

If  $\ell_j = C_L \sigma_{j, r_j}^{-1/\alpha}$  for some sufficiently large constant  $C_L$  and  $m \asymp N^{1/(2\alpha+1)}$ , then it holds that

$$\|\widehat{A} \times_1 \widehat{\mathcal{P}}_1 \cdots \times_d \widehat{\mathcal{P}}_d - A^*\|_{\mathbf{L}_2(\mathcal{O}^d)}^2 = \text{O}_{\mathbb{P}} \left( \frac{\sum_{j=1}^d \sigma_{j, r_j}^{-2}}{N^{2\alpha/(2\alpha+1)}} + \frac{\sum_{j=1}^d \sigma_{j, r_j}^{-(d-1)/\alpha-2}}{N} + \frac{\prod_{j=1}^d r_j}{N} \right). \quad (27)$$

The proof of Theorem 2 can be found in the appendix. To interpret Theorem 2, consider the simplified scenario where the ranks  $r_j$  and the minimal spectral values  $\sigma_{r_j}$  are both positive constants for  $j = 1, \dots, d$ . Then (27) implies that

$$\|\widehat{A} \times_1 \widehat{\mathcal{P}}_1 \cdots \times_d \widehat{\mathcal{P}}_d - A^*\|_{\mathbf{L}_2(\mathcal{O}^d)}^2 = \text{O}_{\mathbb{P}} \left( \frac{1}{N^{2\alpha/(2\alpha+1)}} \right),$$

which matches the minimax optimal rate of estimating non-parametric functions in  $W_2^\alpha(\mathbb{R})$ . Note that the error rate of estimating a nonparametric density in  $W_2^\alpha(\mathbb{R}^d)$  using classical kernel methods is of order  $N^{-2\alpha/(2\alpha+d)}$ . Therefore, as long as

$$\max \left\{ \sigma_{\min}^{-2}, \prod_{j=1}^d r_j \right\} = o(N^{d/(2\alpha+d)}),$$

then by (27), with high probability

$$\|\widehat{A} \times_1 \widehat{\mathcal{P}}_1 \cdots \times_d \widehat{\mathcal{P}}_d - A^*\|_{\mathbf{L}_2(\mathcal{O}^d)}^2 = o_{\mathbb{P}}(N^{-2\alpha/(2\alpha+d)}),$$

and the error bound we obtain in Theorem 2 is strictly better than classical kernel methods.

## 4 Extension: image PCA denoising

In this section, we demonstrate that our nonparametric sketching methodology, introduced in Section 2, can be used to estimate the principal component functions in the continuum limit. The most representative application of PCA is image denoising, which has a wide range of application in machine learning and data science, such as image clustering, classification, and segmentation. We refer the readers to Mika et al. (1998) and Bakır et al. (2004) for a detailed introduction on image processing.

Let  $\kappa \in \mathbb{N}$ . We define  $[\kappa] = [1, \dots, \kappa]$  and  $[\kappa]^2 = [1, \dots, \kappa] \times [1, \dots, \kappa]$ . Motivated by the image denoising model, in our approach, data are treated as discrete functions in  $\mathbf{L}_2([\kappa]^2)$  and therefore the resolution of the image data is  $\kappa^2$ . In such a setting for  $U, V \in \mathbf{L}_2([\kappa]^2)$  and  $x = (x_1, x_2) \in [\kappa]^2$ , we have

$$\|U\|_{\mathbf{L}_2([\kappa]^2)}^2 = \frac{1}{\kappa^2} \sum_{(x_1, x_2) \in [\kappa]^2} \{U(x_1, x_2)\}^2 \quad \text{and} \quad \langle U, V \rangle = \frac{1}{\kappa^2} \sum_{(x_1, x_2) \in [\kappa]^2} U(x_1, x_2)V(x_1, x_2)$$

where  $U(x_1, x_2)$  indicates the  $(x_1, x_2)$  pixel of  $U$ . Note that the norm in  $\mathbf{L}_2([\kappa]^2)$  differs from the Euclidean norm in  $\mathbb{R}^{\kappa^2}$  by a factor of  $\kappa^2$ . Let  $\Gamma \in \mathbf{L}_2([\kappa]^2) \otimes \mathbf{L}_2([\kappa]^2)$  and define

$$\Gamma[U, V] = \frac{1}{\kappa^4} \sum_{x \in [\kappa]^2, y \in [\kappa]^2} \Gamma(x, y)U(x)V(y). \quad (28)$$

The operator norm of  $\Gamma(x, y) \in \mathbf{L}_2([\kappa]^2) \otimes \mathbf{L}_2([\kappa]^2)$  is defined as

$$\|\Gamma(x, y)\|_{\text{op}(\mathbf{L}_2([\kappa]^2) \otimes \mathbf{L}_2([\kappa]^2))} = \sup_{\|U\|_{\mathbf{L}_2([\kappa]^2)} = \|V\|_{\mathbf{L}_2([\kappa]^2)} = 1} \Gamma[U, V]. \quad (29)$$

Motivated by the tremendous success of the discrete wavelet basis functions in the image denoising literature (e.g., see [Mohideen et al. \(2008\)](#)), we study PCA in reproducing kernel Hilbert spaces (RKHS) generated by wavelet functions. Specifically, let  $\{\phi_k^{\mathbb{S}}\}_{k=1}^{\kappa}$  be a collection of orthonormal discrete wavelet functions in  $\mathbf{L}_2([\kappa])$ . The RKHS generated by  $\{\phi_k^{\mathbb{S}}\}_{k=1}^{\kappa}$  is

$$\mathcal{H}([\kappa]) = \left\{ f \in \mathbf{L}_2([\kappa]) : \|f\|_{\mathcal{H}([\kappa])}^2 = \sum_{k=1}^{\kappa} \gamma_k^{-1} \langle f, \phi_k^{\mathbb{S}} \rangle^2 < \infty \right\}. \quad (30)$$

For  $d \in \mathbb{N}$ , define  $\mathcal{H}([\kappa]^d) = \mathcal{H}([\kappa]) \otimes \dots \otimes \mathcal{H}([\kappa])$ . For any  $F \in \mathcal{H}([\kappa]^d)$ , we have

$$\|F\|_{\mathcal{H}([\kappa]^d)}^2 = \sum_{k_1, \dots, k_d=1}^{\kappa} \gamma_{k_1}^{-1} \dots \gamma_{k_d}^{-1} (H[\phi_{k_1}^{\mathbb{S}}, \dots, \phi_{k_d}^{\mathbb{S}}])^2.$$

Let  $\mathcal{M} \subset \mathbf{L}_2([\kappa]^2)$  be the estimation space and  $\mathcal{L} \subset \mathbf{L}_2([\kappa]^2)$  be the sketching space such that

$$\mathcal{M} = \text{span} \left\{ \phi_{\mu_1}^{\mathbb{S}}(x_1) \phi_{\mu_2}^{\mathbb{S}}(x_2) \right\}_{\mu_1, \mu_2=1}^m \quad \text{and} \quad \mathcal{L} = \text{span} \left\{ \phi_{\eta_1}^{\mathbb{S}}(y_1) \phi_{\eta_2}^{\mathbb{S}}(y_2) \right\}_{\eta_1, \eta_2=1}^{\ell}, \quad (31)$$

where  $x_1, x_2, y_1, y_2 \in [\kappa]$ .

Suppose we observe a collection of noisy images  $\{W_i\}_{i=1}^N \subset \mathbf{L}_2([\kappa]^2)$  where for each  $x \in [\kappa]^2$ ,

$$W_i(x) = I_i(x) + \epsilon_i(x). \quad (32)$$

Here  $\{\epsilon_i(x)\}_{i=1, \dots, N, x \in [\kappa]^2} \subset \mathbb{R}$  are i.i.d. sub-Gaussian random variables and  $\{I_i\}_{i=1}^N$  are i.i.d. sub-Gaussian stochastic functions in  $\mathbf{L}_2([\kappa]^2)$  such that for every  $x, y \in [\kappa]^2$  and  $i = 1, \dots, n$ ,

$$\mathbb{E}(I_i(x)) = I^*(x) \quad \text{and} \quad \text{Cov}\{I_i(x)I_i(y)\} = \Sigma^*(x, y). \quad (33)$$

Our objective is to estimate the principle components of  $\Sigma^*$ . Denote  $\overline{W}(x) = \frac{1}{N} \sum_{i=1}^N W_i(x)$ , and define the covariance operator estimator as

$$\widehat{\Sigma}(x, y) = \frac{1}{N-1} \sum_{i=1}^N \{W_i(x) - \overline{W}(x)\} \{W_i(y) - \overline{W}(y)\}. \quad (34)$$

The following theorem shows that the principle components of  $\Sigma^*$  can be consistently estimated by the singular value decomposition of  $\widehat{\Sigma} \times_x \mathcal{P}_{\mathcal{M}} \times_y \mathcal{P}_{\mathcal{L}}$  with suitably chosen subspaces  $\mathcal{M}$  and  $\mathcal{L}$ .

**Corollary 1.** *Suppose the data  $\{W_i\}_{i=1}^N \subset \mathbf{L}_2([\kappa]^2)$  satisfy (32) and (33), and that  $\|\Sigma^*\|_{\mathcal{H}([\kappa]^4)} < \infty$ . Suppose in addition that for  $x, y \in [\kappa]^2$ ,  $\Sigma^*(x, y) = \sum_{\rho=1}^r \sigma_{\rho} \Phi_{\rho}^*(x) \Phi_{\rho}^*(y)$  where  $\sigma_1 \geq \sigma_2 \geq \dots \geq \sigma_r > 0$ , and  $\{\Phi_{\rho}^*\}_{\rho=1}^r$  are orthonormal discrete functions in  $\mathbf{L}_2([\kappa]^2)$ .*

*Suppose that  $\gamma_k \asymp k^{-2\alpha}$  in (30). Let  $\mathcal{M}$  and  $\mathcal{L}$  be defined as in (31). For sufficiently large constant  $C$ , suppose that*

$$|\sigma_r| > C \max \left\{ \ell^{-\alpha}, m^{-\alpha}, \frac{(m+\ell)}{\sqrt{N}}, \frac{1}{\kappa^2} \right\}. \quad (35)$$

*Denote  $\mathcal{P}_x^*$  as the projection operator onto the  $\text{Span}\{\Phi_{\rho}^*\}_{\rho=1}^r$ , and  $\widehat{\mathcal{P}}_x$  the projection operator onto the space spanned by the leading  $r$  singular functions in variable  $x$  of  $\widehat{\Sigma} \times_x \mathcal{P}_{\mathcal{M}} \times_y \mathcal{P}_{\mathcal{L}}$ . Then*

$$\|\widehat{\mathcal{P}}_x - \mathcal{P}_x^*\|_{\text{op}(\mathbf{L}_2([\kappa]^2) \otimes \mathbf{L}_2([\kappa]^2))}^2 = \text{O}_{\mathbb{P}} \left( \frac{\sigma_r^{-2}}{N^{2\alpha/(2\alpha+2)}} + \frac{\sigma_r^{-2}}{\kappa^4} \right). \quad (36)$$

The proof of Corollary 1 can be found in Appendix E. To interpret the result in Corollary 1, consider the scenario where the minimal spectral value  $\sigma_r$  is a positive constant. Then (36) simplifies to

$$\|\widehat{\mathcal{P}}_x - \mathcal{P}_x^*\|_{\text{op}(\mathbf{L}_2([\kappa]^2) \otimes \mathbf{L}_2([\kappa]^2))}^2 = \text{O}_{\mathbb{P}} \left( \frac{1}{N^{2\alpha/(2\alpha+2)}} + \frac{1}{\kappa^4} \right).$$

The term  $\frac{1}{N^{2\alpha/(2\alpha+2)}}$  aligns with the optimal rate for estimating a function in RKHS with degree of smoothness  $\alpha$  in a two-dimensional space. The additional term  $\frac{1}{\kappa^4}$  accounts for the measurement errors  $\{\epsilon_i\}_{i=1}^N$ . This term is typically negligible in application as  $\kappa$ , the resolution of the images, is typically much larger than the sample size  $N$  for high-resolution images.

## 5 Simulations and real data examples

In this section, we compare the numerical performance of the proposed estimator VRS with classical kernel methods and neural network estimators through density estimation models and image denoising models.

## 5.1 Implementations

As detailed in Algorithm 2, our approach involves three groups of tuning parameters:  $m$ ,  $\{\ell_j\}_{j=1}^d$ , and  $\{r_j\}_{j=1}^d$ . In all our numerical experiments, the optimal choices for  $m$  and  $\{\ell_j\}_{j=1}^d$  are determined through cross-validation. To select  $\{r_j\}_{j=1}^d$ , we apply a popular method in low-rank matrix estimation known as adaptive thresholding. Specifically, for each  $j = 1, \dots, d$ , we compute  $\{\widehat{\sigma}_{j,k}\}_{k=1}^\infty$ , the set of singular values of  $\widehat{A} \times_x \mathcal{P}_{\mathcal{M}_j} \times_y \mathcal{P}_{\mathcal{L}_j}$  and set

$$r_j = \arg \max_{k \geq 1} \frac{\widehat{\sigma}_{j,k}}{\widehat{\sigma}_{j,k+1}}.$$

Adaptive thresholding is a very popular strategy in the matrix completion literature (Candes and Plan (2010)) and it has been proven to be empirical robust in many scientific and engineering applications. We use built-in functions provided by the popular Python package scikit-learn to train kernel estimators, and scikit-learn also utilizes cross-validation for tuning parameter selection. For neural networks, we use PyTorch to train various models and make predictions. The implementations of our numerical studies can be found at this [link](#).

## 5.2 Density estimation

We study the numerical performance of Variance-Reduced Sketching (VRS), kernel density estimators (KDE), and neural networks (NN) in various density estimation problems. We use Legendre polynomials to span linear subspaces  $\{\mathcal{M}_j\}_{j=1}^d$  as in (24) and  $\{\mathcal{L}_j\}_{j=1}^d$  as in (25) in Algorithm 2 and the inputs of VRS in the density estimation setting are detailed in Theorem 2. Once we compute the density function via VRS, we use Gibbs sampling to efficiently generate samples from this multivariate probability distribution. The details are listed in Appendix I. For neural network estimators, we use two popular density estimation architectures: Masked Autoregressive Flow (MAF) (Papamakarios et al. (2017)) and Neural Autoregressive Flows (NAF) (Huang et al. (2018)) for comparisons. The details of implementing neural network density estimators are provided in Appendix I. We measure the estimation accuracy by the relative  $\mathbf{L}_2$ -error defined as

$$\frac{\|p^* - \widetilde{p}\|_{\mathbf{L}_2(\Omega)}}{\|p^*\|_{\mathbf{L}_2(\Omega)}},$$

where  $\widetilde{p}$  is the density estimator of a given estimator. We also compute the standard Kullback–Leibler (KL) divergence to measure the distance between two probability density functions:

$$D_{KL} = \mathbb{E}_{p^*}[\log(p^*/\widetilde{p})].$$

• **Simulation I.** In the first simulation, we use a two-dimensional two-modes Gaussian mixture model to numerically compare VRS, KDE and neural network estimators. We generate 1,000 samples from the density function

$$p^*(\mathbf{x}) = 0.4 \frac{\exp\left(-\frac{1}{2}(\mathbf{x} - \boldsymbol{\mu}_1)^T \boldsymbol{\Sigma}_1^{-1}(\mathbf{x} - \boldsymbol{\mu}_1)\right)}{\sqrt{(2\pi)^2 |\boldsymbol{\Sigma}_1|}} + 0.6 \frac{\exp\left(-\frac{1}{2}(\mathbf{x} - \boldsymbol{\mu}_2)^T \boldsymbol{\Sigma}_2^{-1}(\mathbf{x} - \boldsymbol{\mu}_2)\right)}{\sqrt{(2\pi)^2 |\boldsymbol{\Sigma}_2|}},$$

where  $\boldsymbol{\mu}_1 = \begin{pmatrix} -0.35 \\ -0.35 \end{pmatrix}$ ,  $\boldsymbol{\Sigma}_1 = \begin{pmatrix} 0.25^2 & -0.03^2 \\ -0.03^2 & 0.25^2 \end{pmatrix}$ ,  $\boldsymbol{\mu}_2 = \begin{pmatrix} 0.35 \\ 0.35 \end{pmatrix}$ ,  $\boldsymbol{\Sigma}_2 = \begin{pmatrix} 0.35^2 & 0.1^2 \\ 0.1^2 & 0.35^2 \end{pmatrix}$ . The relative  $\mathbf{L}_2$  error and KL divergence for each method are reported in Table 1. As demonstrated in this example, VRS achieves decent accuracy in the classical low-dimensional setting.

	VRS	KDE	NN-MAF	NN-NAF
relative $\mathbf{L}_2$ error	0.1270(0.0054)	0.1636(0.0068)	0.2225(0.0135)	0.3265(0.0103)
KL divergence	0.0092(0.0033)	0.0488(0.0029)	0.0785(0.0134)	0.0983(0.0098)

Table 1: Relative  $\mathbf{L}_2$  errors and KL divergences for four different methods of the two-dimensional Gaussian mixture model in **Simulation I**. The experiments are repeated for 50 times. The average errors are reported and standard deviations are shown in the bracket.

To further visualize the performance of the four different methods, the true density and the estimated density from each method are plotted in Figure 3. Direct comparison in Figure 3 demonstrates that VRS provides a relatively better estimator for the true density.

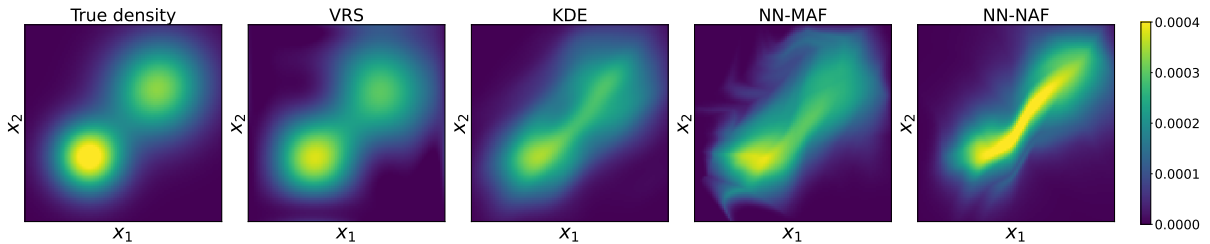


Figure 3: Density functions from the two-dimensional Gaussian mixture model in **Simulation I**. From left to right: the ground truth density, and estimations from VRS, KDE, MAF, and NAF. The values in the colorbar on the right represent function values.

• **Simulation II.** We consider a moderate high-dimensional density model in this simulation. Specifically, we generate  $10^5$  data from the 30-dimensional Gaussian mixture density function

$$\begin{aligned} \begin{pmatrix} x_1 \\ x_2 \\ x_3 \end{pmatrix} &\stackrel{\text{i.i.d.}}{\sim} \frac{1}{2} \mathcal{N} \left( \begin{pmatrix} -0.5 \\ -0.5 \\ -0.5 \end{pmatrix}, \begin{pmatrix} 0.1^2 & 0.06^2 & 0 \\ 0.06^2 & 0.1^2 & 0 \\ 0 & 0 & 0.1^2 \end{pmatrix} \right) + \frac{1}{2} \mathcal{N} \left( \begin{pmatrix} 0.5 \\ 0.5 \\ 0.5 \end{pmatrix}, 0.1^2 I_{3 \times 3} \right), \\ x_4, x_5 &\stackrel{\text{i.i.d.}}{\sim} \mathcal{N}(0, 0.04), \\ x_6, \dots, x_{30} &\stackrel{\text{i.i.d.}}{\sim} \frac{1}{2} \mathcal{N}(-0.4, 0.3^2) + \frac{1}{2} \mathcal{N}(0.4, 0.3^2), \text{ for } d > 5. \end{aligned}$$

The experiments are repeated for 50 times. Since computing high-dimensional  $\mathbf{L}_2$  errors is NP-hard, we only report the averaged KL divergence for performance evaluation. Table 2 showcases that VRS outperforms kernel and neural network estimators with a remarkable margin.

	VRS	KDE	MAF	NAF
KL divergence	0.0195(0.0056)	4.3823(0.0047)	0.9260(0.0523)	0.1613(0.0823)

Table 2: KL divergence for four methods of the 30-dimensional density model in **Simulation II**. The experiments are repeated for 50 times. The average errors are reported and standard deviations are shown in the bracket.

To further visualize the performance of the four different methods, we provide visualization of a few estimated marginal densities and compare them with the ground truth marginal density. Figure 4 depicts the comparison of the two-dimensional marginal densities corresponding to  $(x_1, x_2)$ ,  $(x_4, x_8)$ , and  $(x_{10}, x_{20})$ , respectively. Direct comparison in Figure 4 demonstrates VRS provides a relatively better fit for the true density.

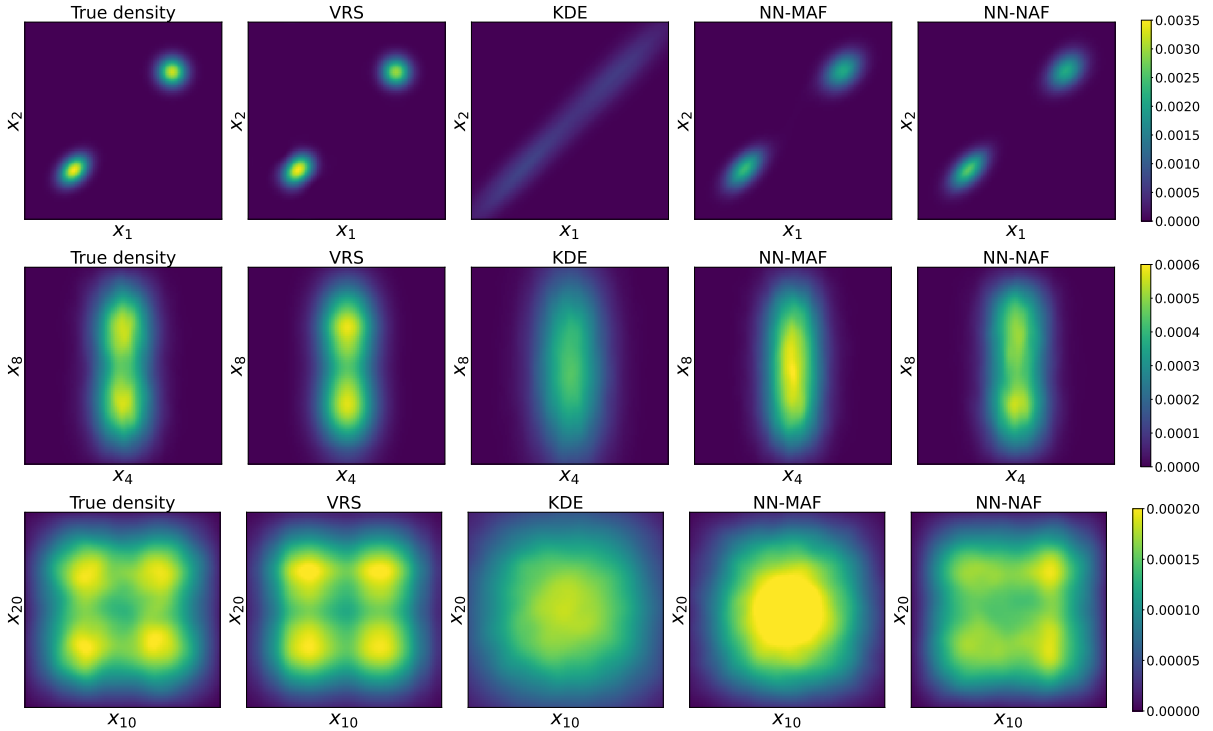


Figure 4: Marginal densities from the 30-dimensional Gaussian mixture model in **Simulation II**. From left to right: the ground truth density, and estimations from VRS, KDE, MAF, and NAF. From top to bottom: two-dimensional marginal densities corresponding to  $(x_1, x_2)$ ,  $(x_4, x_8)$ , and  $(x_{10}, x_{20})$ . The values in the colorbar on the right represent function values.

• **Simulation III.** Ginzburg-Landau theory is widely used to model microscopic behavior of superconductors. The Ginzburg-Landau density has the following expression

$$p^*(x_1, \dots, x_d) \propto \exp \left( -\beta \left\{ \sum_{j=0}^d \frac{\lambda}{2} \left( \frac{x_j - x_{j+1}}{h} \right)^2 + \sum_{j=1}^d \frac{1}{4\lambda} (x_j^2 - 1)^2 \right\} \right), \quad (37)$$

where  $x_0 = x_{d+1} = 0$ . We sample data from the Ginzburg-Landau density with coefficient  $\beta = 1/8, \lambda = 0.02, h = 1/(d+1)$  using Metropolis-Hastings sampling algorithm. This type of density would concentrate on two centers  $(+1, +1, \dots, +1)$  and  $(-1, -1, \dots, -1)$ ,

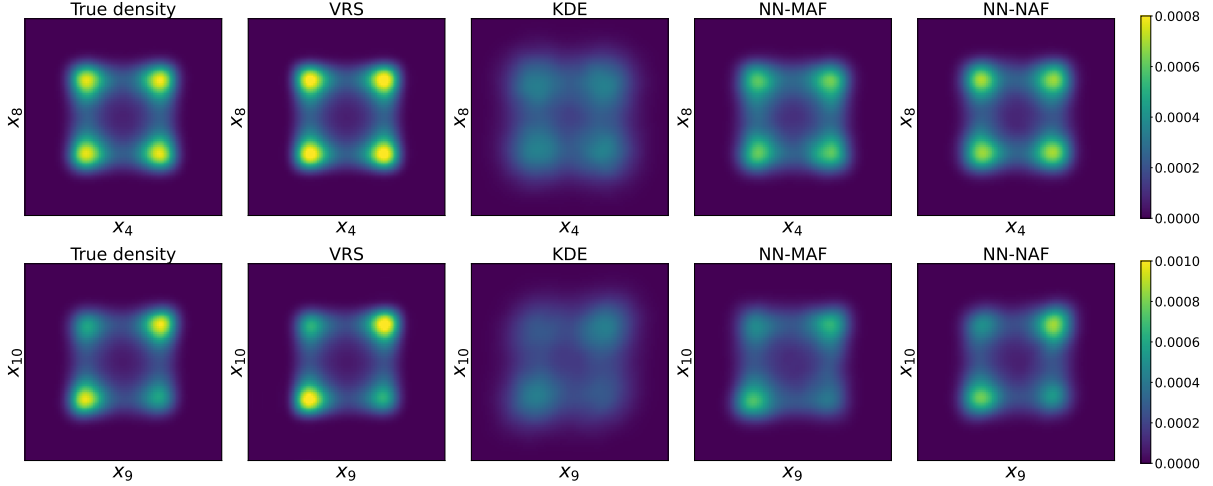


Figure 6: Marginal densities from the 10-dimensional Ginzburg-Landau model in **Simulation III**, and estimations from VRS, KDE, MAF, and NAF. From top to bottom: two-dimensional marginal densities corresponding to  $(x_4, x_8)$  and  $(x_9, x_{10})$ . The values in the colorbar on the right represent the density function values.

and all the coordinates  $(x_1, \dots, x_d)$  are correlated in a non-trivial way due to the interaction term  $\exp\left(-\beta \sum_{j=0}^d \frac{\lambda}{2} \left(\frac{x_j - x_{j+1}}{h}\right)^2\right)$  in the density function. We consider two sets of experiments for the Ginzburg-Landau density model. In the first set of experiments, we fix  $d = 10$  and change the sample size  $N$  from  $1 \times 10^5$  to  $5 \times 10^5$ . In the second set of experiments, we keep the sample size  $N$  at  $1 \times 10^5$  and vary  $d$  from 2 to 10. We summarize the averaged relative  $L_2$ -error for each method in Figure 5. Furthermore in Figure 6, we visualize several two-dimensional marginal densities estimated by the four different methods with sample size  $1 \times 10^5$ . Direct comparison showcases that our VRS method recovers these marginal densities with a decent accuracy.

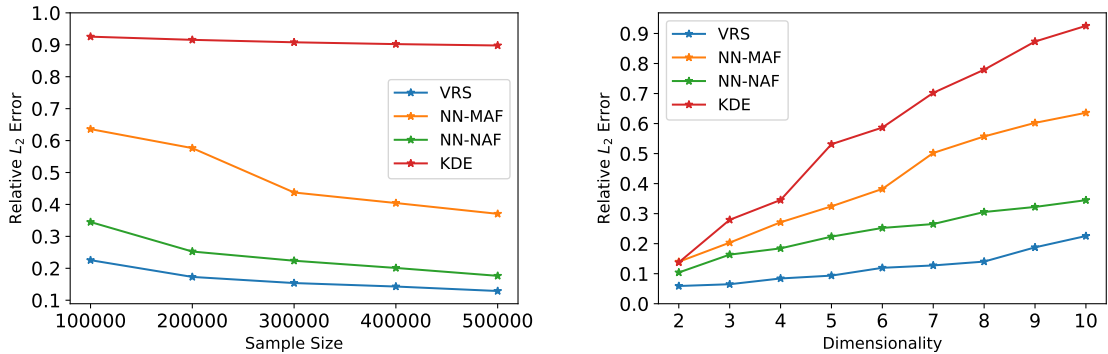


Figure 5: The plot on the left corresponds to **Simulation III** with  $d = 10$  and  $N$  varying from  $1 \times 10^5$  to  $5 \times 10^5$ ; the plot on the right corresponds to **Simulation III** with  $N$  being  $1 \times 10^5$  and  $d$  varying from 2 to 10.

- **Simulation IV.** We consider a four-mode Gaussian mixture model in two dimensions.

We generate 20,000 data from the density

$$p^*(\mathbf{x}) = \sum_{i=1}^4 \frac{1}{4} \frac{\exp\left(-\frac{1}{2}(\mathbf{x} - \boldsymbol{\mu}_i)^T \boldsymbol{\Sigma}_i^{-1}(\mathbf{x} - \boldsymbol{\mu}_i)\right)}{\sqrt{(2\pi)^2 |\boldsymbol{\Sigma}_i|}},$$

where  $\boldsymbol{\mu}_1 = \begin{pmatrix} -0.5 \\ -0.5 \end{pmatrix}$ ,  $\boldsymbol{\mu}_2 = \begin{pmatrix} 0.5 \\ 0.5 \end{pmatrix}$ ,  $\boldsymbol{\mu}_3 = \begin{pmatrix} -0.5 \\ 0.5 \end{pmatrix}$ ,  $\boldsymbol{\mu}_4 = \begin{pmatrix} 0.5 \\ -0.5 \end{pmatrix}$ , and  $\boldsymbol{\Sigma}_1 = \boldsymbol{\Sigma}_2 = \begin{pmatrix} 0.25^2 & 0.03^2 \\ 0.03^2 & 0.25^2 \end{pmatrix}$ ,  $\boldsymbol{\Sigma}_3 = \boldsymbol{\Sigma}_4 = \begin{pmatrix} 0.1^2 & -0.05^2 \\ -0.05^2 & 0.1^2 \end{pmatrix}$ . This setting is more difficult than **Simulation I** due to more modes and stronger singularity in the true density. We report the relative  $L_2$  error and KL divergence for each method in Table 3.

	VRS	KDE	MAF	NAF
Relative $L_1$ Error	0.0721(0.0029)	0.3987(0.0039)	0.2441(0.0411)	0.4617(0.0621)
KL Divergence	0.0142(0.0015)	0.1223(0.0014)	0.0819(0.0161)	0.2356(0.0417)

Table 3: Relative  $L_1$  errors and KL divergences for four different methods of the two-dimensional Gaussian mixture model in **Simulation IV**. The experiments are repeated for 50 times. The average errors are reported and standard deviations are shown in the bracket.

To further visualize the performance of the four different methods, the true density and the estimated density from each method are plotted Figure 7. Direct comparison in Figure 7 demonstrates VRS provides a relatively better estimate for the true density.

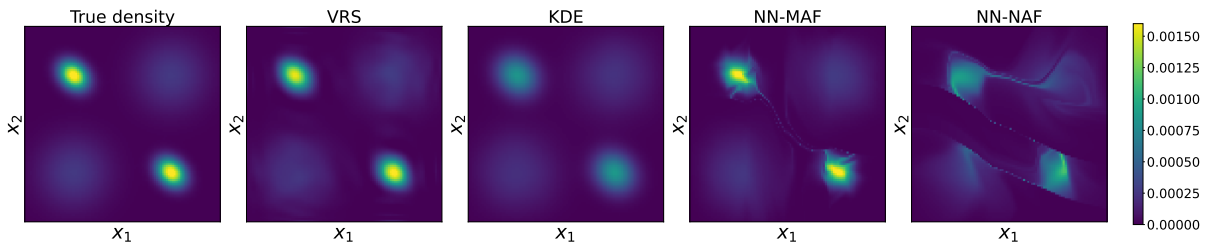


Figure 7: Density functions from the two-dimensional Gaussian mixture model in **Simulation IV**. From left to right are the ground truth density, estimates from VRS, KDE, MAF, and NAF, respectively. The values in the colorbar on the right represent function values.

- **Real data I.** We analyze the density estimation for the [Portugal wine quality](#) dataset from UCI Machine Learning Repository. This dataset contains 6497 samples of red and white wines, along with 8 continuous variables: volatile acidity, citric acid, residual sugar, chlorides, free sulfur dioxide, density, sulphates, and alcohol. To provide a comprehensive comparison between different methods, we estimate the joint density of the first  $d$  variables in this dataset, allowing  $d$  to vary from 2 to 8. For instance,  $d = 2$  corresponds to the joint density of volatile acidity and citric acid. Since the true density is unknown, we randomly split the dataset into 90% training and 10% test data and evaluate the performance of various approaches using the averaged log-likelihood of the test data. The averaged log-likelihood is defined as follows: let  $\tilde{p}$  be the density estimator based on the training data.

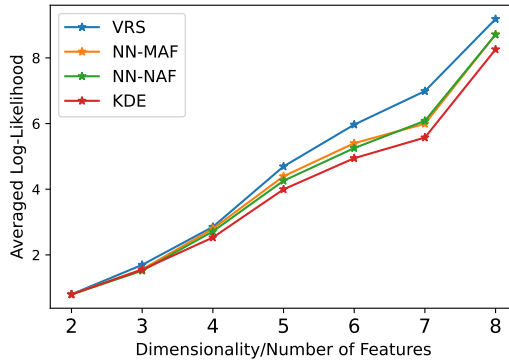


Figure 8: Density estimation for the Portugal wine quality dataset with VRS, KDE, and neural network estimators.

The averaged log-likelihood of the test data  $\{Z_i\}_{i=1}^{N_{\text{test}}}$  is

$$\frac{1}{N_{\text{test}}} \sum_{i=1}^{N_{\text{test}}} \log\{\tilde{p}(Z_i)\}.$$

The numerical performance of VRS, NN, and KDE are summarized in Figure 8. Notably, VRS achieves the highest averaged log-likelihood values, indicating its superior numerical performance.

### 5.3 Image PCA denoising

Principal Component Analysis (PCA) is a popular technique for reducing noise in images. In this subsection, we examine the numerical performance of VRS in image denoising problems. The state-of-the-art method in image denoising literature is kernel PCA. We direct interested readers to [Mika et al. \(1998\)](#) and [Bakır et al. \(2004\)](#) for a comprehensive introduction to the kernel PCA method.

The main advantage of VRS lies in its computational complexity. Consider  $N$  image data with resolution  $\kappa^2$ , where  $N, \kappa \in \mathbb{N}$ . The time complexity of kernel PCA is  $O(N^2\kappa^2 + N^3)$ , where  $O(N^2\kappa^2)$  corresponds to the cost of generating the kernel matrix in  $\mathbb{R}^{N \times N}$ , and  $O(N^3)$  reflects the cost of computing the principal components of this matrix. In contrast, the time complexity of VRS is analyzed in (26) with  $d = 2$ . Empirical evidence (see e.g., [Pope et al. \(2021\)](#)) suggests that image data possesses low intrinsic dimensions, making practical choices of  $\ell_j$  and  $r_j$  in (26) significantly smaller than  $N$  and  $\kappa$ . Even in the worst case scenario where  $M$  takes the upper bound  $\kappa$  in (26), the practical time complexity of VRS is  $O(N\kappa^2 + \kappa^4)$  which is considerably more efficient than the kernel PCA approach.

In the numerical experiments, we work with real datasets and we treat images from these real datasets as the ground truth images. To evaluate the numerical performance of a given approach, we add i.i.d. Gaussian noise to each pixels of the images and randomly split the dataset into 90% training and 10% test data. We then use the training data to compute the principal components based on the given approach and project the test data onto these estimated principal components. Denote the noiseless ground truth image as  $\{I_i^*\}_{i=1}^{N_{\text{test}}}$ , the corresponding projected noisy test data as  $\{\tilde{I}_i\}_{i=1}^{N_{\text{test}}}$  and the corresponding Gaussian noise added in the images as  $\{\epsilon_i\}_{i=1}^{N_{\text{test}}}$  in (32). The numerical performance of

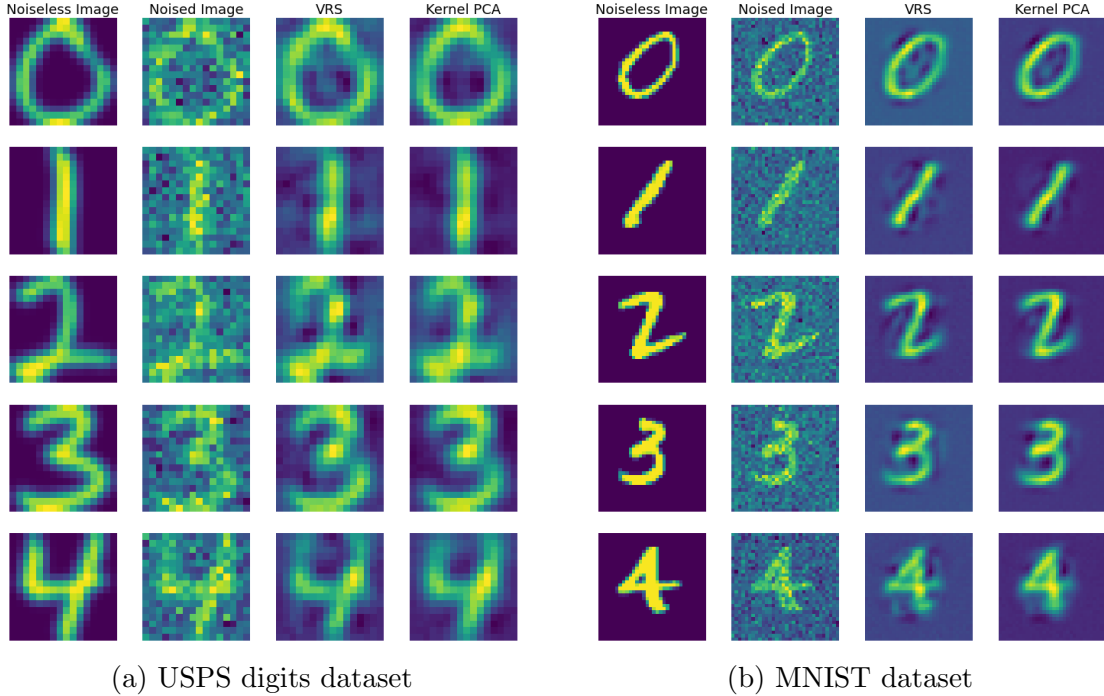


Figure 9: Denoising images from (a) USPS digits dataset and (b) MNIST dataset. In both (a) and (b), the first column shows the ground truth images from the test data, the second column shows the images polluted by Gaussian noise, the third column shows the images denoised using VRS, and the last column shows the images denoised using kernel PCA. Additional numerical results are shown in Appendix I.

the given approach is evaluated through the relative denoising error:

$$\sqrt{\frac{1}{N_{\text{test}}} \sum_{i=1}^{N_{\text{test}}} \frac{\|\tilde{I}_i - I_i^*\|_2^2}{\|I_i^*\|_2^2}}$$

where  $\|I_i^*\|_2$  indicates the euclidean norm of  $I_i^*$ . Besides, we use the relative variance  $\sqrt{\frac{1}{N_{\text{test}}} \sum_{i=1}^{N_{\text{test}}} \|\epsilon_i\|_2^2 / \|I_i^*\|_2^2}$  to measure the noise level. For the time complexity comparison, we execute on Google Colab’s CPU with high RAM and the execution time of each method is recorded.

- Real data III.** Our first study focuses the USPS digits dataset. This dataset comprises images of handwritten digits (0 through 9) that were originally scanned from envelopes by the USPS. It contains a total of 9,298 images, each with a resolution of  $16 \times 16$ . After adding the Gaussian noise, the relative noise variance of the noisy data is 0.7191. The relative denoising errors for VRS and kernel PCA are 0.2951 and 0.2959, respectively, which reflects excellent denoising performance of both two methods. Although the error shows minimal difference, the computational cost of VRS is significantly lower than that of kernel PCA: the execution time for VRS is 0.40 seconds, compared to 36.91 seconds for kernel PCA. In addition to this numerical comparison, in Figure 9(a) we have randomly selected five images from the test set to illustrate the denoised results using VRS and kernel PCA.

- Real data IV.** We analyze the MNIST dataset, which comprises 70,000 images of

handwritten digits (0 through 9), each labeled with the true digit. The size of each image is  $28 \times 28$ . After adding the Gaussian noise, the relative noise variance of the noisy data is 0.9171. The relative denoising errors for VRS and kernel PCA are 0.4044 and 0.4170, respectively. Although the numerical accuracy of the two methods is quite similar, the computational cost of VRS is significantly lower than that of kernel PCA. The execution time for VRS is only 4.33 seconds, in contrast to 3218.35 seconds for kernel PCA. In addition to this numerical comparison, Figure 9 includes a random selection of five images from the test set to demonstrate the denoised images using VRS and kernel PCA.

## 6 Conclusion

In this paper, we develop a comprehensive framework Variance-Reduced Sketching (VRS) for nonparametric density estimation problems in higher dimensions. Our approach leverages the concept of sketching from numerical linear algebra to address the curse of dimensionality in function spaces. Our method treats multivariable functions as infinite-dimensional matrices or tensors and the selection of sketching is specifically tailored to the regularity of the estimated function. This design takes the variance of random samples in nonparametric problems into consideration, intended to reduce curse of dimensionality in density estimation problems. Extensive simulated experiments and real data examples demonstrate that our sketching-based method substantially outperforms both neural network estimators and classical kernel density methods in terms of numerical performance.

## References

- Hussam Al Daas, Grey Ballard, Paul Cazeaux, Eric Hallman, Agnieszka Miedlar, Mirjeta Pasha, Tim W Reid, and Arvind K Saibaba. Randomized algorithms for rounding in the tensor-train format. *SIAM Journal on Scientific Computing*, 45(1):A74–A95, 2023.
- Ahmed Alaoui and Michael W Mahoney. Fast randomized kernel ridge regression with statistical guarantees. *Advances in neural information processing systems*, 28, 2015.
- Gökhan H Bakır, Jason Weston, and Bernhard Schölkopf. Learning to find pre-images. *Advances in neural information processing systems*, 16:449–456, 2004.
- Jordan Bell. The singular value decomposition of compact operators on hilbert spaces, 2014.
- David M Blei, Alp Kucukelbir, and Jon D McAuliffe. Variational inference: A review for statisticians. *Journal of the American statistical Association*, 112(518):859–877, 2017.
- Emmanuel J Candes and Yaniv Plan. Matrix completion with noise. *Proceedings of the IEEE*, 98(6):925–936, 2010.
- Kamalika Chaudhuri, Sanjoy Dasgupta, Samory Kpotufe, and Ulrike Von Luxburg. Consistent procedures for cluster tree estimation and pruning. *IEEE Transactions on Information Theory*, 60(12):7900–7912, 2014.

- Maolin Che and Yimin Wei. Randomized algorithms for the approximations of tucker and the tensor train decompositions. *Advances in Computational Mathematics*, 45(1):395–428, 2019.
- Yen-Chi Chen. A tutorial on kernel density estimation and recent advances. *Biostatistics & Epidemiology*, 1(1):161–187, 2017.
- Yian Chen and Yuehaw Khoo. Combining particle and tensor-network methods for partial differential equations via sketching. *arXiv preprint arXiv:2305.17884*, 2023.
- Yuxin Chen, Yuejie Chi, Jianqing Fan, Cong Ma, et al. Spectral methods for data science: A statistical perspective. *Foundations and Trends® in Machine Learning*, 14(5):566–806, 2021.
- Richard A Davis, Keh-Shin Lii, and Dimitris N Politis. Remarks on some nonparametric estimates of a density function. *Selected Works of Murray Rosenblatt*, pages 95–100, 2011.
- Arthur Dempster. Maximum likelihood estimation from incomplete data via the em algorithm. *Journal of the Royal Statistical Society*, 39:1–38, 1977.
- Laurent Dinh, David Krueger, and Yoshua Bengio. Nice: Non-linear independent components estimation. *arXiv preprint arXiv:1410.8516*, 2014.
- Laurent Dinh, Jascha Sohl-Dickstein, and Samy Bengio. Density estimation using real nvp. *arXiv preprint arXiv:1605.08803*, 2016.
- Petros Drineas and Michael W Mahoney. Randnla: randomized numerical linear algebra. *Communications of the ACM*, 59(6):80–90, 2016.
- Michael D Escobar and Mike West. Bayesian density estimation and inference using mixtures. *Journal of the american statistical association*, 90(430):577–588, 1995.
- Mathieu Germain, Karol Gregor, Iain Murray, and Hugo Larochelle. Made: Masked autoencoder for distribution estimation. In *International conference on machine learning*, pages 881–889. PMLR, 2015.
- Ian Goodfellow, Jean Pouget-Abadie, Mehdi Mirza, Bing Xu, David Warde-Farley, Sherjil Ozair, Aaron Courville, and Yoshua Bengio. Generative adversarial networks. *Communications of the ACM*, 63(11):139–144, 2020.
- Nathan Halko, Per-Gunnar Martinsson, and Joel A Tropp. Finding structure with randomness: Probabilistic algorithms for constructing approximate matrix decompositions. *SIAM review*, 53(2):217–288, 2011.
- Zhao-Yu Han, Jun Wang, Heng Fan, Lei Wang, and Pan Zhang. Unsupervised generative modeling using matrix product states. *Physical Review X*, 8(3):031012, 2018.
- Roger A Horn and Charles R Johnson. *Topics in matrix analysis*. Cambridge university press, 1994.
- Chin-Wei Huang, David Krueger, Alexandre Lacoste, and Aaron Courville. Neural autoregressive flows. In *International Conference on Machine Learning*, pages 2078–2087. PMLR, 2018.

- Yoonhaeng Hur, Jeremy G Hoskins, Michael Lindsey, E Miles Stoudenmire, and Yuehaw Khoo. Generative modeling via tensor train sketching. *Applied and Computational Harmonic Analysis*, 67:101575, 2023.
- Diederik P Kingma and Jimmy Ba. Adam: A method for stochastic optimization. *arXiv preprint arXiv:1412.6980*, 2014.
- Daniel Kressner, Bart Vandereycken, and Rik Voorhaar. Streaming tensor train approximation. *SIAM Journal on Scientific Computing*, 45(5):A2610–A2631, 2023.
- Sanjiv Kumar, Mehryar Mohri, and Ameet Talwalkar. Sampling methods for the nyström method. *The Journal of Machine Learning Research*, 13(1):981–1006, 2012.
- Edo Liberty, Franco Woolfe, Per-Gunnar Martinsson, Vladimir Rokhlin, and Mark Tygert. Randomized algorithms for the low-rank approximation of matrices. *Proceedings of the National Academy of Sciences*, 104(51):20167–20172, 2007.
- Han Liu, John Lafferty, and Larry Wasserman. Sparse nonparametric density estimation in high dimensions using the rodeo. In *Artificial Intelligence and Statistics*, pages 283–290. PMLR, 2007.
- Linxi Liu, Dangna Li, and Wing Hung Wong. Convergence rates of a class of multivariate density estimation methods based on adaptive partitioning. *Journal of machine learning research*, 24(50):1–64, 2023.
- Qiao Liu, Jiaze Xu, Rui Jiang, and Wing Hung Wong. Density estimation using deep generative neural networks. *Proceedings of the National Academy of Sciences*, 118(15):e2101344118, 2021.
- Michael W Mahoney et al. Randomized algorithms for matrices and data. *Foundations and Trends® in Machine Learning*, 3(2):123–224, 2011.
- Per-Gunnar Martinsson. Randomized methods for matrix computations. *The Mathematics of Data*, 25(4):187–231, 2019.
- Per-Gunnar Martinsson and Joel A Tropp. Randomized numerical linear algebra: Foundations and algorithms. *Acta Numerica*, 29:403–572, 2020.
- Sebastian Mika, Bernhard Schölkopf, Alex Smola, Klaus-Robert Müller, Matthias Scholz, and Gunnar Rätsch. Kernel pca and de-noising in feature spaces. *Advances in neural information processing systems*, 11, 1998.
- Rachel Minster, Arvind K Saibaba, and Misha E Kilmer. Randomized algorithms for low-rank tensor decompositions in the tucker format. *SIAM Journal on Mathematics of Data Science*, 2(1):189–215, 2020.
- S Kother Mohideen, S Arumuga Perumal, and M Mohamed Sathik. Image de-noising using discrete wavelet transform. *International Journal of Computer Science and Network Security*, 8(1):213–216, 2008.
- Yuji Nakatsukasa and Joel A Tropp. Fast & accurate randomized algorithms for linear systems and eigenvalue problems. *arXiv preprint arXiv:2111.00113*, 2021.

- George Papamakarios, Theo Pavlakou, and Iain Murray. Masked autoregressive flow for density estimation. *Advances in neural information processing systems*, 30, 2017.
- Emanuel Parzen. On estimation of a probability density function and mode. *The annals of mathematical statistics*, 33(3):1065–1076, 1962.
- Yifan Peng, Yian Chen, E Miles Stoudenmire, and Yuehaw Khoo. Generative modeling via hierarchical tensor sketching. *arXiv preprint arXiv:2304.05305*, 2023.
- Phillip Pope, Chen Zhu, Ahmed Abdelkader, Micah Goldblum, and Tom Goldstein. The intrinsic dimension of images and its impact on learning. *arXiv preprint arXiv:2104.08894*, 2021.
- Ali Rahimi and Benjamin Recht. Random features for large-scale kernel machines. *Advances in neural information processing systems*, 20, 2007.
- Garvesh Raskutti and Michael W Mahoney. A statistical perspective on randomized sketching for ordinary least-squares. *The Journal of Machine Learning Research*, 17(1):7508–7538, 2016.
- Yinuo Ren, Hongli Zhao, Yuehaw Khoo, and Lexing Ying. High-dimensional density estimation with tensorizing flow. *Research in the Mathematical Sciences*, 10(3):30, 2023.
- Danilo Rezende and Shakir Mohamed. Variational inference with normalizing flows. In *International conference on machine learning*, pages 1530–1538. PMLR, 2015.
- Espen Sande, Carla Manni, and Hendrik Speleers. Explicit error estimates for spline approximation of arbitrary smoothness in isogeometric analysis. *Numerische Mathematik*, 144(4):889–929, 2020.
- David W Scott. On optimal and data-based histograms. *Biometrika*, 66(3):605–610, 1979.
- David W Scott. Averaged shifted histograms: effective nonparametric density estimators in several dimensions. *The Annals of Statistics*, pages 1024–1040, 1985.
- Tianyi Shi, Maximilian Ruth, and Alex Townsend. Parallel algorithms for computing the tensor-train decomposition. *SIAM Journal on Scientific Computing*, 45(3):C101–C130, 2023.
- Bharath Sriperumbudur and Ingo Steinwart. Consistency and rates for clustering with dbscan. In *Artificial Intelligence and Statistics*, pages 1090–1098. PMLR, 2012.
- Yiming Sun, Yang Guo, Charlene Luo, Joel Tropp, and Madeleine Udell. Low-rank tucker approximation of a tensor from streaming data. *SIAM Journal on Mathematics of Data Science*, 2(4):1123–1150, 2020.
- Xun Tang and Lexing Ying. Solving high-dimensional fokker-planck equation with functional hierarchical tensor. *arXiv preprint arXiv:2312.07455*, 2023.
- Xun Tang, Yoonhaeng Hur, Yuehaw Khoo, and Lexing Ying. Generative modeling via tree tensor network states. *arXiv preprint arXiv:2209.01341*, 2022.

- Joel A Tropp, Alp Yurtsever, Madeleine Udell, and Volkan Cevher. Fixed-rank approximation of a positive-semidefinite matrix from streaming data. *Advances in Neural Information Processing Systems*, 30, 2017a.
- Joel A Tropp, Alp Yurtsever, Madeleine Udell, and Volkan Cevher. Practical sketching algorithms for low-rank matrix approximation. *SIAM Journal on Matrix Analysis and Applications*, 38(4):1454–1485, 2017b.
- Benigno Uribe, Marc-Alexandre Côté, Karol Gregor, Iain Murray, and Hugo Larochelle. Neural autoregressive distribution estimation. *The Journal of Machine Learning Research*, 17(1):7184–7220, 2016.
- Roman Vershynin. *High-dimensional probability: An introduction with applications in data science*, volume 47. Cambridge university press, 2018.
- Martin J Wainwright. *High-dimensional statistics: A non-asymptotic viewpoint*, volume 48. Cambridge university press, 2019.
- Shusen Wang, Alex Gittens, and Michael W Mahoney. Sketched ridge regression: Optimization perspective, statistical perspective, and model averaging. In *International Conference on Machine Learning*, pages 3608–3616. PMLR, 2017.
- Larry Wasserman. *All of nonparametric statistics*. Springer Science & Business Media, 2006.
- Christopher Williams and Matthias Seeger. Using the nyström method to speed up kernel machines. *Advances in neural information processing systems*, 13, 2000.
- David P Woodruff et al. Sketching as a tool for numerical linear algebra. *Foundations and Trends® in Theoretical Computer Science*, 10(1–2):1–157, 2014.
- Yuan Xu. Approximation by polynomials in sobolev spaces with jacobi weight. *Journal of Fourier Analysis and Applications*, 24:1438–1459, 2018.
- Yun Yang, Mert Pilanci, and Martin J Wainwright. Randomized sketches for kernels: Fast and optimal nonparametric regression. *Annals of Statistics*, pages 991–1023, 2017.
- Adriano Z Zambom and Ronaldo Dias. A review of kernel density estimation with applications to econometrics. *International Econometric Review*, 5(1):20–42, 2013.

## A Examples of finite-rank functions

In this section, we present three examples commonly encountered in nonparametric statistical literature that satisfy Assumption 1. Note that the range of  $A(x, y) : \Omega_1 \times \Omega_2 \rightarrow \mathbb{R}$  is defined as

$$\text{Range}_x(A) = \left\{ f(x) : f(x) = \int A(x, y)g(y)dy \text{ for any } g(y) \in \mathbf{L}_2(\Omega_2) \right\}. \quad (38)$$

In addition, we provide a classical result in function spaces that allows us to conceptualize multivariable functions as infinite-dimensional matrices. Let  $d_1$  and  $d_2$  be arbitrary positive integers, and let  $\Omega_1 \subset \mathbb{R}^{d_1}$  and  $\Omega_2 \subset \mathbb{R}^{d_2}$  be two measurable sets.

**Theorem 3.** *[Singular value decomposition in function space] Let  $A(x, y) : \Omega_1 \times \Omega_2 \rightarrow \mathbb{R}$  be any function such that  $\|A\|_{\mathbf{L}_2(\Omega_1 \times \Omega_2)} < \infty$ . There exists a collection of strictly positive singular values  $\{\sigma_\rho(A)\}_{\rho=1}^r \in \mathbb{R}^+$ , and two collections of orthonormal basis functions  $\{\Phi_\rho(x)\}_{\rho=1}^r \subset \mathbf{L}_2(\Omega_1)$  and  $\{\Psi_\rho(y)\}_{\rho=1}^r \subset \mathbf{L}_2(\Omega_2)$  where  $r \in \mathbb{N} \cup \{+\infty\}$  such that*

$$A(x, y) = \sum_{\rho=1}^r \sigma_\rho(A) \Phi_\rho(x) \Psi_\rho(y). \quad (39)$$

By viewing  $A(x, y)$  as an infinite-dimensional matrix, it follows that the rank of  $A(x, y)$  is  $r$  and that an equivalent definition of  $\text{Range}_x(A)$  is that

$$\text{Range}_x(A) = \text{Span}\{\Phi_\rho(x)\}_{\rho=1}^r. \quad (40)$$

where the definition of Span can be found in (3). Consequently, the rank of  $A(x, y)$  is the same as the dimensionality of  $\text{Range}_x(A)$ .

**Example 1** (Additive models in regression). *In multivariate nonparametric statistical literature, it is commonly assumed that the underlying unknown nonparametric function  $f^* : [0, 1]^d \rightarrow \mathbb{R}$  process an additive structure, meaning that there exists a collection of univariate functions  $\{f_j^*(z_j) : [0, 1] \rightarrow \mathbb{R}\}_{j=1}^d$  such that*

$$f^*(z_1, \dots, z_d) = f_1^*(z_1) + \dots + f_d^*(z_d) \text{ for all } (z_1, \dots, z_d) \in [0, 1]^d$$

*To connect this with Assumption 1, let  $x = z_1$  and  $y = (z_2, \dots, z_d)$ . Then by (38),  $\text{Range}_x(f^*) = \text{Span}\{1, f_1^*(z_1)\}$  and  $\text{Range}_y(f^*) = \text{Span}\{1, g^*(y)\}$ , where*

$$g^*(y) = g^*(z_2, \dots, z_d) = f_2^*(z_2) + \dots + f_d^*(z_d).$$

*The dimensionality of  $\text{Range}_x(f^*)$  is at most 2, and consequently the rank of  $f^*(x, y) \in \mathbf{L}_2([0, 1]) \otimes \mathbf{L}_2([0, 1]^{d-1})$  is at most 2.*

**Example 2** (Mean-field models in density estimation). *Mean-field theory is a popular framework in computational physics and Bayesian probability as it studies the behavior of high-dimensional stochastic models. The main idea of the mean-field theory is to replace all interactions to any one body with an effective interaction in a physical system. Specifically, the mean-field model assumes that the density function  $p^*(z_1, \dots, z_d) : [0, 1]^d \rightarrow \mathbb{R}^+$  can be well-approximated by  $p_1^*(z_1) \dots p_d^*(z_d)$ , where for  $j = 1, \dots, d$ ,  $p_j^*(z_j) : [0, 1] \rightarrow \mathbb{R}^+$  are univariate marginal density functions. The readers are referred to Blei et al. (2017) for further discussion.*

In a large physical system with multiple interacting sub-systems, the underlying density can be well-approximated by a mixture of mean-field densities. Specifically, let  $\{\tau_\rho\}_{\rho=1}^r \subset \mathbb{R}^+$  be a collection of positive probabilities summing to 1. In the mean-field mixture model, with probability  $\tau_\rho$ , data are sampled from a mean-field density  $p_\rho^*(z_1, \dots, z_d) = p_{\rho,1}^*(z_1) \cdots p_{\rho,d}^*(z_d)$ . Therefore

$$p^*(z_1, \dots, z_d) = \sum_{\rho=1}^r \tau_\rho p_{\rho,1}^*(z_1) \cdots p_{\rho,d}^*(z_d).$$

To connect the mean-field mixture model to Assumption 1, let  $x = z_1$  and  $y = (z_2, \dots, z_d)$ . Then according to (38),  $\text{Range}_x(f^*) = \text{Span}\{p_{\rho,1}^*(z_1)\}_{\rho=1}^r$  and  $\text{Range}_y(f^*) = \text{Span}\{g_\rho^*(y)\}_{\rho=1}^r$ , where

$$g_\rho^*(y) = p_{\rho,2}^*(z_2) \cdots p_{\rho,d}^*(z_d).$$

The dimensionality of  $\text{Range}_x(p^*)$  is at most  $r$ , and therefore the rank of  $p^*(x, y)$  is at most  $r$ .

**Example 3** (Multivariate Taylor expansion). Suppose  $G : [0, 1]^d \rightarrow \mathbb{R}$  is an  $\alpha$ -times continuously differentiable function. Then Taylor's theorem in the multivariate setting states that for  $z = (z_1, \dots, z_d) \in \mathbb{R}^d$  and  $t = (t_1, \dots, t_d) \in \mathbb{R}^d$ ,  $G(z) \approx T_t(z)$ , where

$$T_t(z) = G(t) + \sum_{k=1}^{\alpha} \frac{1}{k!} \mathcal{D}^k G(t, z - t), \quad (41)$$

and  $\mathcal{D}^k G(x, h) = \sum_{i_1, \dots, i_k=1}^d \partial_{i_1} \cdots \partial_{i_k} G(x) h_{i_1} \cdots h_{i_k}$ . For example,  $\mathcal{D}G(x, h) = \sum_{i=1}^d \partial_i G(x) h_i$ ,  $\mathcal{D}^2 G(x, h) = \sum_{i=1}^d \sum_{j=1}^d \partial_i \partial_j G(x) h_i h_j$ , and so on. To simplify our discussion, let  $t = 0 \in \mathbb{R}^d$ . Then (41) becomes

$$T_0(z) = G(0) + \sum_{i=1}^d \partial_i G(0) z_i + \frac{1}{2!} \sum_{i=1}^d \sum_{j=1}^d \partial_i \partial_j G(0) z_i z_j + \dots + \frac{1}{\alpha!} \sum_{i_1, \dots, i_\alpha=1}^d \partial_{i_1} \cdots \partial_{i_\alpha} G(0) z_{i_1} \cdots z_{i_\alpha}.$$

Let  $x = z_1$  and  $y = (z_2, \dots, z_d)$ . Then by (38),  $\text{Range}_x(T_0) = \text{Span}\{1, z_1, z_1^2, \dots, z_1^\alpha\}$ . The dimensionality of  $\text{Range}_x(T_0)$  is at most  $\alpha + 1$ , and therefore  $G$  can be well-approximated by finite rank functions.

## B Examples of $\mathcal{M}$ and $\mathcal{L}$ satisfying Assumption 2

In this section, we provide three examples of the subspaces  $\mathcal{M}$  and  $\mathcal{L}$  such that Assumption 2 holds.

### B.1 Reproducing kernel Hilbert space basis

Let  $\mathcal{O}$  be a measurable set in  $\mathbb{R}$ . The two most used examples are  $\mathcal{O} = [0, 1]$  for non-parametric estimation and  $\mathcal{O} = \{1, \dots, \kappa\}$  for image PCA.

For  $x, y \in \mathcal{O}$ , let  $\mathbb{K} : \mathcal{O} \times \mathcal{O} \rightarrow \mathbb{R}$  be a kernel function such that

$$\mathbb{K}(x, y) = \sum_{k=1}^{\infty} \lambda_k^{\mathbb{K}} \phi_k^{\mathbb{K}}(x) \phi_k^{\mathbb{K}}(y), \quad (42)$$

where  $\{\lambda_k^{\mathbb{K}}\}_{k=1}^{\infty} \subset \mathbb{R}^+ \cup \{0\}$ , and  $\{\phi_k^{\mathbb{K}}\}_{k=1}^{\infty}$  is a collection of basis functions in  $\mathbf{L}_2(\mathcal{O})$ . If  $\mathcal{O} = [0, 1]$ ,  $\{\phi_k^{\mathbb{K}}\}_{k=1}^{\infty}$  are orthonormal  $\mathbf{L}_2([0, 1])$  functions. If  $\mathcal{O} = \{1, \dots, \kappa\}$ , then  $\{\phi_k^{\mathbb{K}}\}_{k=1}^{\infty}$  can be identified as orthogonal vectors in  $\mathbb{R}^{\kappa}$ . In this case,  $\lambda_k^{\mathbb{K}} = 0$  for all  $k > \kappa$ .

The reproducing kernel Hilbert space generated by  $\mathbb{K}$  is

$$\mathcal{H}(\mathbb{K}) = \left\{ f \in \mathbf{L}_2([0, 1]) : \|f\|_{\mathcal{H}(\mathbb{K})}^2 = \sum_{k=1}^{\infty} (\lambda_k^{\mathbb{K}})^{-1} \langle f, \phi_k^{\mathbb{K}} \rangle^2 < \infty \right\}. \quad (43)$$

For any functions  $f, g \in \mathcal{H}(\mathbb{K})$ , the inner product in  $\mathcal{H}(\mathbb{K})$  is given by

$$\langle f, g \rangle_{\mathcal{H}(\mathbb{K})} = \sum_{k=1}^{\infty} (\lambda_k^{\mathbb{K}})^{-1} \langle f, \phi_k^{\mathbb{K}} \rangle \langle g, \phi_k^{\mathbb{K}} \rangle.$$

Denote  $\Theta_k^{\mathbb{K}} = (\lambda_k^{\mathbb{K}})^{-1/2} \phi_k^{\mathbb{K}}$ . Then  $\{\Theta_k^{\mathbb{K}}\}_{k=1}^{\infty}$  are the orthonormal basis functions in  $\mathcal{H}(\mathbb{K})$  as we have that

$$\langle \Theta_{k_1}^{\mathbb{K}}, \Theta_{k_2}^{\mathbb{K}} \rangle_{\mathcal{H}(\mathbb{K})} = \begin{cases} 1, & \text{if } k_1 = k_2; \\ 0, & \text{if } k_1 \neq k_2. \end{cases}$$

an that

$$\|f\|_{\mathcal{H}(\mathbb{K})}^2 = \sum_{k=1}^{\infty} (\lambda_k^{\mathbb{K}})^{-1} \langle f, \phi_k^{\mathbb{K}} \rangle^2 = \sum_{k=1}^{\infty} \langle f, \Theta_k^{\mathbb{K}} \rangle^2.$$

Define the tensor product space

$$\underbrace{\mathcal{H}(\mathbb{K}) \otimes \dots \otimes \mathcal{H}(\mathbb{K})}_{d \text{ copies}} = \{\mathcal{H}(\mathbb{K})\}^{\otimes d}.$$

The induced Frobenius norm in  $\{\mathcal{H}(\mathbb{K})\}^{\otimes d}$  is

$$\|A\|_{\{\mathcal{H}(\mathbb{K})\}^{\otimes d}}^2 = \sum_{k_1, \dots, k_d=1}^{\infty} (A[\Theta_{k_1}^{\mathbb{K}}, \dots, \Theta_{k_d}^{\mathbb{K}}])^2 = \sum_{k_1, \dots, k_d=1}^{\infty} (\lambda_{k_1}^{\mathbb{K}} \dots \lambda_{k_d}^{\mathbb{K}})^{-1} (A[\phi_{k_1}^{\mathbb{K}}, \dots, \phi_{k_d}^{\mathbb{K}}])^2, \quad (44)$$

where  $A[\phi_{k_1}^{\mathbb{K}}, \dots, \phi_{k_d}^{\mathbb{K}}]$  is defined by (4). The following lemma shows that the space  $\{\mathcal{H}(\mathbb{K})\}^{\otimes d}$  is naturally motivated by multidimensional Sobolev spaces.

**Lemma 1.** *Let  $\mathcal{O} = [0, 1]$ . With  $\lambda_k^{\mathbb{K}} \asymp k^{-2\alpha}$  and suitable choices of  $\{\phi_k^{\mathbb{K}}\}_{k=1}^{\infty}$ , it holds that*

$$\{\mathcal{H}(\mathbb{K})\}^{\otimes d} = W_2^{\alpha}([0, 1]^d).$$

*Proof.* Let  $\mathcal{O} = [0, 1]$ . When  $d = 1$ , it is a classical Sobolev space result that with  $\lambda_k^{\mathbb{K}} \asymp k^{-2\alpha}$  and suitable choices of  $\{\phi_k^{\mathbb{K}}\}_{k=1}^{\infty}$ ,

$$\mathcal{H}(\mathbb{K}) = W_2^{\alpha}([0, 1]).$$

We refer interested readers to Chapter 12 of [Wainwright \(2019\)](#) for more details. In general, it is well-known in functional analysis that for  $\Omega_1 \subset \mathbb{R}^{d_1}$  and  $\Omega_2 \subset \mathbb{R}^{d_2}$ , then

$$W_2^{\alpha}(\Omega_1) \otimes W_2^{\alpha}(\Omega_2) = W_2^{\alpha}(\Omega_1 \times \Omega_2).$$

Therefore by induction

$$\{\mathcal{H}(\mathbb{K})\}^{\otimes d} = \{\mathcal{H}(\mathbb{K})\}^{\otimes d-1} \otimes \{\mathcal{H}(\mathbb{K})\} = W_2^{\alpha}([0, 1]^{d-1}) \otimes W_2^{\alpha}([0, 1]) = W_2^{\alpha}([0, 1]^d). \quad (45)$$

□

Let  $(z_1, \dots, z_{d_1}, z_{d_1+1}, \dots, z_d) \in \mathcal{O}^d$ . In what follows, we show Assumption 2 holds when

$$\mathcal{M} = \text{span} \left\{ \phi_{\mu_1}^{\mathbb{K}}(z_1) \cdots \phi_{\mu_{d_1}}^{\mathbb{K}}(z_{d_1}) \right\}_{\mu_1, \dots, \mu_{d_1}=1}^m \quad \text{and} \quad \mathcal{L} = \text{span} \left\{ \phi_{\eta_1}^{\mathbb{K}}(z_{d_1+1}) \cdots \phi_{\eta_{d_2}}^{\mathbb{K}}(z_d) \right\}_{\eta_1, \dots, \eta_{d_2}=1}^{\ell}.$$

**Lemma 2.** *Let  $\mathbb{K}$  be a kernel in the form of (42). Suppose that  $\lambda_k^{\mathbb{K}} \asymp k^{-2\alpha}$ , and that  $A : \mathcal{O}^d \rightarrow \mathbb{R}$  is such that  $\|A\|_{\{\mathcal{H}(\mathbb{K})\}^{\otimes d}} < \infty$ . Then for any two positive integers  $m, \ell \in \mathbb{Z}^+$ , it holds that*

$$\|A - A \times_x \mathcal{P}_{\mathcal{M}} \times_y \mathcal{P}_{\mathcal{L}}\|_{\mathbf{L}_2(\mathcal{O}^d)}^2 \leq C(d_1 m^{-2\alpha} + d_2 \ell^{-2\alpha}) \|A\|_{\{\mathcal{H}(\mathbb{K})\}^{\otimes d}}^2, \quad (46)$$

where  $C$  is some absolute constant. Consequently

$$\|A - A \times_y \mathcal{P}_{\mathcal{L}}\|_{\mathbf{L}_2(\mathcal{O}^d)}^2 \leq C d_2 \ell^{-2\alpha} \|A\|_{\{\mathcal{H}(\mathbb{K})\}^{\otimes d}}^2 \quad \text{and} \quad (47)$$

$$\|A \times_y \mathcal{P}_{\mathcal{L}} - A \times_x \mathcal{P}_{\mathcal{M}} \times_y \mathcal{P}_{\mathcal{L}}\|_{\mathbf{L}_2(\mathcal{O}^d)}^2 \leq C d_1 m^{-2\alpha} \|A\|_{\{\mathcal{H}(\mathbb{K})\}^{\otimes d}}^2. \quad (48)$$

*Proof.* Since  $\lambda_k^{\mathbb{K}} \asymp k^{-2\alpha}$ , without loss of generality, throughout the proof we assume that

$$\lambda_k^{\mathbb{K}} = k^{-2\alpha},$$

as otherwise all of our analysis still holds up to an absolute constant. Observe that

$$\begin{aligned} & (A \times_x \mathcal{P}_{\mathcal{M}} \times_y \mathcal{P}_{\mathcal{L}}) [\phi_{\mu_1}^{\mathbb{K}}, \dots, \phi_{\mu_{d_1}}^{\mathbb{K}}, \phi_{\eta_1}^{\mathbb{K}}, \dots, \phi_{\eta_{d_2}}^{\mathbb{K}}] \\ &= \begin{cases} A[\phi_{\mu_1}^{\mathbb{K}}, \dots, \phi_{\mu_{d_1}}^{\mathbb{K}}, \phi_{\eta_1}^{\mathbb{K}}, \dots, \phi_{\eta_{d_2}}^{\mathbb{K}}], & \text{if } 1 \leq \mu_1, \dots, \mu_{d_1} \leq m \text{ and } 1 \leq \eta_1, \dots, \eta_{d_2} \leq \ell, \\ 0, & \text{otherwise.} \end{cases} \end{aligned}$$

Then

$$\begin{aligned} \|A - A \times_x \mathcal{P}_{\mathcal{M}} \times_y \mathcal{P}_{\mathcal{L}}\|_{\mathbf{L}_2(\mathcal{O}^d)}^2 &= \sum_{\mu_1=m+1}^{\infty} \sum_{\mu_2, \dots, \mu_{d_1}=1}^m \sum_{\eta_1, \dots, \eta_{d_2}=1}^{\ell} (A[\phi_{\mu_1}^{\mathbb{K}}, \dots, \phi_{\mu_{d_1}}^{\mathbb{K}}, \phi_{\eta_1}^{\mathbb{K}}, \dots, \phi_{\eta_{d_2}}^{\mathbb{K}}])^2 \\ &\quad + \dots \\ &\quad + \sum_{\mu_1, \dots, \mu_{d_1}=1}^m \sum_{\eta_1, \dots, \eta_{d_2-1}=1}^{\ell} \sum_{\eta_{d_2}=\ell+1}^{\infty} (A[\phi_{\mu_1}^{\mathbb{K}}, \dots, \phi_{\mu_{d_1}}^{\mathbb{K}}, \phi_{\eta_1}^{\mathbb{K}}, \dots, \phi_{\eta_{d_2}}^{\mathbb{K}}])^2. \end{aligned}$$

Observe that

$$\begin{aligned} & \sum_{\mu_1=m+1}^{\infty} \sum_{\mu_2, \dots, \mu_{d_1}=1}^m \sum_{\eta_1, \dots, \eta_{d_2}=1}^{\ell} (A[\phi_{\mu_1}^{\mathbb{K}}, \dots, \phi_{\mu_{d_1}}^{\mathbb{K}}, \phi_{\eta_1}^{\mathbb{K}}, \dots, \phi_{\eta_{d_2}}^{\mathbb{K}}])^2 \\ & \leq \sum_{\mu_1=m+1}^{\infty} m^{-2\alpha} \mu_1^{2\alpha} \sum_{\mu_2, \dots, \mu_{d_1}=1}^m \sum_{\eta_1, \dots, \eta_{d_2}=1}^{\ell} (A[\phi_{\mu_1}^{\mathbb{K}}, \dots, \phi_{\mu_{d_1}}^{\mathbb{K}}, \phi_{\eta_1}^{\mathbb{K}}, \dots, \phi_{\eta_{d_2}}^{\mathbb{K}}])^2 \\ & \leq m^{-2\alpha} \sum_{\mu_1=m+1}^{\infty} \sum_{\mu_2, \dots, \mu_{d_1}=1}^m \sum_{\eta_1, \dots, \eta_{d_2}=1}^{\ell} \mu_1^{2\alpha} \cdots \mu_{d_1}^{2\alpha} \eta_1^{2\alpha} \cdots \eta_{d_2}^{2\alpha} (A[\phi_{\mu_1}^{\mathbb{K}}, \dots, \phi_{\mu_{d_1}}^{\mathbb{K}}, \phi_{\eta_1}^{\mathbb{K}}, \dots, \phi_{\eta_{d_2}}^{\mathbb{K}}])^2 \\ & \leq m^{-2\alpha} \sum_{\mu_1=1}^{\infty} \sum_{\mu_2, \dots, \mu_{d_1}=1}^{\infty} \sum_{\eta_1, \dots, \eta_{d_2}=1}^{\infty} \mu_1^{2\alpha} \cdots \mu_{d_1}^{2\alpha} \eta_1^{2\alpha} \cdots \eta_{d_2}^{2\alpha} (A[\phi_{\mu_1}^{\mathbb{K}}, \dots, \phi_{\mu_{d_1}}^{\mathbb{K}}, \phi_{\eta_1}^{\mathbb{K}}, \dots, \phi_{\eta_{d_2}}^{\mathbb{K}}])^2 \\ & = m^{-2\alpha} \|A\|_{\{\mathcal{H}(\mathbb{K})\}^{\otimes d}}^2 \end{aligned}$$

where the first inequality holds because  $\mu_1 \geq m + 1 \geq m$  and the last equality follows from (44). Similarly

$$\begin{aligned}
& \sum_{\mu_1, \dots, \mu_{d_1}=1}^m \sum_{\eta_1, \dots, \eta_{d_2-1}=1}^{\ell} \sum_{\eta_{d_2}=\ell+1}^{\infty} (A[\phi_{\mu_1}^{\mathbb{K}}, \dots, \phi_{\mu_{d_1}}^{\mathbb{K}}, \phi_{\eta_1}^{\mathbb{K}}, \dots, \phi_{\eta_{d_2}}^{\mathbb{K}}])^2 \\
& \leq \sum_{\mu_1, \dots, \mu_{d_1}=1}^m \sum_{\eta_1, \dots, \eta_{d_2-1}=1}^{\ell} \sum_{\eta_{d_2}=\ell+1}^{\infty} \ell^{-2\alpha} \eta_{d_2}^{2\alpha} (A[\phi_{\mu_1}^{\mathbb{K}}, \dots, \phi_{\mu_{d_1}}^{\mathbb{K}}, \phi_{\eta_1}^{\mathbb{K}}, \dots, \phi_{\eta_{d_2}}^{\mathbb{K}}])^2 \\
& \leq \ell^{-2\alpha} \sum_{\mu_1, \dots, \mu_{d_1}=1}^m \sum_{\eta_1, \dots, \eta_{d_2-1}=1}^{\ell} \sum_{\eta_{d_2}=\ell+1}^{\infty} \mu_1^{2\alpha} \cdots \mu_{d_1}^{2\alpha} \eta_1^{2\alpha} \cdots \eta_{d_2}^{2\alpha} (A[\phi_{\mu_1}^{\mathbb{K}}, \dots, \phi_{\mu_{d_1}}^{\mathbb{K}}, \phi_{\eta_1}^{\mathbb{K}}, \dots, \phi_{\eta_{d_2}}^{\mathbb{K}}])^2 \\
& \leq \ell^{-2\alpha} \|A\|_{\{\mathcal{H}(\mathbb{K})\}^{\otimes d}}^2,
\end{aligned}$$

where the first inequality holds because  $\eta_{d_2} \geq \ell + 1 \geq \ell$  and the last inequality follows from (44). Thus (46) follows immediately.

For (47), note that when  $m = \infty$ ,  $\mathcal{M} = \mathbf{L}_2(\mathcal{O}^{d_1})$ . In this case  $\mathcal{P}_{\mathcal{M}}$  becomes the identity operator and

$$A \times_x \mathcal{P}_{\mathcal{M}} \times_y \mathcal{P}_{\mathcal{L}} = A \times_y \mathcal{P}_{\mathcal{L}}.$$

Therefore (47) follows from (46) by taking  $m = \infty$ .

For (48), similar to (47), we have that

$$\|A - A \times_x \mathcal{P}_{\mathcal{M}}\|_{\mathbf{L}_2(\mathcal{O}^d)}^2 \leq Cd_1 m^{-2\alpha} \|A\|_{\{\mathcal{H}(\mathbb{K})\}^{\otimes d}}^2.$$

It follows that

$$\|A \times_y \mathcal{P}_{\mathcal{L}} - A \times_x \mathcal{P}_{\mathcal{M}} \times_y \mathcal{P}_{\mathcal{L}}\|_{\mathbf{L}_2(\mathcal{O}^d)}^2 \leq \|A - A \times_x \mathcal{P}_{\mathcal{M}}\|_{\mathbf{L}_2(\mathcal{O}^d)}^2 \|\mathcal{P}_{\mathcal{L}}\|_{\text{op}}^2 \leq Cd_1 m^{-2\alpha} \|A\|_{\{\mathcal{H}(\mathbb{K})\}^{\otimes d}}^2,$$

where last inequality follows from the fact that  $\|\mathcal{P}_{\mathcal{L}}\|_{\text{op}} \leq 1$ .  $\square$

## B.2 Legendre polynomial basis

Legendre polynomials is a well-known classical orthonormal polynomial system in  $\mathbf{L}_2([-1, 1])$ .

We can define the Legendre polynomials in the following inductive way. Let  $p_0 = 1$  and suppose  $\{p_k\}_{k=1}^{n-1}$  are defined. Let  $p_n : [-1, 1] \rightarrow \mathbb{R}$  be a polynomial of degree  $n$  such that

- $\|p_n\|_{\mathbf{L}_2([-1,1])} = 1$ , and
- $\int_{-1}^1 p_n(x) p_k(x) dx = 0$  for all  $0 \leq k \leq n-1$ .

As a quick example, we have that

$$p_0(x) = 1, \quad p_1(x) = \sqrt{\frac{3}{2}}x, \quad \text{and} \quad p_2(x) = \sqrt{\frac{5}{3}} \frac{3x^2 - 1}{2}.$$

Let  $q_k(x) = \sqrt{2} p_k(2x - 1)$ . Then  $\{q_k\}_{k=0}^{\infty}$  are the orthonormal polynomial system in  $\mathbf{L}_2([0, 1])$ . In this subsection, we show that Assumption 2 holds when  $\{\phi_k^{\mathbb{S}}\}_{k=1}^{\infty}$  in (3) is chosen to be  $\{q_k\}_{k=0}^{\infty}$ . More precisely, let

$$\mathbb{S}_n = \text{Span}\{q_k\}_{k=0}^n$$

and  $\mathcal{P}_{\mathbb{S}_n}$  denote the projection operator from  $\mathbf{L}_2([0, 1])$  to  $\mathbb{S}_n$ . Then  $\mathbb{S}_n$  is the subspace of polynomials of degree at most  $n$ . In addition, for any  $f \in \mathbf{L}_2([0, 1])$ ,  $\mathcal{P}_{\mathbb{S}_n}(f)$  is the best  $n$ -degree polynomial approximation of  $f$  in the sense that

$$\|\mathcal{P}_{\mathbb{S}_n(z)}(f) - f\|_{\mathbf{L}_2([0,1])} = \min_{g \in \mathbb{S}_n} \|g - f\|_{\mathbf{L}_2([0,1])}. \quad (49)$$

We begin with a well-known polynomial approximation result. For  $\alpha \in \mathbb{Z}^+$ , denote  $C^\alpha([0, 1])$  to be the class of functions that are  $\alpha$  times continuously differentiable.

**Theorem 4.** *Suppose  $f \in C^\alpha([0, 1])$ . Then for any  $n \in \mathbb{Z}^+$ , there exists a polynomial  $p_{2n}(f)$  of degree  $2n$  such that*

$$\|f - p_{2n}(f)\|_{\mathbf{L}_2([0,1])}^2 \leq Cn^{-2\alpha} \|f^{(\alpha)}\|_{\mathbf{L}_2([0,1])}^2,$$

where  $C$  is an absolute constant.

*Proof.* This is Theorem 1.2 of [Xu \(2018\)](#). □

Therefore by (49) and Theorem 4,

$$\|\mathcal{P}_{\mathbb{S}_n(z)}(f) - f\|_{\mathbf{L}_2([0,1])}^2 \leq \|f - p_{[n/2]}(f)\|_{\mathbf{L}_2([0,1])}^2 \leq C'n^{-2\alpha} \|f^{(\alpha)}\|_{\mathbf{L}_2([0,1])}^2. \quad (50)$$

Let  $z = (z_1, \dots, z_d) \in \mathbb{R}^d$  and let  $\mathbb{S}_n(z_j)$  denote the linear space spanned by polynomials of  $z_j$  of degree at most  $n$ .

**Corollary 2.** *Suppose  $B(z_1, \dots, z_d) \in C^\alpha([0, 1]^d)$ . Then for any  $1 \leq p \leq d$ ,*

$$\|B - B \times_p \mathcal{P}_{\mathbb{S}_n(z_p)}\|_{\mathbf{L}_2([0,1]^d)} \leq Cn^{-\alpha} \|B\|_{W_2^\alpha([0,1]^d)}.$$

*Proof.* It suffices to consider  $p = 1$ . For any fixed  $(z_2, \dots, z_d)$ ,  $B(\cdot, z_2, \dots, z_d) \in C^\alpha([0, 1])$ . Therefore by (50),

$$\int \left\{ B(z_1, z_2, \dots, z_d) - \mathcal{P}_{\mathbb{S}_n(z_1)}(B(z_1, z_2, \dots, z_d)) \right\}^2 dz_1 \leq Cn^{-2\alpha} \int \left\{ \frac{\partial^\alpha}{\partial^\alpha z_1} B(z_1, z_2, \dots, z_d) \right\}^2 dz_1.$$

Therefore

$$\begin{aligned} & \int \cdots \int \left\{ B(z_1, z_2, \dots, z_d) - \mathcal{P}_{\mathbb{S}_n(z_1)}(B(z_1, z_2, \dots, z_d)) \right\}^2 dz_1 dz_2 \cdots dz_d \\ & \leq \int \cdots \int Cn^{-2\alpha} \int \left\{ \frac{\partial^\alpha}{\partial^\alpha z_1} B(z_1, z_2, \dots, z_d) \right\}^2 dz_1 dz_2 \cdots dz_d. \end{aligned}$$

The desired result follows from the observation that

$$\mathcal{P}_{\mathbb{S}_n(z_1)}(B(z_1, z_2, \dots, z_d)) = (B \times_1 \mathcal{P}_{\mathbb{S}_n(z_1)})(z_1, z_2, \dots, z_d)$$

and that  $\int \cdots \int \left\{ \frac{\partial^\alpha}{\partial^\alpha z_1} B(z_1, z_2, \dots, z_d) \right\}^2 dz_1 \cdots dz_d \leq \|B\|_{W_2^\alpha([0,1]^d)}^2$ . □

**Lemma 3.** *Under the same conditions as in Corollary 2, it holds that*

$$\mathcal{P}_{\mathbb{S}_n(z_1)}(B(z_1, z_2, \dots, z_d)) = (B \times_1 \mathcal{P}_{\mathbb{S}_n(z_1)})(z_1, z_2, \dots, z_d). \quad (51)$$

*Proof.* Note that  $\mathcal{P}_{\mathbb{S}_n(z_1)}$  is a projection operator. So for any  $f, g \in \mathbf{L}_2([0, 1])$ ,

$$\int_0^1 \mathcal{P}_{\mathbb{S}_n(z_1)}(f(z_1))g(z_1)dz_1 = \langle \mathcal{P}_{\mathbb{S}_n(z_1)}(f), g \rangle = \langle f, \mathcal{P}_{\mathbb{S}_n(z_1)}(g) \rangle = \int_0^1 f(z_1)\mathcal{P}_{\mathbb{S}_n(z_1)}(g(z_1))dz_1 \quad (52)$$

Given  $(z_2, \dots, z_d)$ ,  $B(\cdot, z_2, \dots, z_d) \in C^\alpha([0, 1])$  and therefore  $\mathcal{P}_{\mathbb{S}_n(z_1)}(B(z_1, z_2, \dots, z_d))$  is well-defined and is a function mapping from  $[0, 1]^d$  to  $\mathbb{R}$ . To show that (51), it suffices to observe that for any test functions  $\{u_j(z_j)\}_{j=1}^d \in \mathbf{L}_2([0, 1])$ ,

$$\begin{aligned} & \mathcal{P}_{\mathbb{S}_n(z_1)}(B(z_1, z_2, \dots, z_d))[u_1(z_1), \dots, u_d(z_d)] \\ &= \int_0^1 \cdots \int_0^1 \mathcal{P}_{\mathbb{S}_n(z_1)}(B(z_1, z_2, \dots, z_d))u_1(z_1) \cdots u_d(z_d)dz_1 \cdots dz_d \\ &= \int_0^1 \cdots \int_0^1 \left( \int_0^1 \mathcal{P}_{\mathbb{S}_n(z_1)}(B(z_1, z_2, \dots, z_d))u_1(z_1)dz_1 \right) u_2(z_2) \cdots u_d(z_d)dz_2 \cdots dz_d \\ &= \int_0^1 \cdots \int_0^1 \left( \int_0^1 B(z_1, z_2, \dots, z_d)\mathcal{P}_{\mathbb{S}_n(z_1)}(u_1(z_1))dz_1 \right) u_2(z_2) \cdots u_d(z_d)dz_2 \cdots dz_d \\ &= (B \times_1 \mathcal{P}_{\mathbb{S}_n(z_1)})[u_1(z_1), \dots, u_d(z_d)]. \end{aligned}$$

□

In what follows, we present a polynomial approximation theory in multidimensions.

**Lemma 4.** For  $j \in [1, \dots, d]$ , let  $\mathbb{S}_{n_j}(z_j)$  denote the linear space spanned by polynomials of  $z_j$  of degree  $n_j$  and let  $\mathcal{P}_{\mathbb{S}_{n_j}(z_j)}$  be the corresponding projection operator. Then for any  $B \in W_2^\alpha([0, 1]^d)$ , it holds that

$$\|B - B \times_1 \mathcal{P}_{\mathbb{S}_{n_1}(z_1)} \cdots \times_d \mathcal{P}_{\mathbb{S}_{n_d}(z_d)}\|_{\mathbf{L}_2([0, 1]^d)} \leq C \sum_{j=1}^d n_j^{-\alpha} \|B\|_{W_2^\alpha([0, 1]^d)}. \quad (53)$$

*Proof.* Since  $C^\alpha([0, 1]^d)$  is dense in  $W_2^\alpha([0, 1]^d)$ , it suffices to show (53) for all  $f \in C^\alpha([0, 1]^d)$ . We proceed by induction. The base case

$$\|B - B \times_1 \mathcal{P}_{\mathbb{S}_{n_1}(z_1)}\|_{\mathbf{L}_2([0, 1]^d)} \leq C n_1^{-\alpha} \|B\|_{W_2^\alpha([0, 1]^d)}$$

is a direct consequence of Corollary 2. Suppose by induction, the following inequality holds for  $p$ ,

$$\|B - B \times_1 \mathcal{P}_{\mathbb{S}_{n_1}(z_1)} \cdots \times_p \mathcal{P}_{\mathbb{S}_{n_p}(z_p)}\|_{\mathbf{L}_2([0, 1]^d)} \leq C \sum_{j=1}^p n_j^{-\alpha} \|B\|_{W_2^\alpha([0, 1]^d)}. \quad (54)$$

Then

$$\begin{aligned} & \|B - B \times_1 \mathcal{P}_{\mathbb{S}_{n_1}(z_1)} \cdots \times_p \mathcal{P}_{\mathbb{S}_{n_p}(z_p)} \times_{p+1} \mathcal{P}_{\mathbb{S}_{n_{p+1}}(z_{p+1})}\|_{\mathbf{L}_2([0, 1]^d)} \\ & \leq \|B \times_1 \mathcal{P}_{\mathbb{S}_{n_1}(z_1)} \cdots \times_p \mathcal{P}_{\mathbb{S}_{n_p}(z_p)} \times_{p+1} \mathcal{P}_{\mathbb{S}_{n_{p+1}}(z_{p+1})} - B \times_1 \mathcal{P}_{\mathbb{S}_{n_1}(z_1)} \cdots \times_p \mathcal{P}_{\mathbb{S}_{n_p}(z_p)}\|_{\mathbf{L}_2([0, 1]^d)} \\ & \quad + \|B - B \times_1 \mathcal{P}_{\mathbb{S}_{n_1}(z_1)} \cdots \times_p \mathcal{P}_{\mathbb{S}_{n_p}(z_p)}\|_{\mathbf{L}_2([0, 1]^d)}. \end{aligned}$$

The desired result follows from (54) and the observation that  $\|\mathcal{P}_{\mathbb{S}_{n_j}(z_j)}\|_{\text{op}} \leq 1$  for all  $j$ , and therefore

$$\begin{aligned} & \|B \times_1 \mathcal{P}_{\mathbb{S}_{n_1}(z_1)} \cdots \times_p \mathcal{P}_{\mathbb{S}_{n_p}(z_p)} \times_{p+1} \mathcal{P}_{\mathbb{S}_{n_{p+1}}(z_{p+1})} - B \times_1 \mathcal{P}_{\mathbb{S}_{n_1}(z_1)} \cdots \times_p \mathcal{P}_{\mathbb{S}_{n_p}(z_p)}\|_{\mathbf{L}_2([0,1]^d)} \\ & \leq \|B \times_{p+1} \mathcal{P}_{\mathbb{S}_{n_{p+1}}(z_{p+1})} - B\|_{\mathbf{L}_2([0,1]^d)} \|\mathcal{P}_{\mathbb{S}_{n_1}(z_1)}\|_{\text{op}} \cdots \|\mathcal{P}_{\mathbb{S}_{n_p}(z_p)}\|_{\text{op}} \\ & \leq C n_{p+1}^{-\alpha} \|B\|_{W_2^\alpha([0,1]^d)}, \end{aligned}$$

where the last inequality follows from Corollary 2.  $\square$

Note that Lemma 4 directly implies that Assumption 2 holds when

$$\mathcal{M} = \mathbb{S}_m(z_1) \otimes \cdots \otimes \mathbb{S}_m(z_{d_1}) \quad \text{and} \quad \mathcal{L} = \mathbb{S}_\ell(z_{d_1+1}) \otimes \cdots \otimes \mathbb{S}_\ell(z_d).$$

This is summarized in the following lemma.

**Lemma 5.** *Suppose  $\|A\|_{W_2^\alpha([0,1]^d)} < \infty$ . Then for  $1 \leq m \leq \infty$  and  $1 \leq \ell \leq \infty$ ,*

$$\|A - A \times_x \mathcal{P}_{\mathcal{M}} \times_y \mathcal{P}_{\mathcal{L}}\|_{\mathbf{L}_2([0,1]^d)}^2 = O(m^{-2\alpha} + \ell^{-2\alpha}) \quad (55)$$

$$\|A - A \times_y \mathcal{P}_{\mathcal{L}}\|_{\mathbf{L}_2([0,1]^d)}^2 = O(\ell^{-2\alpha}) \quad \text{and} \quad (56)$$

$$\|A \times_y \mathcal{P}_{\mathcal{L}} - A \times_x \mathcal{P}_{\mathcal{M}} \times_y \mathcal{P}_{\mathcal{L}}\|_{\mathbf{L}_2([0,1]^d)}^2 = O(m^{-2\alpha}). \quad (57)$$

*Proof.* For (55), by Lemma 4,

$$\begin{aligned} \|A - A \times_x \mathcal{P}_{\mathcal{M}} \times_y \mathcal{P}_{\mathcal{L}}\|_{\mathbf{L}_2([0,1]^d)} & \leq C(d_1(m - \alpha - 1)^{-\alpha} + d_2(\ell - \alpha - 1)^{-\alpha}) \|A\|_{W_2^\alpha([0,1]^d)} \\ & = O(m^{-\alpha} + \ell^{-\alpha}), \end{aligned}$$

where the equality follows from the fact that  $\alpha$ ,  $d_1$  and  $d_2$  are constants.

For (56), note that when  $m = \infty$ ,  $\mathcal{M} = \mathbf{L}_2([0,1]^{d_1})$ . In this case  $\mathcal{P}_{\mathcal{M}}$  becomes the identity operator and

$$A \times_x \mathcal{P}_{\mathcal{M}} \times_y \mathcal{P}_{\mathcal{L}} = A \times_y \mathcal{P}_{\mathcal{L}}.$$

Therefore (56) follows from (55) by taking  $m = \infty$ .

For (57), similar to (56), we have that

$$\|A - A \times_x \mathcal{P}_{\mathcal{M}}\|_{\mathbf{L}_2([0,1]^d)}^2 = O(m^{-2\alpha}).$$

It follows that

$$\|A \times_y \mathcal{P}_{\mathcal{L}} - A \times_x \mathcal{P}_{\mathcal{M}} \times_y \mathcal{P}_{\mathcal{L}}\|_{\mathbf{L}_2([0,1]^d)}^2 \leq \|A - A \times_x \mathcal{P}_{\mathcal{M}}\|_{\mathbf{L}_2([0,1]^d)}^2 \|\mathcal{P}_{\mathcal{L}}\|_{\text{op}}^2 = O(m^{-2\alpha}),$$

where last inequality follows from the fact that  $\|\mathcal{P}_{\mathcal{L}}\|_{\text{op}} \leq 1$ .  $\square$

### B.3 Spline basis

Let  $\alpha \in \mathbb{Z}^+$  be given and  $\{\xi_k\}_{k=1}^n \subset [0, 1]$  be a collection of grid points such that

$$\xi_k = \frac{k}{n}.$$

Denote  $\mathbb{S}_{n,\alpha}(x)$  the subspace in  $\mathbf{L}_2([0, 1])$  spanned by the spline functions being peicewise polynomials defined on  $\{\xi_k\}_{k=1}^n$  of degree  $\alpha$ . Specifically

$$\mathbb{S}_{n,\alpha}(x) = \{\beta_0 + \beta_1 b_1(x) + \dots + \beta_{\alpha+n} b_{\alpha+n}(x) : \{\beta_k\}_{k=0}^{\alpha+n} \subset \mathbb{R}\},$$

where

$$b_1(x) = x^1, \dots, b_\alpha(x) = x^\alpha, b_{k+\alpha}(x) = (x - \xi_k)_+^\alpha \text{ for } k = 1, \dots, n,$$

and

$$(x - \xi_k)_+^\alpha = \begin{cases} (x - \xi_k)^\alpha, & \text{if } x \geq \xi_k; \\ 0, & \text{if } x < \xi_k. \end{cases}$$

Let  $\{\phi_k^{n,\alpha}(x)\}_{k=1}^{n+\alpha+1}$  be the  $\mathbf{L}_2([0, 1])$  sub-basis functions spanning  $\mathbb{S}_{n,\alpha}(x)$ . In this section, we show that Assumption 2 holds when

$$\begin{aligned} \mathcal{M} &= \mathbb{S}_{m-\alpha-1,\alpha}(z_1) \otimes \dots \otimes \mathbb{S}_{m-\alpha-1,\alpha}(z_{d_1}) = \text{span} \left\{ \phi_{\mu_1}^{m-\alpha-1,\alpha}(z_1) \dots \phi_{\mu_{d_1}}^{m-\alpha-1,\alpha}(z_{d_1}) \right\}_{\mu_1, \dots, \mu_{d_1}=1}^m, \quad \text{and} \\ \mathcal{L} &= \mathbb{S}_{\ell-\alpha-1,\alpha}(z_{d_1+1}) \otimes \dots \otimes \mathbb{S}_{\ell-\alpha-1,\alpha}(z_d) = \text{span} \left\{ \phi_{\eta_1}^{\ell-\alpha-1,\alpha}(z_{d_1+1}) \dots \phi_{\eta_{d_2}}^{\ell-\alpha-1,\alpha}(z_d) \right\}_{\eta_1, \dots, \eta_{d_2}=1}^\ell. \end{aligned}$$

where  $m$  and  $\ell$  are positive integers such that  $m > \alpha + 1$  and  $\ell > \alpha + 1$ . We begin with a spline space approximation theorem for multivariate functions.

**Lemma 6.** *Suppose  $\|A\|_{W_2^\alpha([0,1]^d)} < \infty$ . Suppose in addition  $\{n_j\}_{j=1}^d$  is a collection positive integer strictly greater than  $\alpha + 1$ . Then*

$$\|A - A \times_1 \mathcal{P}_{\mathbb{S}_{n_1-\alpha-1,\alpha}}(z_1) \dots \times_d \mathcal{P}_{\mathbb{S}_{n_d-\alpha-1,\alpha}}(z_d)\| \leq C \sum_{j=1}^d (n_j - \alpha - 1)^{-\alpha} \|A\|_{W_2^\alpha([0,1]^d)}$$

*Proof.* This is Example 13 on page 26 of Sande et al. (2020).  $\square$

In the following lemma, we justify Assumption 2 when  $\mathcal{M} = \mathbb{S}_{m-\alpha-1,\alpha}(z_1) \otimes \dots \otimes \mathbb{S}_{m-\alpha-1,\alpha}(z_{d_1})$  and  $\mathcal{L} = \mathbb{S}_{\ell-\alpha-1,\alpha}(z_{d_1+1}) \otimes \dots \otimes \mathbb{S}_{\ell-\alpha-1,\alpha}(z_d)$ .

**Lemma 7.** *Suppose  $\|A\|_{W_2^\alpha([0,1]^d)} < \infty$  where  $\alpha \in \mathbb{Z}^+$  is a fixed constant. Then for  $1 + \alpha \leq m \leq \infty$  and  $1 + \alpha \leq \ell \leq \infty$ ,*

$$\|A - A \times_x \mathcal{P}_{\mathcal{M}} \times_y \mathcal{P}_{\mathcal{L}}\|_{\mathcal{L}_2([0,1]^d)}^2 = O(m^{-2\alpha} + \ell^{-2\alpha}) \quad (58)$$

$$\|A - A \times_y \mathcal{P}_{\mathcal{L}}\|_{\mathcal{L}_2([0,1]^d)}^2 = O(\ell^{-2\alpha}) \quad \text{and} \quad (59)$$

$$\|A \times_y \mathcal{P}_{\mathcal{L}} - A \times_x \mathcal{P}_{\mathcal{M}} \times_y \mathcal{P}_{\mathcal{L}}\|_{\mathcal{L}_2([0,1]^d)}^2 = O(m^{-2\alpha}). \quad (60)$$

*Proof.* For (58), by Lemma 6,

$$\begin{aligned} \|A - A \times_x \mathcal{P}_{\mathcal{M}} \times_y \mathcal{P}_{\mathcal{L}}\|_{\mathcal{L}_2([0,1]^d)} &\leq C(d_1(m - \alpha - 1)^{-\alpha} + d_2(\ell - \alpha - 1)^{-\alpha}) \|A\|_{W_2^\alpha([0,1]^d)} \\ &= O(m^{-\alpha} + \ell^{-\alpha}), \end{aligned}$$

where the equality follows from the fact that  $\alpha$ ,  $d_1$  and  $d_2$  are constants.

For (59), note that when  $m = \infty$ ,  $\mathcal{M} = \mathbf{L}_2([0, 1]^{d_1})$ . In this case  $\mathcal{P}_{\mathcal{M}}$  becomes the identity operator and

$$A \times_x \mathcal{P}_{\mathcal{M}} \times_y \mathcal{P}_{\mathcal{L}} = A \times_y \mathcal{P}_{\mathcal{L}}.$$

Therefore (59) follows from (58) by taking  $m = \infty$ .

For (60), similar to (59), we have that

$$\|A - A \times_x \mathcal{P}_{\mathcal{M}}\|_{\mathbf{L}_2([0,1]^d)}^2 = O(m^{-2\alpha}).$$

It follows that

$$\|A \times_y \mathcal{P}_{\mathcal{L}} - A \times_x \mathcal{P}_{\mathcal{M}} \times_y \mathcal{P}_{\mathcal{L}}\|_{\mathbf{L}_2([0,1]^d)}^2 \leq \|A - A \times_x \mathcal{P}_{\mathcal{M}}\|_{\mathbf{L}_2([0,1]^d)}^2 \|\mathcal{P}_{\mathcal{L}}\|_{\text{op}}^2 = O(m^{-2\alpha}),$$

where last inequality follows from the fact that  $\|\mathcal{P}_{\mathcal{L}}\|_{\text{op}} \leq 1$ .  $\square$

## C Proofs of the main results

### C.1 Proofs related to Theorem 1

*Proof of Theorem 1.* By Lemma 8,  $\mathcal{P}_x^*$  is the projection operator of  $\text{Range}_x(A^* \times_y \mathcal{P}_{\mathcal{L}})$ . By Corollary 3,

$$\|(\widehat{A} - A^*) \times_x \mathcal{P}_{\mathcal{M}} \times_y \mathcal{P}_{\mathcal{L}}\|_{\text{op}} = O_{\mathbb{P}} \left( \sqrt{\frac{m^{d_1} + \ell^{d_2}}{N}} \right). \quad (61)$$

Supposed this good event holds. Observe that

$$\begin{aligned} & \|\widehat{A} \times_x \mathcal{P}_{\mathcal{M}} \times_y \mathcal{P}_{\mathcal{L}} - A^* \times_y \mathcal{P}_{\mathcal{L}}\|_{\text{op}} \\ & \leq \|A^* \times_x \mathcal{P}_{\mathcal{M}} \times_y \mathcal{P}_{\mathcal{L}} - A^* \times_y \mathcal{P}_{\mathcal{L}}\|_{\text{op}} + \|\widehat{A} \times_x \mathcal{P}_{\mathcal{M}} \times_y \mathcal{P}_{\mathcal{L}} - A^* \times_x \mathcal{P}_{\mathcal{M}} \times_y \mathcal{P}_{\mathcal{L}}\|_{\text{op}} \\ & \leq O_{\mathbb{P}} \left( m^{-\alpha} + \sqrt{\frac{m^{d_1} + \ell^{d_2}}{N}} \right), \end{aligned} \quad (62)$$

where the last inequality follows from Assumption 2 and (61). In addition by (64) in Lemma 8, the minimal eigenvalue of  $A^* \times_y \mathcal{P}_{\mathcal{L}}$  is lower bounded by  $|\sigma_r|/2$ .

The rank of  $A^* \times_y \mathcal{P}_{\mathcal{L}}$  is bounded by the dimensionality of  $\dim(\mathcal{L}) = \ell^{d_2}$ , so the rank of  $A^* \times_y \mathcal{P}_{\mathcal{L}}$  is finite. Similarly,  $\widehat{A} \times_x \mathcal{P}_{\mathcal{M}} \times_y \mathcal{P}_{\mathcal{L}}$  has finite rank. Corollary 4 in Appendix F.2 implies that

$$\|\widehat{\mathcal{P}}_x - \mathcal{P}_x^*\|_{\text{op}} \leq \frac{\sqrt{2} \|\widehat{A} \times_x \mathcal{P}_{\mathcal{M}} \times_y \mathcal{P}_{\mathcal{L}} - A^* \times_y \mathcal{P}_{\mathcal{L}}\|_{\text{op}}}{\sigma_r/2 - \|\widehat{A} \times_x \mathcal{P}_{\mathcal{M}} \times_y \mathcal{P}_{\mathcal{L}} - A^* \times_y \mathcal{P}_{\mathcal{L}}\|_{\text{op}}}.$$

By (62), we have that  $\|\widehat{A} \times_x \mathcal{P}_{\mathcal{M}} \times_y \mathcal{P}_{\mathcal{L}} - A^* \times_y \mathcal{P}_{\mathcal{L}}\|_{\text{op}} = O_{\mathbb{P}} \left( m^{-\alpha} + \sqrt{\frac{m^{d_1} + \ell^{d_2}}{N}} \right)$ , and by condition (21) in Theorem 1, we have that  $\sigma_r/2 - \|\widehat{A} \times_x \mathcal{P}_{\mathcal{M}} \times_y \mathcal{P}_{\mathcal{L}} - A^* \times_y \mathcal{P}_{\mathcal{L}}\|_{\text{op}} \geq \sigma_r/4$ . The desired result follows immediately:

$$\|\widehat{\mathcal{P}}_x - \mathcal{P}_x^*\|_{\text{op}}^2 = O_{\mathbb{P}} \left\{ \sigma_r^{-2} \left( \frac{m^{d_1} + \ell^{d_2}}{N} + m^{-2\alpha} \right) \right\}. \quad (63)$$

$\square$

**Lemma 8.** *Suppose Assumption 1 and 2 hold. If  $\sigma_r > C_L \ell^{-\alpha}$  for sufficiently large constant  $C_L$ , then*

$$\text{Range}_x(A^* \times_y \mathcal{P}_{\mathcal{L}}) = \text{Range}_x(A^*).$$

*Proof of Lemma 8.* By Lemma 15 in Appendix F and Assumption 2, the singular values  $\{\sigma_\rho(A^* \times_y \mathcal{P}_{\mathcal{L}})\}_{\rho=1}^\infty$  of the operator  $A^* \times_y \mathcal{P}_{\mathcal{L}}$  satisfies

$$|\sigma_\rho - \sigma_\rho(A^* \times_y \mathcal{P}_{\mathcal{L}})| \leq \|A^* - A^* \times_y \mathcal{P}_{\mathcal{L}}\|_F = O(\ell^{-\alpha}) \text{ for all } 1 \leq \rho < \infty.$$

As a result if  $\sigma_r > C_L \ell^{-\alpha}$  for sufficiently large constant  $C_L$ , then

$$\sigma_1(A^* \times_y \mathcal{P}_{\mathcal{L}}) \geq \dots \geq \sigma_r(A^* \times_y \mathcal{P}_{\mathcal{L}}) \geq \sigma_r - \|A^* - A^* \times_y \mathcal{P}_{\mathcal{L}}\|_F > \sigma_r/2. \quad (64)$$

Since by construction,  $\text{Range}_x(A^* \times_y \mathcal{P}_{\mathcal{L}}) \subset \text{Range}_x(A^*)$ , and the leading  $r$  singular values of  $A^* \times_y \mathcal{P}_{\mathcal{L}}$  is positive, it follows that the rank of  $\text{Range}_x(A^* \times_y \mathcal{P}_{\mathcal{L}})$  is  $r$ . So  $\text{Range}_x(A^* \times_y \mathcal{P}_{\mathcal{L}}) = \text{Range}_x(A^*)$ .  $\square$

**Lemma 9.** *Suppose  $\widehat{A}$  and  $A^*$  are defined as in Theorem 2. Let  $d_1, d_2 \in \mathbb{Z}^+$  be such that  $d_1 + d_2 = d$ . Suppose  $\{\phi_k^{\mathbb{S}}\}_{k=1}^\infty$  be a collection of  $\mathbf{L}_2([0, 1])$  basis such that  $\|\phi_k^{\mathbb{S}}\|_\infty \leq C_{\mathbb{S}}$ . For positive integers  $m$  and  $\ell$ , denote*

$$\mathcal{M} = \text{span} \left\{ \phi_{\mu_1}^{\mathbb{S}}(z_1) \cdots \phi_{\mu_{d_1}}^{\mathbb{S}}(z_{d_1}) \right\}_{\mu_1, \dots, \mu_{d_1}=1}^m \quad \text{and} \quad \mathcal{L} = \text{span} \left\{ \phi_{\eta_1}^{\mathbb{S}}(z_{d_1+1}) \cdots \phi_{\eta_{d_2}}^{\mathbb{S}}(z_d) \right\}_{\eta_1, \dots, \eta_{d_2}=1}^\ell. \quad (65)$$

Then it holds that

$$\|(\widehat{A} - A^*) \times_x \mathcal{P}_{\mathcal{M}} \times_y \mathcal{P}_{\mathcal{L}}\|_{\text{op}} = O_{\mathbb{P}} \left( \sqrt{\frac{m^{d_1} + \ell^{d_2}}{N}} + \frac{m^{3d_1/2} \ell^{d_2/2} + m^{d_1/2} \ell^{3d_2/2}}{N} \right).$$

*Proof.* Denote

$$x = (z_1, \dots, z_{d_1}) \quad \text{and} \quad y = (z_{d_1+1}, \dots, z_d).$$

For positive integers  $m$  and  $\ell$ , by ordering the indexes  $(\mu_1, \dots, \mu_{d_1})$  and  $(\eta_1, \dots, \eta_{d_2})$  in (65), we can also write

$$\mathcal{M} = \text{span}\{\Phi_\mu(x)\}_{\mu=1}^{m^{d_1}} \quad \text{and} \quad \mathcal{L} = \text{span}\{\Psi_\eta(y)\}_{\eta=1}^{\ell^{d_2}}. \quad (66)$$

Note that  $\widehat{A} \times_x \mathcal{P}_{\mathcal{M}} \times_y \mathcal{P}_{\mathcal{L}}$  and  $A^* \times_x \mathcal{P}_{\mathcal{M}} \times_y \mathcal{P}_{\mathcal{L}}$  are both zero outside the subspace  $\mathcal{M} \otimes \mathcal{L}$ . Recall  $\{Z_i\}_{i=1}^N \subset [0, 1]^d$  are independently samples forming  $\widehat{A}$ . Let  $\widehat{B}$  and  $B^*$  be two matrices in  $\mathbb{R}^{m^{d_1} \times \ell^{d_2}}$  such that

$$\widehat{B}_{\mu, \eta} = \widehat{A}[\Phi_\mu, \Psi_\eta] = \frac{1}{N} \sum_{i=1}^N \Phi_\mu(X_i) \Psi_\eta(Y_i) \quad \text{and} \quad B_{\mu, \eta}^* = A^*[\Phi_\mu, \Psi_\eta] = \mathbb{E}(\widehat{A}[\Phi_\mu, \Psi_\eta]),$$

where  $X_i = (Z_{i,1}, \dots, Z_{i,d_1}) \in \mathbb{R}^{d_1}$  and  $Y_i = (Z_{i,d_1+1}, \dots, Z_{i,d}) \in \mathbb{R}^{d_2}$ . Note that

$$\|\widehat{B} - B^*\|_{\text{op}} = \|(\widehat{A} - A^*) \times_x \mathcal{P}_{\mathcal{M}} \times_y \mathcal{P}_{\mathcal{L}}\|_{\text{op}}. \quad (67)$$

**Step 1.** Let  $v = (v_1, \dots, v_{m^{d_1}}) \in \mathbb{R}^{m^{d_1}}$  and suppose that  $\|v\|_2 = 1$ . Then by orthonormality of  $\{\Phi_\mu(x)\}_{\mu=1}^{m^{d_1}}$  in  $\mathbf{L}_2([0, 1]^{d_1})$  it follows that

$$\left\| \sum_{\mu=1}^{m^{d_1}} v_\mu \Phi_\mu \right\|_{\mathbf{L}_2([0, 1]^{d_1})}^2 = 1.$$

In addition, since

$$\|\phi_{\mu_1}^{\mathbb{S}}(z_1) \cdots \phi_{\mu_{d_1}}^{\mathbb{S}}(z_{d_1})\|_{\infty} \leq \prod_{j=1}^{d_1} \|\phi_{\mu_j}^{\mathbb{S}}\|_{\infty} \leq C_{\mathbb{S}}^{d_1},$$

it follows that  $\|\Phi_{\mu}\|_{\infty} \leq C_{\mathbb{S}}^p$  for all  $1 \leq \mu \leq m^{d_1}$  and

$$\left\| \sum_{\mu=1}^{m^{d_1}} v_{\mu} \Phi_{\mu} \right\|_{\infty} \leq \sqrt{\sum_{\mu=1}^{m^{d_1}} v_{\mu}^2} \sqrt{\sum_{\mu=1}^{m^{d_1}} \|\Phi_{\mu}\|_{\infty}^2} = O(\sqrt{m^{d_1}}).$$

**Step 2.** Let  $w = (w_1, \dots, w_{\ell^{d_2}}) \in \mathbb{R}^{\ell^{d_2}}$  and suppose that  $\|w\|_2 = 1$ . Then by orthonormality of  $\{\Psi_{\eta}(y)\}_{\eta=1}^{\ell^{d_2}}$  in  $\mathbf{L}_2([0, 1]^{d_2})$ ,

$$\left\| \sum_{\eta=1}^{\ell^{d_2}} w_{\eta} \Psi_{\eta} \right\|_{\mathbf{L}_2([0, 1]^{d_2})}^2 = 1.$$

In addition, since

$$\|\phi_{\eta_1}^{\mathbb{S}}(z_{d_1+1}) \cdots \phi_{\eta_{d_2}}^{\mathbb{S}}(z_d)\|_{\infty} \leq \prod_{j=1}^{d_2} \|\phi_{\eta_j}^{\mathbb{S}}\|_{\infty} \leq C_{\mathbb{S}}^{d_2},$$

it follows that  $\|\Psi_{\eta}\|_{\infty} \leq C_{\mathbb{S}}^{d_2}$ . Therefore

$$\left\| \sum_{\eta=1}^{\ell^{d_2}} w_{\eta} \Psi_{\eta} \right\|_{\infty} \leq \sqrt{\sum_{\eta=1}^{\ell^{d_2}} w_{\eta}^2} \sqrt{\sum_{\eta=1}^{\ell^{d_2}} \|\Psi_{\eta}\|_{\infty}^2} = O(\sqrt{\ell^{d_2}}).$$

**Step 3.** For fixed  $v = (v_1, \dots, v_{m^{d_1}})$  and  $w = (w_1, \dots, w_{\ell^{d_2}})$ , we bound  $v^{\top}(B^* - \widehat{B})w$ . Let  $\Delta_i = \sum_{\mu=1}^{m^{d_1}} v_{\mu} \Phi_{\mu}(X_i) \sum_{\eta=1}^{\ell^{d_2}} w_{\eta} \Psi_{\eta}(Y_i)$ . Then

$$\begin{aligned} \text{Var}(\Delta_i) &\leq \mathbb{E}(\Delta_i^2) = \iint \left\{ \sum_{\mu=1}^{m^{d_1}} v_{\mu} \Phi_{\mu}(x) \right\}^2 \left\{ \sum_{\eta=1}^{\ell^{d_2}} w_{\eta} \Psi_{\eta}(y) \right\}^2 A^*(x, y) dx dy \\ &\leq \|A^*\|_{\infty} \int \left\{ \sum_{\mu=1}^{m^{d_1}} v_{\mu} \Phi_{\mu}(x) \right\}^2 dx \int \left\{ \sum_{\eta=1}^{\ell^{d_2}} w_{\eta} \Psi_{\eta}(y) \right\}^2 dy \\ &= \|A^*\|_{\infty} \left\| \sum_{\mu=1}^{m^{d_1}} v_{\mu} \Phi_{\mu} \right\|_{\mathbf{L}_2([0, 1]^{d_1})}^2 \left\| \sum_{\eta=1}^{\ell^{d_2}} w_{\eta} \Psi_{\eta} \right\|_{\mathbf{L}_2([0, 1]^{d_2})}^2 = \|A^*\|_{\infty}. \end{aligned}$$

where the last equality follows from **Step 1** and **Step 2**. In addition,

$$|\Delta_i| \leq \left\| \sum_{\mu=1}^{m^{d_1}} v_{\mu} \Phi_{\mu}(X_i) \right\|_{\infty} \left\| \sum_{\eta=1}^{\ell^{d_2}} w_{\eta} \Psi_{\eta}(Y_i) \right\|_{\infty} = O(\sqrt{m^{d_1} \ell^{d_2}}).$$

So for given  $v, w$ , by Bernstein's inequality

$$\mathbb{P}\left(\left|v^\top(B^* - \widehat{B})w\right| \geq t\right) = \mathbb{P}\left(\left|\frac{1}{N} \sum_{i=1}^N \Delta_i - \mathbb{E}(\Delta_i)\right| \geq t\right) \leq 2 \exp\left(\frac{-cNt^2}{\|A^*\|_\infty + t\sqrt{m^{d_1}\ell^{d_2}}}\right).$$

**Step 4.** Let  $\mathcal{N}(\frac{1}{4}, m^{d_1})$  be a  $1/4$  covering net of unit ball in  $\mathbb{R}^{m^{d_1}}$  and  $\mathcal{N}(\frac{1}{4}, \ell^{d_2})$  be a  $1/4$  covering net of unit ball in  $\mathbb{R}^{\ell^{d_2}}$ , then by 4.4.3 on page 90 of [Vershynin \(2018\)](#)

$$\|B^* - \widehat{B}\|_{\text{op}} \leq 2 \sup_{v \in \mathcal{N}(\frac{1}{4}, m^{d_1}), w \in \mathcal{N}(\frac{1}{4}, \ell^{d_2})} v^\top(B^* - \widehat{B})w.$$

So by union bound and the fact that the size of  $\mathcal{N}(\frac{1}{4}, m^{d_1})$  is bounded by  $9^{m^{d_1}}$  and the size of  $\mathcal{N}(\frac{1}{4}, \ell^{d_2})$  is bounded by  $9^{\ell^{d_2}}$ ,

$$\begin{aligned} \mathbb{P}\left(\|B^* - \widehat{B}\|_{\text{op}} \geq t\right) &\leq \mathbb{P}\left(\sup_{v \in \mathcal{N}(\frac{1}{4}, m^{d_1}), w \in \mathcal{N}(\frac{1}{4}, \ell^{d_2})} v^\top(B^* - \widehat{B})w \geq t/2\right) \\ &\leq 2 \cdot 9^{m^{d_1} + \ell^{d_2}} \exp\left(\frac{-cNt^2}{\|A^*\|_\infty + t\sqrt{m^{d_1}\ell^{d_2}}}\right). \end{aligned}$$

This implies that

$$\|B^* - \widehat{B}\|_{\text{op}} = O_{\mathbb{P}}\left(\sqrt{\frac{m^{d_1} + \ell^{d_2}}{N}} + \frac{m^{3d_1/2}\ell^{d_2/2} + m^{d_1/2}\ell^{3d_2/2}}{N}\right).$$

□

**Corollary 3.** Suppose  $\widehat{A}$  and  $A^*$  are defined as in [Theorem 2](#). Let  $\{\phi_k^{\mathbb{S}}\}_{k=1}^\infty$  be a collection of  $L_2([0, 1])$  basis such that  $\|\phi_k^{\mathbb{S}}\|_\infty \leq C_{\mathbb{S}}$ . Let

$$\mathcal{M} = \text{Span}\left\{\phi_{\mu_1}^{\mathbb{S}}(z_1)\right\}_{\mu_1=1}^m \quad \text{and} \quad \mathcal{L} = \text{Span}\left\{\phi_{\eta_1}^{\mathbb{S}}(z_2) \cdots \phi_{\eta_{d-1}}^{\mathbb{S}}(z_d)\right\}_{\eta_1, \dots, \eta_{d-1}=1}^\ell.$$

If in addition that  $m \asymp N^{1/(2\alpha+1)}$  and that  $\ell^{d-1} = o(N^{\frac{2\alpha-1}{2(2\alpha+1)}})$ , then

$$\|(\widehat{A} - A^*) \times_x \mathcal{P}_{\mathcal{M}} \times_y \mathcal{P}_{\mathcal{L}}\|_{\text{op}} = O_{\mathbb{P}}\left(\sqrt{\frac{\dim(\mathcal{M}) + \dim(\mathcal{L})}{N}}\right). \quad (68)$$

*Proof.* Since  $m\ell^{d-1}(m + \ell^{d-1}) \leq m\ell^{d-1}m\ell^{d-1} \leq N$  with above choice of  $m$  and  $\ell$ , [Corollary 3](#) is a direct consequence of [Lemma 9](#). □

## C.2 Proof of [Theorem 2](#)

*Proof of [Theorem 2](#).* It suffices to confirm that all the conditions in [Theorem 5](#) in [Appendix C.3](#) are met.

In particular, [Assumption 2](#) is verified in [Appendix B.1](#) for reproducing kernel Hilbert spaces, [Appendix B.2](#) for Legendre polynomials, and [Appendix B.3](#) for spline basis. [Assumption 4](#) is shown in [\(69\)](#) and [\(70\)](#). Therefore, [Theorem 2](#) immediately follows. □

### C.3 Proofs related to Theorem 5

**Assumption 4.** Suppose  $\mathbb{E}(\langle \widehat{A}, G \rangle) = \langle A^*, G \rangle$  for any non-random function  $G \in \mathbf{L}_2(\mathcal{O}^d)$ . In addition, suppose that

$$\sup_{\|G\|_{\mathbf{L}_2(\mathcal{O}^d)} \leq 1} \text{Var}\{\langle \widehat{A}, G \rangle\} = \mathcal{O}\left(\frac{1}{N}\right).$$

Assumption 4 requires that  $\langle \widehat{A}, G \rangle$  is a consistent estimator of  $\langle A^*, G \rangle$  for any generic non-random function  $G \in \mathbf{L}_2(\mathcal{O}^d)$ . It is straight forward to check that  $\widehat{A} = \frac{1}{N} \sum_{i=1}^N \mathbb{I}_{\{Z_i\}}$  in the density estimation model satisfies Assumption 4: for any  $G \in \mathbf{L}_2(\mathcal{O}^d)$ ,

$$\mathbb{E}(\langle \widehat{A}, G \rangle) = \mathbb{E}\left(\frac{1}{N} \sum_{i=1}^N G(Z_i)\right) = \mathbb{E}(G(Z_1)) = \int_{\mathcal{O}^d} A^*(z)G(z)dz = \langle A^*, G \rangle \quad \text{and} \quad (69)$$

$$\text{Var}(\langle \widehat{A}, G \rangle) = \frac{1}{N} \text{Var}(G(Z_1)) \leq \frac{1}{N} \mathbb{E}(G^2(Z_1)) = \frac{1}{N} \int_{\mathcal{O}^d} A^*(z)G^2(z)dz \leq \frac{\|A^*\|_{\infty} \|G\|_{\mathbf{L}_2(\mathcal{O}^d)}^2}{N}. \quad (70)$$

**Theorem 5.** Suppose Assumption 3 and Assumption 4 hold with  $\alpha \geq 1$ . Let  $\{\mathcal{M}_j, \mathcal{L}_j\}_{j=1}^d$  be defined in (24) and (25), and suppose Assumption 2 holds with  $(\mathcal{M}_j, \mathcal{L}_j)$  for  $j \in \{1, \dots, d\}$ . Let  $\sigma_{\min} = \min_{j=1, \dots, d} \{\sigma_{j, r_j}\}$  and suppose for a sufficiently large constant  $C_{snr}$ ,

$$N^{2\alpha/(2\alpha+1)} > C_{snr} \max \left\{ \prod_{j=1}^d r_j, \frac{1}{\sigma_{\min}^{(d-1)/\alpha+2}}, \frac{1}{\sigma_{\min}^{2\alpha/(\alpha-1/2)}} \right\}. \quad (71)$$

Let  $\widehat{f} \times_1 \widehat{\mathcal{P}}_1 \cdots \times_d \widehat{\mathcal{P}}_d$  be the output of Algorithm 2. If  $\ell_j = C_L \sigma_{j, r_j}^{-1/\alpha}$  for some sufficiently large constant  $C_L$  and  $m \asymp N^{1/(2\alpha+1)}$ , then it holds that

$$\|\widehat{A} \times_1 \widehat{\mathcal{P}}_1 \cdots \times_d \widehat{\mathcal{P}}_d - A^*\|_{\mathbf{L}_2(\mathcal{O}^d)}^2 = \mathcal{O}_{\mathbb{P}} \left( \frac{\sum_{j=1}^d \sigma_{j, r_j}^{-2}}{N^{2\alpha/(2\alpha+1)}} + \frac{\sum_{j=1}^d \sigma_{j, r_j}^{-(d-1)/\alpha-2}}{N} + \frac{\prod_{j=1}^d r_j}{N} \right). \quad (72)$$

*Proof of Theorem 5.* Observe that  $A^* = A^* \times_1 \mathcal{P}_1^* \cdots \times_d \mathcal{P}_d^*$ , where  $\mathcal{P}_j^*$  the projection matrix of  $\text{Range}_j(A^*)$ . As a result,

$$\begin{aligned} \widehat{A} \times_1 \widehat{\mathcal{P}}_1 \cdots \times_d \widehat{\mathcal{P}}_d - A^* &= \widehat{A} \times_1 \widehat{\mathcal{P}}_1 \cdots \times_d \widehat{\mathcal{P}}_d - A^* \times_1 \mathcal{P}_1^* \cdots \times_d \mathcal{P}_d^* \\ &= \widehat{A} \times_1 (\widehat{\mathcal{P}}_1 - \mathcal{P}_1^*) \times_2 \widehat{\mathcal{P}}_2 \cdots \times_d \widehat{\mathcal{P}}_d \\ &\quad + \dots \\ &\quad + \widehat{A} \times_1 \mathcal{P}_1^* \times_2 \mathcal{P}_2^* \cdots \times_{d-1} \mathcal{P}_{d-1}^* \times_d (\widehat{\mathcal{P}}_d - \mathcal{P}_d^*) \\ &\quad + (\widehat{A} - A^*) \times_1 \mathcal{P}_1^* \cdots \times_d \mathcal{P}_d^*. \end{aligned}$$

In the following, we bound each above term individually.

Let  $\mathcal{T}_1$  denote the linear subspace spanned by basis  $\{\Phi_{1, \rho}^*\}_{\rho=1}^{r_1}$  and  $\mathcal{M}_1$ . So  $\mathcal{P}_{\mathcal{T}_1}$  is non-random projection with rank at most  $m + r_1$ . Since the column space of  $\mathcal{P}_1^*$  is spanned by basis  $\{\Phi_{1, \rho}^*\}_{\rho=1}^{r_1}$  and the column space of  $\widehat{\mathcal{P}}_1$  is contained in  $\mathcal{M}_1$ , it follows

that  $\mathcal{P}_{\mathcal{T}_1}(\mathcal{P}_1^* - \widehat{\mathcal{P}}_1) = \mathcal{P}_1^* - \widehat{\mathcal{P}}_1$ . Besides, by condition (71) in Theorem 5, both (21) in Theorem 1 and (74) in Lemma 11 hold. Therefore

$$\begin{aligned}
& \|\widehat{A} \times_1 (\widehat{\mathcal{P}}_1 - \mathcal{P}_1^*) \times_2 \widehat{\mathcal{P}}_2 \cdots \times_d \widehat{\mathcal{P}}_d\|_F^2 \\
&= \|\widehat{A} \times_1 \mathcal{P}_{\mathcal{T}_1}(\widehat{\mathcal{P}}_1 - \mathcal{P}_1^*) \times_2 \widehat{\mathcal{P}}_2 \cdots \times_d \widehat{\mathcal{P}}_d\|_F^2 \\
&\leq \|\widehat{\mathcal{P}}_1 - \mathcal{P}_1^*\|_{\text{op}}^2 \|\widehat{A} \times_1 \mathcal{P}_{\mathcal{T}_1} \times_2 \widehat{\mathcal{P}}_2 \cdots \times_d \widehat{\mathcal{P}}_d\|_F^2 \\
&\leq O_{\mathbb{P}} \left( \frac{1}{\sigma_{1,r_1}^2} \left\{ \frac{m + \ell_1^{d-1}}{N} + m^{-2\alpha} \right\} \left\{ \frac{(m + r_1) \prod_{j=2}^d r_j}{N} + \|A^*\|_F^2 \right\} \right) \\
&= O_{\mathbb{P}} \left( \frac{1}{\sigma_{1,r_1}^2} \left\{ \frac{m + \ell_1^{d-1}}{N} + m^{-2\alpha} \right\} \right)
\end{aligned}$$

where the second inequality follows from Theorem 1 and Lemma 11, and the last equality follows from the fact that  $m \asymp N^{1/(2\alpha+1)}$  so that  $\frac{m \prod_{j=1}^d r_j}{N} = O(1)$  from the condition (71) in Theorem 5 and  $\|A^*\|_F^2 = O(1)$ .

Similarly, let  $\mathcal{T}_d$  denote the linear subspace space spanned by basis  $\{\Phi_{d,\rho}^*\}_{\rho=1}^{r_d}$  and  $\mathcal{M}_d$ . So  $\mathcal{P}_{\mathcal{T}_d}$  is non-random with rank at most  $m + r_d$ . Since the column space of  $\mathcal{P}_d^*$  is spanned by basis  $\{\Phi_{d,\rho}^*\}_{\rho=1}^{r_d}$  and the the column space of  $\widehat{\mathcal{P}}_d$  is contained in  $\mathcal{M}_d$ , it follows that  $\mathcal{P}_{\mathcal{T}_d}(\mathcal{P}_d^* - \widehat{\mathcal{P}}_d) = \mathcal{P}_d^* - \widehat{\mathcal{P}}_d$ .

$$\begin{aligned}
& \|\widehat{A} \times_1 \mathcal{P}_1^* \times_2 \mathcal{P}_2^* \cdots \times_{d-1} \mathcal{P}_{d-1}^* \times_d (\widehat{\mathcal{P}}_d - \mathcal{P}_d^*)\|_F^2 \\
&= \|\widehat{A} \times_1 \mathcal{P}_1^* \times_2 \mathcal{P}_2^* \cdots \times_{d-1} \mathcal{P}_{d-1}^* \times_d \mathcal{P}_{\mathcal{T}_d}(\widehat{\mathcal{P}}_d - \mathcal{P}_d^*)\|_F^2 \\
&\leq \|\widehat{\mathcal{P}}_d - \mathcal{P}_d^*\|_{\text{op}}^2 \|\widehat{A} \times_1 \mathcal{P}_1^* \times_2 \mathcal{P}_2^* \cdots \times_{d-1} \mathcal{P}_{d-1}^* \times_d \mathcal{P}_{\mathcal{T}_d}\|_F^2 \\
&\leq O_{\mathbb{P}} \left( \frac{1}{\sigma_{d,r_d}^2} \left\{ \frac{m + \ell_d^{d-1}}{N} + m^{-2\alpha} \right\} \left\{ \frac{(m + r_d) \prod_{j=1}^{d-1} r_j}{N} + \|A^*\|_F^2 \right\} \right) \\
&= O_{\mathbb{P}} \left( \frac{1}{\sigma_{d,r_d}^2} \left\{ \frac{m + \ell_d^{d-1}}{N} + m^{-2\alpha} \right\} \right)
\end{aligned}$$

where the inequalities hold following the same logic as above. Similarly, for any  $2 \leq p \leq d-1$ , it holds

$$\|\widehat{A} \times_1 \mathcal{P}_1^* \cdots \times_{p-1} \mathcal{P}_{p-1}^* \times_p (\widehat{\mathcal{P}}_p - \mathcal{P}_p^*) \times_{p+1} \widehat{\mathcal{P}}_{p+1} \cdots \times_d \widehat{\mathcal{P}}_d\|_F^2 = O_{\mathbb{P}} \left( \frac{1}{\sigma_{p,r_p}^2} \left\{ \frac{m + \ell_p^{d-1}}{N} + m^{-2\alpha} \right\} \right).$$

from Lemma 11. In addition by Lemma 10,

$$\mathbb{E} \|\widehat{A} - A_*\|_F^2 = O \left( \frac{\prod_{j=1}^d r_j}{N} \right).$$

Therefore,

$$\|\widehat{A} \times_1 \widehat{\mathcal{P}}_1 \cdots \times_d \widehat{\mathcal{P}}_d - A^*\|_F^2 = O_{\mathbb{P}} \left( \sum_{j=1}^d \frac{1}{\sigma_{j,r_j}^2} \left\{ \frac{m + \ell_j^{d-1}}{N} + m^{-2\alpha} \right\} + \frac{\prod_{j=1}^d r_j}{N} \right).$$

The desired result follows from the condition  $m \asymp N^{1/(2\alpha+1)}$  and  $\ell_j \asymp \sigma_{j,r_j}^{-1/\alpha}$  in Theorem 5.  $\square$

Here we provide two lemmas required in the above proof.

**Lemma 10.** *Suppose for each  $j = 1, \dots, d$ ,  $\mathcal{Q}_j$  is a non-random linear operator on  $\mathbf{L}_2(\mathcal{O}) \otimes \mathbf{L}_2(\mathcal{O})$  and that the rank of  $\mathcal{Q}_j$  is  $q_j$ . Then under Assumption 4, it holds that*

$$\mathbb{E}(\|(\widehat{A} - A^*) \times_1 \mathcal{Q}_1 \cdots \times_d \mathcal{Q}_d\|_F^2) = \mathcal{O}\left(\frac{\prod_{j=1}^d q_j \|\mathcal{Q}_j\|_{\text{op}}^2}{N}\right). \quad (73)$$

Consequently

$$\|\widehat{A} \times_1 \mathcal{Q}_1 \times_2 \mathcal{Q}_2 \cdots \times_d \mathcal{Q}_d\|_F^2 = \mathcal{O}_{\mathbb{P}}\left(\prod_{j=1}^d \|\mathcal{Q}_j\|_{\text{op}}^2 \left\{\frac{\prod_{j=1}^d q_j}{N} + \|A^*\|_F^2\right\}\right).$$

*Proof.* Since the rank of  $\mathcal{Q}_j$  is  $q_j$ , we can write

$$\mathcal{Q}_j = \sum_{\mu_j=1}^{q_j} \nu_{j,\mu_j} \phi_{j,\mu_j} \otimes \psi_{j,\mu_j},$$

where  $\{\psi_{j,\mu_j}\}_{\mu_j=1}^{q_j}$  and  $\{\phi_{j,\mu_j}\}_{\mu_j=1}^{q_j}$  are both orthonormal in  $\mathbf{L}_2(\mathcal{O})$ . Note that  $|\nu_{j,\mu_j}| \leq \|\mathcal{Q}_j\|_{\text{op}}$  for any  $\mu_j$ . Denote

$$\mathcal{S}_j = \text{Span}\{\psi_{j,\mu_j}\}_{\mu_j=1}^{q_j}.$$

Note that  $(\widehat{A} - A^*) \times_1 \mathcal{Q}_1 \cdots \times_d \mathcal{Q}_d$  is zero in the orthogonal complement of the subspace  $\mathcal{S}_1 \otimes \cdots \otimes \mathcal{S}_d$ . Therefore,

$$\begin{aligned} & \|(\widehat{A} - A^*) \times_1 \mathcal{Q}_1 \cdots \times_d \mathcal{Q}_d\|_F^2 \\ &= \sum_{\mu_1=1}^{q_1} \cdots \sum_{\mu_d=1}^{q_d} \left\{ (\widehat{A} - A^*) \times_1 \mathcal{Q}_1 \cdots \times_d \mathcal{Q}_d[\psi_{1,\mu_1}, \dots, \psi_{d,\mu_d}] \right\}^2 \\ &= \sum_{\mu_1=1}^{q_1} \cdots \sum_{\mu_d=1}^{q_d} \left\{ (\widehat{A} - A^*)[\mathcal{Q}_1(\psi_{1,\mu_1}), \dots, \mathcal{Q}_d(\psi_{d,\mu_d})] \right\}^2 \\ &= \sum_{\mu_1=1}^{q_1} \cdots \sum_{\mu_d=1}^{q_d} \left\{ (\widehat{A} - A^*)[\nu_{1,\mu_1} \phi_{1,\mu_1}, \dots, \nu_{d,\mu_d} \phi_{d,\mu_d}] \right\}^2 \\ &\leq \prod_{j=1}^d \|\mathcal{Q}_j\|_{\text{op}}^2 \sum_{\mu_1=1}^{q_1} \cdots \sum_{\mu_d=1}^{q_d} \left\{ (\widehat{A} - A^*)[\phi_{1,\mu_1}, \dots, \phi_{d,\mu_d}] \right\}^2 \end{aligned}$$

and so

$$\begin{aligned} & \mathbb{E}\|(\widehat{A} - A^*) \times_1 \mathcal{Q}_1 \cdots \times_d \mathcal{Q}_d\|_F^2 \\ &\leq \prod_{j=1}^d \|\mathcal{Q}_j\|_{\text{op}}^2 \sum_{\mu_1=1}^{q_1} \cdots \sum_{\mu_d=1}^{q_d} \mathbb{E}\left\{ (\widehat{A} - A^*)[\phi_{1,\mu_1}, \dots, \phi_{d,\mu_d}] \right\}^2 \\ &= \prod_{j=1}^d \|\mathcal{Q}_j\|_{\text{op}}^2 \sum_{\mu_1=1}^{q_1} \cdots \sum_{\mu_d=1}^{q_d} \text{Var}\left\{ \widehat{A}[\phi_{1,\mu_1}, \dots, \phi_{d,\mu_d}] \right\} = \mathcal{O}\left(\frac{\prod_{j=1}^d q_j \|\mathcal{Q}_j\|_{\text{op}}^2}{N}\right), \end{aligned}$$

where the equality follows from the assumption that  $\mathbb{E}(\langle \widehat{A}, G \rangle) = \langle A^*, G \rangle$  for any  $G \in \mathbf{L}_2(\mathcal{O}^d)$ . Consequently,

$$\begin{aligned} \|\widehat{A} \times_1 \mathcal{Q}_1 \times_2 \mathcal{Q}_2 \cdots \times_d \mathcal{Q}_d\|_F^2 &\leq 2\|(\widehat{A} - A^*) \times_1 \mathcal{Q}_1 \times_2 \mathcal{Q}_2 \cdots \times_d \mathcal{Q}_d\|_F^2 + 2\|A^* \times_1 \mathcal{Q}_1 \times_2 \mathcal{Q}_2 \cdots \times_d \mathcal{Q}_d\|_F^2 \\ &\leq 2\|(\widehat{A} - A^*) \times_1 \mathcal{Q}_1 \times_2 \mathcal{Q}_2 \cdots \times_d \mathcal{Q}_d\|_F^2 + 2 \prod_{j=1}^d \|\mathcal{Q}_j\|_{\text{op}}^2 \|A^*\|_F^2 \\ &= \mathcal{O}_{\mathbb{P}} \left( \prod_{j=1}^d \|\mathcal{Q}_j\|_{\text{op}}^2 \left\{ \frac{\prod_{j=1}^d q_j}{N} + \|A^*\|_F^2 \right\} \right). \end{aligned}$$

□

**Lemma 11.** *Let  $\widehat{A}$  be any estimator satisfying Assumption 4. Suppose  $\{\mathcal{Q}_j\}_{j=1}^d$  is collection of non-random operators on  $\mathbf{L}_2 \otimes \mathbf{L}_2$  such that  $\mathcal{Q}_j$  has rank  $q_j$  and  $\|\mathcal{Q}_j\|_{\text{op}} \leq 1$ . Let  $\sigma_{\min} = \min_{j=1, \dots, d} \{\sigma_{j, r_j}\}$  and suppose in addition it holds that*

$$\frac{m}{\sigma_{\min}^2} \left( \frac{m + \ell^{d-1}}{N} + m^{-2\alpha} \right) = \mathcal{O}(1). \quad (74)$$

Then for any  $0 \leq p \leq d-1$ , it holds that

$$\|\widehat{A} \times_1 \mathcal{Q}_1 \cdots \times_{p+1} \mathcal{Q}_{p+1} \times_{p+2} \widehat{\mathcal{P}}_{p+2} \cdots \times_d \widehat{\mathcal{P}}_d\|_F^2 = \mathcal{O}_{\mathbb{P}} \left( \frac{(\prod_{j=1}^{p+1} q_j)(\prod_{j=p+2}^d r_j)}{N} + \|A^*\|_F^2 \right). \quad (75)$$

*Proof.* We prove (75) by induction. The base case  $p+1 = d$  is exactly Lemma 10. Suppose (75) holds for any  $p+1$ . Then

$$\begin{aligned} &\|\widehat{A} \times_1 \mathcal{Q}_1 \cdots \times_p \mathcal{Q}_p \times_{p+1} \widehat{\mathcal{P}}_{p+1} \cdots \times_d \widehat{\mathcal{P}}_d\|_F^2 \\ &\leq 2\|\widehat{A} \times_1 \mathcal{Q}_1 \cdots \times_p \mathcal{Q}_p \times_{p+1} \mathcal{P}_{p+1}^* \times_{p+2} \widehat{\mathcal{P}}_{p+2} \cdots \times_d \widehat{\mathcal{P}}_d\|_F^2 \end{aligned} \quad (76)$$

$$+ 2\|\widehat{A} \times_1 \mathcal{Q}_1 \cdots \times_p \mathcal{Q}_p \times_{p+1} (\mathcal{P}_{p+1}^* - \widehat{\mathcal{P}}_{p+1}) \times_{p+2} \widehat{\mathcal{P}}_{p+2} \cdots \times_d \widehat{\mathcal{P}}_d\|_F^2. \quad (77)$$

By induction,

$$\begin{aligned} (76) &\leq \mathcal{O}_{\mathbb{P}} \left( \frac{(\prod_{j=1}^p q_j) \text{Rank}(\mathcal{P}_{p+1}^*) (\prod_{j=p+2}^d r_j)}{N} + \|A^*\|_F^2 \right) \\ &= \mathcal{O}_{\mathbb{P}} \left( \frac{(\prod_{j=1}^p q_j) (\prod_{j=p+1}^d r_j)}{N} + \|A^*\|_F^2 \right). \end{aligned}$$

Let  $\mathcal{T}_{p+1}$  denote space spanned by basis  $\{\Phi_{p+1, \rho}^*\}_{\rho=1}^{r_{p+1}}$  defined in Assumption 3 and  $\mathcal{M}_{p+1}$ . So  $\mathcal{P}_{\mathcal{T}_{p+1}}$  is non-random with rank at most  $m + r_{p+1}$ . Since the column space of  $\mathcal{P}_{p+1}^*$  is spanned by  $\{\Phi_{p+1, \rho}^*\}_{\rho=1}^{r_{p+1}}$  and the column space of  $\widehat{\mathcal{P}}_{p+1}$  is contained in  $\mathcal{M}_{p+1}$ , it follows

that  $\mathcal{P}_{\mathcal{T}_{p+1}}(\mathcal{P}_{p+1}^* - \widehat{\mathcal{P}}_{p+1}) = \mathcal{P}_{p+1}^* - \widehat{\mathcal{P}}_{p+1}$ . Consequently,

$$\begin{aligned}
(77) &= \|\widehat{A} \times_1 \mathcal{Q}_1 \cdots \times_p \mathcal{Q}_p \times_{p+1} \mathcal{P}_{\mathcal{T}_{p+1}}(\mathcal{P}_{p+1}^* - \widehat{\mathcal{P}}_{p+1}) \times_{p+2} \widehat{\mathcal{P}}_{p+2} \cdots \times_d \widehat{\mathcal{P}}_d\|_F^2 \\
&\leq \|\widehat{A} \times_1 \mathcal{Q}_1 \cdots \times_p \mathcal{Q}_p \times_{p+1} \mathcal{P}_{\mathcal{T}_{p+1}} \times_{p+2} \widehat{\mathcal{P}}_{p+2} \cdots \times_d \widehat{\mathcal{P}}_d\|_F^2 \|\mathcal{P}_{p+1}^* - \widehat{\mathcal{P}}_{p+1}\|_{\text{op}}^2 \\
&\leq \text{O}_{\mathbb{P}} \left( \left\{ \frac{(\prod_{j=1}^p q_j)(m + r_{p+1})(\prod_{j=p+2}^d r_j)}{N} + \|A^*\|_F^2 \right\} \frac{1}{\sigma_{p+1, r_{p+1}}^2} \left\{ \frac{m + \ell^{d-1}}{N} + m^{-2\alpha} \right\} \right) \\
&= \text{O}_{\mathbb{P}} \left( \left\{ \frac{(\prod_{j=1}^p q_j) \prod_{j=p+1}^d r_j}{N} + \|A^*\|_F^2 \right\} \frac{1}{\sigma_{p+1, r_{p+1}}^2} \left\{ \frac{m + \ell^{d-1}}{N} + m^{-2\alpha} \right\} \right) \\
&+ \text{O}_{\mathbb{P}} \left( \frac{(\prod_{j=1}^p q_j) \prod_{j=p+2}^d r_j}{N} \frac{m}{\sigma_{p+1, r_{p+1}}^2} \left\{ \frac{m + \ell^{d-1}}{N} + m^{-2\alpha} \right\} \right) \\
&= \text{O}_{\mathbb{P}} \left( \frac{(\prod_{j=1}^p q_j)(\prod_{j=p+1}^d r_j)}{N} + \|A^*\|_F^2 \right)
\end{aligned}$$

where the second inequality follows from induction and Theorem 1, and the last inequality follows from the assumption that  $\frac{m}{\sigma_{p+1, r_{p+1}}^2} \left( \frac{m + \ell^{d-1}}{N} + m^{-2\alpha} \right) \leq \frac{m}{\sigma_{\min}^2} \left( \frac{m + \ell^{d-1}}{N} + m^{-2\alpha} \right) = \text{O}(1)$ . Consequently,

$$\|\widehat{A} \times_1 \mathcal{Q}_1 \cdots \times_p \mathcal{Q}_p \times_{p+1} \widehat{\mathcal{P}}_{p+1} \cdots \times_d \widehat{\mathcal{P}}_d\|_F^2 = \text{O}_{\mathbb{P}} \left( \frac{(\prod_{j=1}^p q_j)(\prod_{j=p+1}^d r_j)}{N} + \|A^*\|_F^2 \right)$$

Therefore, (75) holds for any  $p \in \{1, \dots, d\}$ .  $\square$

## D Additional discussions related to Section 2

### D.1 Implementation details for Algorithm 1

Let  $\mathcal{M} \subset \mathbf{L}_2(\Omega_1)$  and  $\mathcal{L} \subset \mathbf{L}_2(\Omega_2)$  be two subspaces and  $\widehat{A}(x, y) : \Omega_1 \times \Omega_2 \rightarrow \mathbb{R}$  be any (random) function. Suppose that  $\{v_\mu(x)\}_{\mu=1}^{\dim(\mathcal{M})}$  and  $\{w_\eta(y)\}_{\eta=1}^{\dim(\mathcal{L})}$  are the orthonormal basis functions of  $\mathcal{M}$  and  $\mathcal{L}$  respectively, with  $\dim(\mathcal{M}), \dim(\mathcal{L}) \in \mathbb{Z}^+$ . Our general assumption is that  $\widehat{A}[f, g]$  can be computed efficiently for any  $f \in \mathbf{L}_2(\Omega_1)$  and  $g \in \mathbf{L}_2(\Omega_2)$ . This assumption is easily verified for the density estimation model. The following algorithm provide additional implementation details for Algorithm 1.

---

#### Algorithm 3 Range Estimation via Variance-Reduced Sketching

---

**INPUT:** Estimator  $\widehat{A}(x, y)$ , parameter  $r \in \mathbb{Z}^+$ , linear subspaces  $\mathcal{M} = \text{Span}\{v_\mu(x)\}_{\mu=1}^{\dim(\mathcal{M})}$  and  $\mathcal{L} = \text{Span}\{w_\eta(y)\}_{\eta=1}^{\dim(\mathcal{L})}$ .

1: Compute  $B \in \mathbb{R}^{\dim(\mathcal{M}) \times \dim(\mathcal{L})}$ , where for  $1 \leq \mu \leq \dim(\mathcal{M})$  and  $1 \leq \eta \leq \dim(\mathcal{L})$ ,

$$B_{\mu, \eta} = \widehat{A}[v_\mu, w_\eta].$$

2: Compute  $\{\widehat{U}_\rho\}_{\rho=1}^r \subset \mathbb{R}^{\dim(\mathcal{M})}$ , the leading  $r$  left singular vectors of  $B$  using matrix singular value decomposition.

3: Compute  $\widehat{\Phi}_\rho(x) = \sum_{\mu=1}^{\dim(\mathcal{M})} \widehat{U}_{\rho, \mu} v_\mu(x)$  for  $\rho = 1, \dots, r$ .

**OUTPUT:** Functions  $\{\widehat{\Phi}_\rho(x)\}_{\rho=1}^r \subset \mathbf{L}_2(\Omega_1)$ .

---

## D.2 Sketching in finite-dimensional vector spaces

In this subsection, we illustrate the intuition of sketching in a finite-dimensional matrix example. Suppose  $B \in \mathbb{R}^{n_1 \times n_2}$  is a finite-dimensional matrix with rank  $r$ . Let  $\text{Range}(B) \subset \mathbb{R}^{n_1}$  denote the linear subspace spanned by the columns of  $B$ , and  $\text{Row}(B) \subset \mathbb{R}^{n_2}$  the linear subspace spanned by the rows of  $B$ . Our goal is to illustrate how to estimate  $\text{Range}(B)$  with reduced variance and reduced computational complexity when  $n_1 \ll n_2$ .

By singular value decomposition, we can write

$$B = \sum_{\rho=1}^r \sigma_{\rho}(B) U_{\rho} V_{\rho}^{\top},$$

where  $\sigma_1(B) \geq \dots \geq \sigma_r(B) > 0$  are singular values,  $\{U_{\rho}\}_{\rho=1}^r$  are orthonormal vectors in  $\mathbb{R}^{n_1}$ , and  $\{V_{\rho}\}_{\rho=1}^r$  are orthonormal vectors in  $\mathbb{R}^{n_2}$ . Therefore  $\text{Range}(B)$  is spanned by  $\{U_{\rho}\}_{\rho=1}^r$ , and  $\text{Row}(B)$  is spanned by  $\{V_{\rho}\}_{\rho=1}^r$ .

The sketch-based estimation procedure of  $\text{Range}(B)$  is as follows. First, we choose a linear subspace  $\mathcal{S} \subset \mathbb{R}^{n_2}$  such that  $\dim(\mathcal{S}) \ll n_2$  and that  $\mathcal{S}$  forms a  $\delta$ -cover of  $\text{Row}(B)$ . Let  $P_{\mathcal{S}}$  be the projection matrix from  $\mathbb{R}^{n_2}$  to  $\mathcal{S}$  and we form the sketch matrix  $BP_{\mathcal{S}}^{\top} \in \mathbb{R}^{n_1 \times \dim(\mathcal{S})}$ . Then in the second stage, we use the singular value decomposition to compute  $\text{Range}(BP_{\mathcal{S}}^{\top})$  and return  $\text{Range}(BP_{\mathcal{S}}^{\top})$  as the estimator of  $\text{Range}(B)$ .

With the sketching technique, we only need to work with the reduced-size matrix  $BP_{\mathcal{S}}^{\top} \in \mathbb{R}^{n_1 \times \dim(\mathcal{S})}$  instead of  $B \in \mathbb{R}^{n_1 \times n_2}$ . Therefore, the effective variance of the sketching procedure is reduced to  $O(n_1 \dim(\mathcal{S}))$ , significantly smaller than  $O(n_1 n_2)$  which is the cost if we directly use  $B$  to estimate the range.

We also provide an intuitive argument to support the above sketching procedure. Since  $BP_{\mathcal{S}}^{\top} = \sum_{\rho=1}^r \sigma_{\rho}(B) U_{\rho} (P_{\mathcal{S}} V_{\rho})^{\top}$ , it holds that

$$\text{Range}(BP_{\mathcal{S}}^{\top}) \subset \text{Range}(B). \quad (78)$$

Let  $\|\cdot\|_2$  indicate matrix spectral norm for matrix and vector  $l_2$  norm. Since the subspace  $\mathcal{S}$  is a  $\delta$ -cover of  $\text{Row}(B)$ , it follows that  $\|P_{\mathcal{S}} V_{\rho} - V_{\rho}\| \leq \delta$  for  $\rho = 1, \dots, r$ . Therefore

$$\|B - BP_{\mathcal{S}}^{\top}\|_2 = \left\| \sum_{\rho=1}^r \sigma_{\rho}(B) U_{\rho} (V_{\rho} - P_{\mathcal{S}} V_{\rho})^{\top} \right\|_2 \leq \sum_{\rho=1}^r |\sigma_{\rho}(B)| \|U_{\rho}\|_2 \|V_{\rho} - P_{\mathcal{S}} V_{\rho}\|_2 = O(\delta),$$

where the last equality follows from the fact that  $|\sigma_{\rho}(B)| < \infty$  and  $\|U_{\rho}\|_2 = 1$  for  $\rho = 1, \dots, r$ . Let  $\{\sigma_{\rho}(BP_{\mathcal{S}}^{\top})\}_{\rho=1}^r$  be the leading  $r$  singular values of  $BP_{\mathcal{S}}^{\top}$ . By matrix singular value perturbation theory,

$$|\sigma_{\rho}(B) - \sigma_{\rho}(BP_{\mathcal{S}}^{\top})| \leq \|B - BP_{\mathcal{S}}^{\top}\|_2 = O(\delta). \quad (79)$$

for  $\rho = 1, \dots, r$ . Suppose  $\mathcal{S}$  is chosen so that  $\delta \ll \sigma_r(B)$ , where  $\sigma_r(B)$  is the minimal singular value of  $B$ . Then (79) implies that  $\sigma_{\rho}(BP_{\mathcal{S}}^{\top}) \geq \sigma_{\rho}(B) - O(\delta) > 0$  for  $\rho \in \{1, \dots, r\}$ . Therefore,  $BP_{\mathcal{S}}^{\top}$  has at least  $r$  positive singular values and the rank of  $BP_{\mathcal{S}}^{\top}$  is at least  $r$ . This observation, together with (78) and the fact that  $\text{Rank}(B) = r$  implies that

$$\text{Range}(BP_{\mathcal{S}}^{\top}) = \text{Range}(B).$$

This justifies the sketching procedure in finite-dimensions.

## E Proofs in Section 4

**Lemma 12.** Let  $\Gamma(x, y)$  be a generic element in  $\mathbf{L}_2([\kappa]^2) \otimes \mathbf{L}_2([\kappa]^2)$ . Then

$$\|\Gamma(x, y)\|_{\text{op}(\mathbf{L}_2([\kappa]^2) \otimes \mathbf{L}_2([\kappa]^2))} = \frac{\|\Gamma(x, y)\|_{\text{op}}}{\kappa^2}.$$

*Proof.* Let  $f_x = I(x)/\kappa$  and  $g_x = J(x)/\kappa$ . Then

$$\sum_{x \in [\kappa]^2} f_x^2 = \frac{1}{\kappa^2} \sum_{x \in [\kappa]^2} I^2(x) = \|I\|_{\mathbf{L}_2([\kappa]^2)}^2.$$

It suffices to observe that

$$\begin{aligned} \|\Gamma\|_{\text{op}(\mathbf{L}_2([\kappa]^2) \otimes \mathbf{L}_2([\kappa]^2))} &= \sup_{\|I\|_{\mathbf{L}_2([\kappa]^2)} = \|J\|_{\mathbf{L}_2([\kappa]^2)} = 1} \Gamma[I, J] \\ &= \sup_{\|I\|_{\mathbf{L}_2([\kappa]^2)} = \|J\|_{\mathbf{L}_2([\kappa]^2)} = 1} \frac{1}{\kappa^4} \sum_{x, y \in [\kappa]^2} \Gamma(x, y) I(x) J(y) \\ &= \frac{1}{\kappa^2} \sum_{\sum_{x \in [\kappa]^2} f_x^2 = \sum_{y \in [\kappa]^2} g_y^2 = 1} \Gamma(x, y) f_x g_y = \frac{\|\Gamma(x, y)\|_{\text{op}}}{\kappa^2}. \end{aligned}$$

□

*Proof of Corollary 1.* From the proof of Theorem 1 and Lemma 13, it follows that

$$\|\widehat{\mathcal{P}}_x - \mathcal{P}_x^*\|_{\text{op}(\mathbf{L}_2([\kappa]^2) \otimes \mathbf{L}_2([\kappa]^2))}^2 = O_{\mathbb{P}} \left\{ \sigma_r^{-2} \left( m^{-2\alpha} + \frac{m^2 + \ell^2}{N} + \frac{1}{\kappa^4} \right) \right\}. \quad (80)$$

The desired result follows by setting

$$m \asymp N^{-1/(2\alpha+2)} \quad \text{and} \quad \ell = C_L \sigma_r^{-1/\alpha}.$$

□

**Lemma 13.** Let  $\mathcal{M}$  and  $\mathcal{L}$  be subspaces in the form of (31). Suppose in addition that  $\frac{m+\ell}{\sqrt{N}} = O(1)$ . Then under the same conditions as in Corollary 1, it holds that

$$\|(\widehat{\Sigma} - \Sigma^*) \times_x \mathcal{P}_{\mathcal{M}} \times_y \mathcal{P}_{\mathcal{L}}\|_{\text{op}(\mathbf{L}_2([\kappa]^2) \otimes \mathbf{L}_2([\kappa]^2))} = O_{\mathbb{P}} \left( \frac{m + \ell}{\sqrt{N}} + \frac{m^2 + \ell^2}{N} + \frac{1}{\kappa^2} \right).$$

*Proof.* Let  $x = (x_1, x_2) \in [\kappa]^2$  and  $y = (y_1, y_2) \in [\kappa]^2$ . By reordering  $(\mu_1, \mu_2)$  and  $(\eta_1, \eta_2)$  in (31), we can assume that

$$\mathcal{M} = \text{span}\{\Phi_{\mu}(x)\}_{\mu=1}^{m^2} \quad \text{and} \quad \mathcal{L} = \text{span}\{\Psi_{\eta}(y)\}_{\eta=1}^{\ell^2}, \quad (81)$$

where  $\{\Phi_{\mu}(x)\}_{\mu=1}^{m^2}$  and  $\{\Psi_{\eta}(y)\}_{\eta=1}^{\ell^2}$  are orthonormal basis functions of  $\mathbf{L}_2([\kappa]^2)$ . Note that  $\widehat{\Sigma} \times_x \mathcal{P}_{\mathcal{M}} \times_y \mathcal{P}_{\mathcal{L}}$  and  $\Sigma^* \times_x \mathcal{P}_{\mathcal{M}} \times_y \mathcal{P}_{\mathcal{L}}$  are both zero on the orthogonal complement of the subspace  $\mathcal{M} \otimes \mathcal{L}$ . Let

$$W_i(x) = I^*(x) + \delta_i(x) + \epsilon_i(x) \quad (82)$$

where  $I^*(x) = \mathbb{E}(I_i(x))$  and  $\delta_i(x) = I_i(x) - I^*(x)$ . Therefore  $\mathbb{E}(\delta_i(x)) = 0$  and  $Cov(\delta_i(x), \delta_i(y)) = \Sigma^*(x, y)$ . Let  $\widehat{B}, B^* \in \mathbb{R}^{m^2 \times \ell^2}$  be such that for  $\mu = 1, \dots, m^2$  and  $\eta = 1, \dots, \ell^2$ ,

$$\widehat{B}_{\mu, \eta} = \widehat{\Sigma}[\Phi_\mu, \Psi_\eta] \quad \text{and} \quad B_{\mu, \eta}^* = \Sigma^*[\Phi_\mu, \Psi_\eta],$$

where  $\widehat{\Sigma}[\Phi_\mu, \Psi_\eta]$  and  $\Sigma^*[\Phi_\mu, \Psi_\eta]$  are defined according to (28). By the definition of  $\widehat{B}$  and  $B^*$ ,

$$\|\widehat{B} - B^*\|_{\text{op}} = \|(\widehat{\Sigma} - \Sigma^*) \times_x \mathcal{P}_M \times_y \mathcal{P}_L\|_{\text{op}(\mathbf{L}_2([\kappa]^2) \otimes \mathbf{L}_2([\kappa]^2))}. \quad (83)$$

Note that

$$\|\widehat{B} - B^*\|_{\text{op}} \leq \|\widehat{B} - \mathbb{E}(\widehat{B})\|_{\text{op}} + \|\mathbb{E}(\widehat{B}) - B^*\|_{\text{op}}.$$

We estimate above two terms separately.

**Step 1.** In this step, we control  $\|\mathbb{E}(\widehat{B}) - B^*\|_{\text{op}}$ . Denote  $C_\epsilon = \text{Var}(\epsilon_i(x))$ . Since  $\{\epsilon_i(x)\}_{i=1, \dots, N, x \in [\kappa]^2}$  and  $\{\delta_i\}_{i=1}^N$  are independent,

$$\mathbb{E}(W_i(x)W_i(y)) = \begin{cases} I^*(x)I^*(y) + \Sigma^*(x, y) & \text{if } x \neq y, \\ I^*(x)I^*(x) + \Sigma^*(x, x) + C_\epsilon & \text{if } x = y. \end{cases}$$

Therefore for any  $i = 1, \dots, N$ ,

$$\mathbb{E}(W_i(x)\overline{W}(y)) = \begin{cases} I^*(x)I^*(y) + \frac{1}{N}\Sigma^*(x, y) & \text{if } x \neq y, \\ I^*(x)I^*(x) + \frac{1}{N}\Sigma^*(x, x) + \frac{1}{N}C_\epsilon & \text{if } x = y \end{cases}$$

and

$$\mathbb{E}(\overline{W}(x)\overline{W}(y)) = \begin{cases} I^*(x)I^*(y) + \frac{1}{N}\Sigma^*(x, y) & \text{if } x \neq y, \\ I^*(x)I^*(x) + \frac{1}{N}\Sigma^*(x, x) + \frac{1}{N}C_\epsilon & \text{if } x = y. \end{cases}$$

So

$$\mathbb{E}(\widehat{\Sigma}(x, y)) = \begin{cases} \Sigma^*(x, y) & \text{if } x \neq y, \\ \Sigma^*(x, x) + C_\epsilon & \text{if } x = y, \end{cases}$$

and

$$\mathbb{E}(\widehat{\Sigma}(x, y)) - \Sigma^*(x, y) = \begin{cases} 0 & \text{if } x \neq y, \\ C_\epsilon & \text{if } x = y. \end{cases} \quad (84)$$

By Lemma 12, it follows that

$$\|\mathbb{E}(\widehat{\Sigma}) - \Sigma^*\|_{\text{op}(\mathbf{L}_2([\kappa]^2) \otimes \mathbf{L}_2([\kappa]^2))} = \frac{C_\epsilon}{\kappa^2}.$$

Therefore

$$\|\mathbb{E}(\widehat{B}) - B^*\|_{\text{op}} = \|(\mathbb{E}(\widehat{\Sigma}) - \Sigma^*) \times_x \mathcal{P}_M \times_y \mathcal{P}_L\|_{\text{op}(\mathbf{L}_2([\kappa]^2) \otimes \mathbf{L}_2([\kappa]^2))} = \frac{C_\epsilon}{\kappa^2}.$$

**Step 2.** In this step, we bound  $\|\mathbb{E}(\widehat{B}) - \widehat{B}\|_{\text{op}}$ . This procedures are similar to Lemma 9

and Lemma 22. Let  $v = (v_1, \dots, v_{m^2}) \in \mathbb{R}^{m^2}$  and  $w = (w_1, \dots, w_{\ell^2}) \in \mathbb{R}^{\ell^2}$  be such that  $\sum_{\mu=1}^{m^2} v_\mu^2 = 1$  and  $\sum_{\eta=1}^{\ell^2} w_\eta^2 = 1$ . Denote

$$\Phi_v(x) = \sum_{\mu=1}^{m^2} v_\mu \Phi_\mu(x) \quad \text{and} \quad \Psi_w(y) = \sum_{\eta=1}^{\ell^2} w_\eta \Psi_\eta(y).$$

Since  $\{\Phi_\mu(x)\}_{\mu=1}^{m^2}$  and  $\{\Psi_\eta(y)\}_{\eta=1}^{\ell^2}$  are orthonormal basis functions of  $\mathbf{L}_2([\kappa]^2)$ , it follows that

$$\|\Phi_v\|_{\mathbf{L}_2([\kappa]^2)} = 1 \quad \text{and} \quad \|\Psi_w\|_{\mathbf{L}_2([\kappa]^2)} = 1. \quad (85)$$

Therefore,

$$\begin{aligned} v^\top (\mathbb{E}(\widehat{B}) - \widehat{B})w &= \sum_{\mu=1}^{m^2} \sum_{\eta=1}^{\ell^2} v_\mu \widehat{\Sigma}[\Phi_\mu, \Psi_\eta] w_\eta = \sum_{\mu=1}^{m^2} \sum_{\eta=1}^{\ell^2} \widehat{\Sigma}[v_\mu \Phi_\mu, w_\eta \Psi_\eta] \\ &= \frac{1}{N} \sum_{i=1}^N \frac{1}{\kappa^4} \left\{ \sum_{x \in [\kappa]^2} \{W_i(x) - \overline{W}(x)\} \Phi_v(x) \sum_{y \in [\kappa]^2} \{W_i(y) - \overline{W}(y)\} \Psi_w(y) \right\} \\ &= \frac{1}{N\kappa^4} \sum_{i=1}^N \sum_{x \in [\kappa]^2} \{W_i(x) - \mathbb{E}(W(x))\} \Phi_v(x) \sum_{y \in [\kappa]^2} \{W_i(y) - \mathbb{E}(W(y))\} \Psi_w(y) \end{aligned} \quad (86)$$

$$+ \frac{1}{N\kappa^4} \sum_{i=1}^N \sum_{x \in [\kappa]^2} \{\mathbb{E}(W(x)) - \overline{W}(x)\} \Phi_v(x) \sum_{y \in [\kappa]^2} \{W_i(y) - \mathbb{E}(W(y))\} \Psi_w(y) \quad (87)$$

$$+ \frac{1}{N\kappa^4} \sum_{i=1}^N \sum_{x \in [\kappa]^2} \{W_i(x) - \mathbb{E}(W(x))\} \Phi_v(x) \sum_{y \in [\kappa]^2} \{\mathbb{E}(W(y)) - \overline{W}(y)\} \Psi_w(y) \quad (88)$$

$$+ \frac{1}{N\kappa^4} \sum_{i=1}^N \sum_{x \in [\kappa]^2} \{\mathbb{E}(W(x)) - \overline{W}(x)\} \Phi_v(x) \sum_{y \in [\kappa]^2} \{\mathbb{E}(W(y)) - \overline{W}(y)\} \Psi_w(y), \quad (89)$$

where the third equality follows from (34) and (28).

**Step 3.** Here we bound above four terms separately. Observe that

$$(86) = \frac{1}{N} \sum_{i=1}^N \left\{ \frac{1}{\kappa^2} \sum_{x \in [\kappa]^2} (\delta_i(x) + \epsilon_i(x)) \Phi_v(x) \right\} \left\{ \frac{1}{\kappa^2} \sum_{y \in [\kappa]^2} (\delta_i(y) + \epsilon_i(y)) \Psi_w(y) \right\}.$$

Since  $\delta_i \in \mathbf{L}_2([\kappa]^2)$  is a subGaussian process with parameter  $C_\delta$ , and by (85),  $\|\Phi_v\|_{\mathbf{L}_2([\kappa]^2)} = 1$ , it follows that  $\frac{1}{\kappa^2} \sum_{x \in [\kappa]^2} (\delta_i(x) + \epsilon_i(x)) \Phi_v(x)$  is a subGaussian random variable with parameter  $(C_\delta + C_\epsilon)^2$ . Similarly  $\left\{ \frac{1}{\kappa^2} \sum_{y \in [\kappa]^2} (\delta_i(y) + \epsilon_i(y)) \Psi_w(y) \right\}$  is subGaussian with parameter  $(C_\delta + C_\epsilon)^2$ .

Therefore  $\left\{ \frac{1}{\kappa^2} \sum_{x \in [\kappa]^2} (\delta_i(x) + \epsilon_i(x)) \Phi_v(x) \right\} \left\{ \frac{1}{\kappa^2} \sum_{y \in [\kappa]^2} (\delta_i(y) + \epsilon_i(y)) \Psi_w(y) \right\}$  is sub-exponential with parameter  $(C_\delta + C_\epsilon)^4$ . It follows that

$$\mathbb{P} \left( |(86)| \geq t \right) \leq 2 \exp \left( - \frac{cNt^2}{(C_\delta + C_\epsilon)^4 + t(C_\delta + C_\epsilon)^2} \right).$$

For (87), note that  $\frac{1}{\kappa^2} \sum_{x \in [\kappa]^2} \left\{ \frac{1}{N} \sum_{i=1}^N (\delta_i(x) + \epsilon_i(x)) \Phi_v(x) \right\}$  is subGaussian with parameter  $\frac{(C_\delta + C_\epsilon)^2}{N}$  and  $\frac{1}{\kappa^2} \sum_{y \in [\kappa]^2} \left\{ (\delta_i(y) + \epsilon_i(y)) \Psi_w(y) \right\}$  is subGaussian with parameter  $(C_\delta + C_\epsilon)^2$ .

Therefore  $\frac{1}{\kappa^2} \sum_{x \in [\kappa]^2} \left\{ \frac{1}{N} \sum_{i=1}^N (\delta_i(x) + \epsilon_i(x)) \Phi_v(x) \right\} \frac{1}{\kappa^2} \sum_{y \in [\kappa]^2} \left\{ (\delta_i(y) + \epsilon_i(y)) \Psi_w(y) \right\}$  is sub-exponential with parameter  $\frac{(C_\delta + C_\epsilon)^4}{N}$ . Consequently

$$\mathbb{P}\left(|(87)| \geq t\right) \leq 2 \exp\left(-\frac{cNt^2}{(C_\delta + C_\epsilon)^4/N + t(C_\delta + C_\epsilon)^2/\sqrt{N}}\right).$$

Similarly, it holds that

$$\mathbb{P}\left(|(88)| \geq t\right) \leq 2 \exp\left(-\frac{cNt^2}{(C_\delta + C_\epsilon)^4/N + t(C_\delta + C_\epsilon)^2/\sqrt{N}}\right), \quad \text{and that}$$

$$\mathbb{P}\left(|(89)| \geq t\right) \leq 2 \exp\left(-\frac{cNt^2}{(C_\delta + C_\epsilon)^4/N^2 + t(C_\delta + C_\epsilon)^2/N}\right).$$

**Step 4.** By summarizing above four terms, the first term is dominant. Therefore,

$$\mathbb{P}\left(|v^\top(\mathbb{E}(\widehat{B}) - \widehat{B})w| \geq t\right) \leq 8 \exp\left(-\frac{cNt^2}{(C_\delta + C_\epsilon)^4 + t(C_\delta + C_\epsilon)^2}\right).$$

Let  $\mathcal{N}(\frac{1}{4}, m^2)$  be a  $1/4$  covering net of unit ball in  $\mathbb{R}^{m^2}$  and  $\mathcal{N}(\frac{1}{4}, \ell^2)$  be a  $1/4$  covering net of unit ball in  $\mathbb{R}^{\ell^2}$ , then by 4.4.3 on page 90 of [Vershynin \(2018\)](#)

$$\|\mathbb{E}(\widehat{B}) - \widehat{B}\|_{\text{op}} \leq 2 \sup_{v \in \mathcal{N}(\frac{1}{4}, m^2), w \in \mathcal{N}(\frac{1}{4}, \ell^2)} |v^\top(\mathbb{E}(\widehat{B}) - \widehat{B})w|.$$

So by union bound and the fact that the size of  $\mathcal{N}(\frac{1}{4}, m^2)$  is bounded by  $9^{m^2}$  and the size of  $\mathcal{N}(\frac{1}{4}, \ell^2)$  is bounded by  $9^{\ell^2}$ ,

$$\begin{aligned} \mathbb{P}\left(\|\mathbb{E}(\widehat{B}) - \widehat{B}\|_{\text{op}} \geq t\right) &\leq \mathbb{P}\left(\sup_{v \in \mathcal{N}(\frac{1}{4}, m^2), w \in \mathcal{N}(\frac{1}{4}, \ell^2)} |v^\top(\mathbb{E}(\widehat{B}) - \widehat{B})w| \geq \frac{t}{2}\right) \\ &\leq 9^{m^2 + \ell^2} * 16 \exp\left(-\frac{cNt^2}{(C_\delta + C_\epsilon)^4 + t(C_\delta + C_\epsilon)^2}\right). \end{aligned} \quad (90)$$

This implies that

$$\|\mathbb{E}(\widehat{B}) - \widehat{B}\|_{\text{op}} = \text{O}_{\mathbb{P}}\left(\frac{m + \ell}{\sqrt{N}} + \frac{m^2 + \ell^2}{N}\right).$$

Therefore by **Step 1** and **Step 2**

$$\begin{aligned} \|\widehat{B} - B^*\|_{\text{op}} &\leq \|\mathbb{E}(\widehat{B}) - B^*\|_{\text{op}} + \|\widehat{B} - \mathbb{E}(\widehat{B})\|_{\text{op}} = \text{O}_{\mathbb{P}}\left(\frac{m + \ell}{\sqrt{N}} + \frac{m^2 + \ell^2}{N} + \frac{1}{\kappa^2}\right) \\ &= \text{O}_{\mathbb{P}}\left(\frac{m + \ell}{\sqrt{N}} + \frac{1}{\kappa^2}\right). \end{aligned}$$

where the last equality follows from the fact that  $\frac{m + \ell}{\sqrt{N}} = o(1)$ . The desired result follows from (83).  $\square$

## F Perturbation bounds

### F.1 Compact operators on Hilbert spaces

**Lemma 14.** *Let  $A$  and  $B$  be two compact self-adjoint operators on a Hilbert space  $\mathcal{W}$ . Denote  $\lambda_k(A)$  and  $\lambda_k(A+B)$  to be the  $k$ -th eigenvalue of  $A$  and  $A+B$  respectively. Then*

$$|\lambda_k(A+B) - \lambda_k(A)| \leq \|B\|_{\text{op}}.$$

*Proof.* By the min-max principle, for any compact self-adjoint operators  $H$  and any  $S_k \subset \mathcal{W}$  being a  $k$ -dimensional subspace

$$\max_{S_k} \min_{x \in S_k, \|x\|_{\mathcal{W}}=1} H[x, x] = \lambda_k(H).$$

It follows that

$$\begin{aligned} \lambda_k(A+B) &= \max_{S_k} \min_{x \in S_k, \|x\|_{\mathcal{W}}=1} (A+B)[x, x] \\ &\leq \max_{S_k} \min_{x \in S_k, \|x\|_{\mathcal{W}}=1} A[x, x] + \|B\|_{\text{op}} \|x\|_{\mathcal{W}}^2 \\ &= \lambda_k(A) + \|B\|_{\text{op}}. \end{aligned}$$

The other direction follows from symmetry.  $\square$

For any compact operator  $H : \mathcal{W} \otimes \mathcal{W}'$ , by Theorem 13 of [Bell \(2014\)](#), there exists orthogonal basis  $\{u_k\}_{k=1}^{\infty}$  and  $\{v_k\}_{k=1}^{\infty}$  such that

$$H = \sum_{k=1}^{\infty} \sigma_k(H) u_k \otimes v_k,$$

where  $\sigma_1(H) \geq \sigma_2(H) \geq \dots \geq 0$  are the singular values of  $H$ . So

$$\lambda_k(HH^\top) = \sigma_k(H)^2. \quad (91)$$

**Lemma 15.** *Let  $\mathcal{W}$  and  $\mathcal{W}'$  be two separable Hilbert spaces. Suppose  $A$  and  $B$  are two compact operators from  $\mathcal{W} \otimes \mathcal{W}' \rightarrow \mathbb{R}$ . Then*

$$|\sigma_k(A+B) - \sigma_k(A)| \leq \|B\|_{\text{op}}.$$

*Proof.* Let  $\{\phi_i\}_{i=1}^{\infty}$  and  $\{\phi'_i\}_{i=1}^{\infty}$  be the orthogonal basis of  $\mathcal{W}$  and  $\mathcal{W}'$ . Let

$$\mathcal{W}_j = \text{Span}(\{\phi_i\}_{i=1}^j) \quad \text{and} \quad \mathcal{W}'_j = \text{Span}(\{\phi'_i\}_{i=1}^j).$$

Denote

$$A_j = A \times \mathcal{P}_{\mathcal{W}_j} \times \mathcal{P}_{\mathcal{W}'_j} \quad \text{and} \quad (A+B)_j = (A+B) \times \mathcal{P}_{\mathcal{W}_j} \times \mathcal{P}_{\mathcal{W}'_j}.$$

Note that  $(A+B)_j = A_j + B_j$  due to linearity. Since  $A$  and  $A+B$  are compact,

$$\lim_{j \rightarrow \infty} \|A - A_j\|_F = 0 \quad \text{and} \quad \lim_{j \rightarrow \infty} \|(A+B) - (A+B)_j\|_F = 0.$$

Then  $AA^\top$  and  $A_j A_j^\top$  are two compact self-adjoint operators on  $\mathcal{W}$  and that

$$\lim_{j \rightarrow \infty} \|AA^\top - A_j A_j^\top\|_F = 0.$$

By Lemma 14,  $\lim_{j \rightarrow \infty} \lambda_k(A_j A_j^\top) = \lambda_k(AA^\top)$ . Since  $\sigma_k(A_j)$  and  $\sigma_k(A)$  are both positive, by (91)

$$\lim_{j \rightarrow \infty} \sigma_k(A_j) = \sigma_k(A).$$

Similarly

$$\lim_{j \rightarrow \infty} \sigma_k((A+B)_j) = \sigma_k(A+B).$$

By the finite dimensional SVD perturbation theory (see Theorem 3.3.16 on page 178 of Horn and Johnson (1994)), it follows that

$$|\sigma_k((A+B)_j) - \sigma_k(A_j)| \leq \|B_j\|_{\text{op}} \leq \|B\|_{\text{op}}.$$

The desired result follows by taking the limit as  $j \rightarrow \infty$ . □

## F.2 Subspace perturbation bounds

**Theorem 6** (Wedin). *Suppose without loss of generality that  $n_1 \leq n_2$ . Let  $M = M^* + E$ ,  $M^*$  be two matrices in  $\mathbb{R}^{n_1 \times n_2}$  whose svd are given respectively by*

$$M^* = \sum_{i=1}^{n_1} \sigma_i^* u_i^* v_i^{*\top} \quad \text{and} \quad M = \sum_{i=1}^{n_1} \sigma_i u_i v_i^\top$$

where  $\sigma_1^* \geq \dots \geq \sigma_{n_1}^*$  and  $\sigma_1 \geq \dots \geq \sigma_{n_1}$ . For any  $r \leq n_1$ , let

$$\Sigma^* = \text{diag}([\sigma_1^*, \dots, \sigma_r^*]) \in \mathbb{R}^{r \times r}, \quad U^* = [u_1^*, \dots, u_r^*] \in \mathbb{R}^{n_1 \times r}, \quad V = [v_1^*, \dots, v_r^*] \in \mathbb{R}^{n_2 \times r}, \\ \Sigma = \text{diag}([\sigma_1, \dots, \sigma_r]) \in \mathbb{R}^{r \times r}, \quad U = [u_1, \dots, u_r] \in \mathbb{R}^{n_1 \times r}, \quad V = [v_1, \dots, v_r] \in \mathbb{R}^{n_2 \times r}.$$

Denote  $\mathcal{P}_{U^*} = \sum_{i=1}^r u_i^* \otimes u_i^*$  and  $\mathcal{P}_U = \sum_{i=1}^r u_i \otimes u_i$ . If  $\|E\|_{\text{op}} < \sigma_r^* - \sigma_{r+1}^*$ , then

$$\|\mathcal{P}_{U^*} - \mathcal{P}_U\|_{\text{op}} \leq \frac{\sqrt{2} \max\{\|U^* E\|_{\text{op}}, \|E V^*\|_{\text{op}}\}}{\sigma_r^* - \sigma_{r+1}^* - \|E\|_{\text{op}}}.$$

*Proof.* This follows from Lemma 2.6 and Theorem 2.9 of Chen et al. (2021). □

**Corollary 4.** *Let  $\mathcal{W}$  and  $\mathcal{W}'$  be two Hilbert spaces. Let  $M$  and  $E$  be two finite rank operators on  $\mathcal{W} \otimes \mathcal{W}'$  and denote  $M = M^* + E$ . Let the SVD of  $M^*$  and  $M$  are given respectively by*

$$M^* = \sum_{i=1}^{r_1} \sigma_i^* u_i^* \otimes v_i^* \quad \text{and} \quad M = \sum_{i=1}^{r_2} \sigma_i u_i \otimes v_i$$

where  $\sigma_1^* \geq \dots \geq \sigma_{r_1}^*$  and  $\sigma_1 \geq \dots \geq \sigma_{r_2}$ . For  $r \leq \min\{r_1, r_2\}$ , denote

$$U^* = \text{Span}(\{u_i^*\}_{i=1}^r) \quad \text{and} \quad U = \text{Span}(\{u_i\}_{i=1}^r)$$

Let  $\mathcal{P}_{U^*}$  to be projection matrix from  $\mathcal{W}$  to  $U^*$ , and  $\mathcal{P}_U$  to be projection matrix from  $\mathcal{W}$  to  $U$ . If  $\|E\|_{\text{op}} < \sigma_r^* - \sigma_{r+1}^*$ , then

$$\|\mathcal{P}_{U^*} - \mathcal{P}_U\|_{\text{op}} \leq \frac{\sqrt{2} \max\{\|E \times_1 U^*\|_{\text{op}}, \|E \times_2 V^*\|_{\text{op}}\}}{\sigma_r^* - \sigma_{r+1}^* - \|E\|_{\text{op}}} \leq \frac{\sqrt{2} \|E\|_{\text{op}}}{\sigma_r^* - \sigma_{r+1}^* - \|E\|_{\text{op}}}.$$

*Proof.* Let

$$\mathcal{S} = \text{Span}(\{u_i^*\}_{i=1}^{r_1}, \{u_i\}_{i=1}^{r_2}) \quad \text{and} \quad \mathcal{S}' = \text{Span}(\{v_i^*\}_{i=1}^{r_1}, \{v_i\}_{i=1}^{r_2}).$$

Then  $M^*$  and  $M$  can be viewed as finite-dimensional matrices on  $\mathcal{S} \otimes \mathcal{S}'$ . Since  $\mathcal{P}_{U^*} = \sum_{i=1}^r u_i^* \otimes u_i^*$  and  $\mathcal{P}_U = \sum_{i=1}^r u_i \otimes u_i$ , the desired result follows from Theorem 6. □

## G Additional technical results

**Lemma 16.** For positive integers  $\{s_j\}_{j=1}^d \in \mathbb{N}$ , let  $\Omega_j \subset \mathbb{R}^{s_j}$ . Let  $B \in \mathbf{L}_2(\Omega_1) \otimes \mathbf{L}_2(\Omega_2) \cdots \otimes \mathbf{L}_2(\Omega_d)$  and for  $1 \leq j \leq d$ , let  $\mathcal{Q}_j \in \mathbf{L}_2(\Omega_j) \otimes \mathbf{L}_2(\Omega_j)$  be a collection of operators such that  $\|\mathcal{Q}_j\|_F < \infty$ . Then

$$\|B \times_1 \mathcal{Q}_1 \cdots \times_d \mathcal{Q}_d\|_F \leq \|B\|_F \|\mathcal{Q}_1\|_{\text{op}} \cdots \|\mathcal{Q}_d\|_{\text{op}}$$

*Proof.* By Theorem 3, we can write

$$\mathcal{Q}_j = \sum_{\mu_j=1}^{\infty} \nu_{j,\mu_j} \phi_{j,\mu_j} \otimes \psi_{j,\mu_j},$$

where  $\{\psi_{j,\mu_j}\}_{\mu_j=1}^{\infty}$  and  $\{\phi_{j,\mu_j}\}_{\mu_j=1}^{\infty}$  are both orthonormal in  $\mathbf{L}_2(\Omega_j)$ . Note that  $|\nu_{j,\mu_j}| \leq \|\mathcal{Q}_j\|_{\text{op}}$ . Therefore

$$\begin{aligned} \|B \times_1 \mathcal{Q}_1 \cdots \times_d \mathcal{Q}_d\|_F^2 &= \sum_{\mu_1, \dots, \mu_d=1}^{\infty} \{B \times_1 \mathcal{Q}_1 \cdots \times_d \mathcal{Q}_d[\psi_{1,\mu_1}, \dots, \psi_{d,\mu_d}]\}^2 \\ &= \sum_{\mu_1, \dots, \mu_d=1}^{\infty} \{B[\mathcal{Q}_1(\psi_{1,\mu_1}), \dots, \mathcal{Q}_d(\psi_{d,\mu_d})]\}^2 \\ &= \sum_{\mu_1, \dots, \mu_d=1}^{\infty} \{B[\nu_{1,\mu_1} \phi_{1,\mu_1}, \dots, \nu_{d,\mu_d} \phi_{d,\mu_d}]\}^2 \\ &\leq \|\mathcal{Q}_1\|_{\text{op}}^2 \cdots \|\mathcal{Q}_d\|_{\text{op}}^2 \sum_{\mu_1, \dots, \mu_d=1}^{\infty} \{B[\phi_{1,\mu_1}, \dots, \phi_{d,\mu_d}]\}^2 \\ &= \|\mathcal{Q}_1\|_{\text{op}}^2 \cdots \|\mathcal{Q}_d\|_{\text{op}}^2 \|B\|_F^2. \end{aligned}$$

□

**Lemma 17.** For  $j = 1, \dots, d$ , let  $\{\phi_{j,i}\}_{i=1}^{\infty}$  be a collection of orthogonal basis function of  $\mathbf{L}_2(\Omega_j)$ . Suppose  $A \in \mathbf{L}_2(\Omega_1) \otimes \cdots \otimes \mathbf{L}_2(\Omega_d)$  is such that  $\|A\|_F < \infty$ . Then  $A$  is a function in  $\mathbf{L}_2(\Omega_1 \times \cdots \times \Omega_d)$  and that

$$A(z_1, \dots, z_d) = \sum_{i_1, \dots, i_d=1}^{\infty} A[\phi_{1,i_1}, \dots, \phi_{d,i_d}] \phi_{1,i_1}(z_1) \cdots \phi_{d,i_d}(z_d). \quad (92)$$

Note that (92) is independent of choices of basis functions.

*Proof.* This is a classical functional analysis result. □

**Lemma 18.** For  $k \leq d$ , let  $x = (z_1, \dots, z_k) \in \Omega_1 \times \cdots \times \Omega_k$  and  $y = (z_{k+1}, \dots, z_d) \in \Omega_{k+1} \times \cdots \times \Omega_d$ . Let  $A = A(x, y) \in \mathbf{L}_2(\Omega_1 \times \cdots \times \Omega_k) \otimes \mathbf{L}_2(\Omega_{k+1} \times \cdots \times \Omega_d)$ . For  $1 \leq j \leq k$ , let  $\mathcal{U}_j \subset \mathbf{L}_2(\Omega_j)$  be a collection of subspaces and  $\mathcal{U}_x \subset \mathbf{L}_2(\Omega_1 \times \cdots \times \Omega_k)$  is such that  $\mathcal{U}_x = \mathcal{U}_1 \otimes \cdots \otimes \mathcal{U}_k$ , then

$$A \times_x \mathcal{P}_{\mathcal{U}_x} = A \times_1 \mathcal{P}_{\mathcal{U}_1} \cdots \times_k \mathcal{P}_{\mathcal{U}_k}. \quad (93)$$

*Proof.* For generic functions  $f_j \in \mathbf{L}_2(\Omega_j)$ , it holds that

$$\mathcal{P}_{\mathcal{U}_x}[f_1, \dots, f_k](z_1, \dots, z_d) = \mathcal{P}_{\mathcal{U}_1}(f_1)(z_1) \cdots \mathcal{P}_{\mathcal{U}_k}(f_k)(z_k).$$

Therefore (93) follows from the observation that

$$\begin{aligned} & A \times_x \mathcal{P}_{\mathcal{U}_x}[f_1, \dots, f_k, f_{k+1}, \dots, f_d] \\ &= A[\mathcal{P}_{\mathcal{U}_x}(f_1, \dots, f_k), f_{k+1}, \dots, f_d] \\ &= A[\mathcal{P}_{\mathcal{U}_1}(f_1), \dots, \mathcal{P}_{\mathcal{U}_k}(f_k), f_{k+1}, \dots, f_d] \\ &= A \times_1 \mathcal{P}_{\mathcal{U}_1} \cdots \times_k \mathcal{P}_{\mathcal{U}_k}[f_1, \dots, f_k, f_{k+1}, \dots, f_d]. \end{aligned}$$

□

**Lemma 19.** Let  $A \in \mathbf{L}_2(\Omega_1) \otimes \cdots \otimes \mathbf{L}_2(\Omega_d)$  be any tensor. For  $j = 1, \dots, d$ , suppose

$$\text{Range}_j(A) = \text{Span}\{u_{j,\rho_j}\}_{\rho_j=1}^{r_j},$$

where  $\{u_{j,\rho_j}\}_{\rho_j=1}^{r_j}$  are orthonormal functions in  $\mathbf{L}_2(\Omega_j)$ . Then

$$A(z_1, \dots, z_d) = \sum_{\rho_1=1}^{r_1} \cdots \sum_{\rho_d=1}^{r_d} A[u_{1,\rho_1}, \dots, u_{d,\rho_d}] u_{1,\rho_1}(z_1) \cdots u_{d,\rho_d}(z_d).$$

Therefore the core size of the tensor  $A$  is  $\prod_{j=1}^d r_j$ .

*Proof.* It suffices to observe that as a linear map,  $A$  is 0 in the orthogonal complement the subspace  $\text{Range}_1(A) \otimes \cdots \otimes \text{Range}_d(A)$  and  $\{u_{1,\rho_1}(z_1) \cdots u_{d,\rho_d}(z_d)\}_{\rho_1=1, \dots, \rho_d=1}^{r_1, \dots, r_d}$  are the orthonormal basis of  $\text{Range}_1(A) \otimes \cdots \otimes \text{Range}_d(A)$ . □

**Lemma 20.** Let  $\mathcal{M}$  be linear subspace of  $\mathbf{L}_2(\Omega_1)$  spanned by the orthonormal basis function  $= \text{Span}\{v_\mu(x)\}_{\mu=1}^{\dim(\mathcal{M})}$ . Suppose  $g : \Omega_1 \rightarrow \mathbb{R}$  is a generic function in  $\mathbf{L}_2(\Omega_1)$ . If

$$\tilde{g}(x) = \arg \min_{f \in \mathcal{M}} \|g(x) - f(x)\|_{\mathbf{L}_2(\Omega_1)}^2,$$

Then  $\tilde{g}(x) = \sum_{\mu=1}^{\dim(\mathcal{M})} a_\mu v_\mu(x)$ , where

$$a_\mu = \langle g, v_\mu \rangle = \int_{\Omega_1} g(x) v_\mu(x) dx.$$

*Proof.* This is a well-known projection property in Hilbert space. □

## H Extension: multivariable nonparametric regression

In this section, we apply our sketching estimator to study the nonparametric regression models. To begin, suppose the observed data  $\{W_i, Z_i\}_{i=1}^N \subset \mathbb{R} \times \mathbb{R}^d$  satisfy

$$W_i = f^*(Z_i) + \epsilon_i, \tag{94}$$

where  $\{\epsilon_i\}_{i=1}^N$  are measurement errors and  $f^* : [0, 1]^d \rightarrow \mathbb{R}$  is the unknown regression function. We first present our theory assuming that the random design  $\{Z_i\}_{i=1}^N$  are independently sampled from the uniform density on the domain  $[0, 1]^d$  in Corollary 5. The general setting, where  $\{Z_i\}_{i=1}^N$  are sampled from an unknown generic density function, will be discussed in Corollary 6.

Let  $\hat{f}$  be the estimator such that for any non-random function  $G \in \mathbf{L}_2([0, 1]^d)$ ,

$$\langle \hat{f}, G \rangle = \frac{1}{N} \sum_{i=1}^N W_i G(Z_i). \quad (95)$$

where  $G(Z_i)$  is the value of function  $G$  evaluated at the sample point  $Z_i \in [0, 1]^d$ . In the following corollary, we formally summarize the statistical guarantee of the regression function estimator detailed in Algorithm 2.

**Corollary 5.** *Suppose the observed data  $\{W_i, Z_i\}_{i=1}^N \in \mathbb{R} \times [0, 1]^d$  satisfy (94), where  $\{\epsilon_i\}_{i=1}^N$  are i.i.d. centered subGaussian noise with subGaussian parameter  $C_\epsilon$ ,  $\{Z_i\}_{i=1}^N$  are independently sampled from the uniform density distribution on  $[0, 1]^d$ , and that  $\|f^*\|_{W_2^\alpha([0, 1]^d)} < \infty$  with  $\alpha \geq 1$  and  $\|f^*\|_\infty < \infty$ .*

*Suppose in addition that  $f^*$  satisfies Assumption 3, and that  $\{\mathcal{M}_j, \mathcal{L}_j\}_{j=1}^d$  are in the form of (24) and (25), where  $\{\phi_k^\mathbb{S}\}_{k=1}^\infty \subset \mathbf{L}_2([0, 1])$  are derived from reproducing kernel Hilbert spaces, the Legendre polynomial basis, or spline basis functions.*

*Let  $\hat{f}$  in (95),  $\{r_j\}_{j=1}^d$ , and  $\{\mathcal{M}_j, \mathcal{L}_j\}_{j=1}^d$  be the input of Algorithm 2, and  $\hat{f} \times_1 \hat{\mathcal{P}}_1 \cdots \times_d \hat{\mathcal{P}}_d$  be the corresponding output. Denote  $\sigma_{\min} = \min_{j=1, \dots, d} \{\sigma_{j, r_j}\}$  and suppose for a sufficiently large constant  $C_{snr}$ ,*

$$N^{2\alpha/(2\alpha+1)} > C_{snr} \max \left\{ \prod_{j=1}^d r_j, \frac{1}{\sigma_{\min}^{(d-1)/\alpha+2}}, \frac{1}{\sigma_{\min}^{2\alpha/(\alpha-1/2)}} \right\}.$$

*If  $\ell_j = C_L \sigma_{j, r_j}^{-1/\alpha}$  for some sufficiently large constant  $C_L$  and  $m \asymp N^{1/(2\alpha+1)}$ , then it holds that*

$$\|\hat{f} \times_1 \hat{\mathcal{P}}_1 \cdots \times_d \hat{\mathcal{P}}_d - f^*\|_{\mathbf{L}_2([0, 1]^d)}^2 = \mathcal{O}_{\mathbb{P}} \left( \frac{\sum_{j=1}^d \sigma_{j, r_j}^{-2}}{N^{2\alpha/(2\alpha+1)}} + \frac{\sum_{j=1}^d \sigma_{j, r_j}^{-(d-1)/\alpha-2}}{N} + \frac{\prod_{j=1}^d r_j}{N} \right). \quad (96)$$

*Proof.* Assumption 2 is verified in Appendix B.1 for reproducing kernel Hilbert space, Appendix B.2 for Legendre polynomials, and Appendix B.3 for spline basis. Assumption 4 is shown in Lemma 21. Therefore all the conditions in Theorem 5 are met and Corollary 5 immediately follows.  $\square$

In the following result, we extend our approach to the general setting where the random designs  $\{Z_i\}_{i=1}^N$  are sampled from a generic density function  $p^* : [0, 1]^d \rightarrow \mathbb{R}^+$ . To achieve consistent regression estimation in this context, we propose adjusting our estimator to incorporate an additional density estimator. This modification aligns with techniques commonly used in classical nonparametric methods, such as the Nadaraya–Watson kernel regression estimator.

**Corollary 6.** Suppose  $\{Z_i\}_{i=1}^N$  are random designs independently sampled from a common density function  $p^* : [0, 1]^d \rightarrow \mathbb{R}^+$  such that  $p^*(z_1, \dots, z_d) \geq c^*$  for all  $(z_1, \dots, z_d) \in [0, 1]^d$  where  $c^* > 0$  is a universal positive constant. Let

$$\tilde{f} = \hat{f} \times_1 \hat{\mathcal{P}}_1 \cdots \times_d \hat{\mathcal{P}}_d,$$

where  $\hat{f} \times_1 \hat{\mathcal{P}}_1 \cdots \times_d \hat{\mathcal{P}}_d$  is defined in Corollary 5, and  $\tilde{p}$  is any generic density estimator of  $p^*$ . Denote  $\tilde{p}' = \max\left\{\frac{1}{\sqrt{\log(N)}}, \tilde{p}\right\}$ . Suppose in addition that all of the other conditions in Corollary 5 hold. Then

$$\begin{aligned} & \left\| \frac{\tilde{f}}{\tilde{p}'} - f^* \right\|_{\mathbf{L}_2([0,1]^d)}^2 \\ &= O_{\mathbb{P}} \left( \log(N) \left\{ \frac{\sum_{j=1}^d \sigma_{j,r_j}^{-2}}{N^{2\alpha/(2\alpha+1)}} + \frac{\sum_{j=1}^d \sigma_{j,r_j}^{-(d-1)/\alpha-2}}{N} + \frac{\prod_{j=1}^d r_j}{N} \right\} + \log(N) \|p^* - \tilde{p}\|_{\mathbf{L}_2([0,1]^d)}^2 \right). \end{aligned}$$

Note that if  $p^*$  is also a low-rank density function, then we can estimate  $p^*$  via Algorithm 2 with a reduced curse of dimensionality. Consequently, the regression function  $f^*$  can be estimated with a reduced curse of dimensionality even when the random designs are sampled from a non-uniform density.

*Proof of Corollary 6.* Suppose  $N$  is sufficient large so that  $\frac{1}{\sqrt{\log(N)}} \leq c^*$ . Let  $Z$  be a generic element in  $[0, 1]^d$ . Based on the definition,  $\tilde{p}' = \max\left\{\frac{1}{\sqrt{\log(N)}}, \tilde{p}\right\}$ . Thus, when  $\tilde{p}(Z) \geq \frac{1}{\sqrt{\log(N)}}$ ,  $\tilde{p}'(Z) - p^*(Z) = \tilde{p}(Z) - p^*(Z)$ . When  $\tilde{p}(Z) < \frac{1}{\sqrt{\log(N)}}$ , note that

$$|p^*(Z) - \tilde{p}'(Z)| = \left| p^*(Z) - \frac{1}{\sqrt{\log(N)}} \right| = p^*(Z) - \frac{1}{\sqrt{\log(N)}} \leq p^*(Z) - \tilde{p}(Z) = |p^*(Z) - \tilde{p}(Z)|$$

where the first equality follows from  $\tilde{p}'(Z) = \frac{1}{\sqrt{\log(N)}}$ , the second equality follows from  $p^*(Z) \geq c^* \geq \frac{1}{\sqrt{\log(N)}}$ , the inequality follows from  $\tilde{p}(Z) < \frac{1}{\sqrt{\log(N)}}$  and the last equality follows from  $p^*(Z) \geq c^* \geq \frac{1}{\sqrt{\log(N)}} \geq \tilde{p}(Z)$ . Therefore  $|\tilde{p}'(Z) - p^*(Z)| \leq |\tilde{p}(Z) - p^*(Z)|$  for all  $Z \in [0, 1]^d$  and it follows that

$$\|\tilde{p}' - p^*\|_{\mathbf{L}_2([0,1]^d)} \leq \|\tilde{p} - p^*\|_{\mathbf{L}_2([0,1]^d)}. \quad (97)$$

By Corollary 5,

$$\|\tilde{f} - f^* p^*\|_{\mathbf{L}_2([0,1]^d)}^2 = O_{\mathbb{P}} \left( \frac{\sum_{j=1}^d \sigma_{j,r_j}^{-2}}{N^{2\alpha/(2\alpha+1)}} + \frac{\sum_{j=1}^d \sigma_{j,r_j}^{-(d-1)/\alpha-2}}{N} + \frac{\prod_{j=1}^d r_j}{N} \right). \quad (98)$$

Therefore

$$\left\| \frac{\tilde{f}}{\tilde{p}'} - f^* \right\|_{\mathbf{L}_2([0,1]^d)} \leq \left\| \frac{\tilde{f}}{\tilde{p}'} - \frac{f^* p^*}{\tilde{p}'} \right\|_{\mathbf{L}_2([0,1]^d)} + \left\| \frac{f^* p^*}{\tilde{p}'} - f^* \right\|_{\mathbf{L}_2([0,1]^d)}. \quad (99)$$

The desired result follows from the observation that

$$\begin{aligned} & \left\| \frac{\tilde{f}}{\tilde{p}'} - \frac{f^* p^*}{\tilde{p}'} \right\|_{\mathbf{L}_2([0,1]^d)}^2 \leq \left\| \frac{1}{\tilde{p}'} \right\|_{\infty}^2 \|\tilde{f} - f^* p^*\|_{\mathbf{L}_2([0,1]^d)}^2 \\ &= O_{\mathbb{P}} \left( \log(N) \left\{ \frac{\sum_{j=1}^d \sigma_{j,r_j}^{-2}}{N^{2\alpha/(2\alpha+1)}} + \frac{\sum_{j=1}^d \sigma_{j,r_j}^{-(d-1)/\alpha-2}}{N} + \frac{\prod_{j=1}^d r_j}{N} \right\} \right) \end{aligned}$$

and that

$$\begin{aligned} & \left\| \frac{f^* p^*}{\tilde{p}'} - f^* \right\|_{\mathbf{L}_2([0,1]^d)} = \left\| f^* \left( \frac{p^*}{\tilde{p}'} - 1 \right) \right\|_{\mathbf{L}_2([0,1]^d)} = \left\| f^* \left( \frac{p^* - \tilde{p}'}{\tilde{p}'} \right) \right\|_{\mathbf{L}_2([0,1]^d)} \\ & \leq \left\| \frac{f^*}{\tilde{p}'} \right\|_{\infty} \|p^* - \tilde{p}'\|_{\mathbf{L}_2([0,1]^d)} \leq \|f^*\|_{\infty} \sqrt{\log(N)} \|p^* - \tilde{p}'\|_{\mathbf{L}_2([0,1]^d)} \leq \|f^*\|_{\infty} \sqrt{\log(N)} \|p^* - \tilde{p}'\|_{\mathbf{L}_2([0,1]^d)}, \end{aligned}$$

where the last inequality follows from (97).  $\square$

## H.1 Additional technical results for regression

**Lemma 21.** *Let  $\hat{f}$  be defined as in (95). Suppose all the conditions in Corollary 5 holds. Then  $\hat{f}$  satisfies Assumption 4.*

*Proof.* Note that  $\{Z_i\}_{i=1}^N$  are sampled from the uniform density and that  $\mathbb{E}(\epsilon_1) = 0$ ,  $\text{Var}(\epsilon_1) \leq C_\epsilon$ . Therefore

$$\mathbb{E}(\langle \hat{f}, G \rangle) = \mathbb{E}(w_1 G(Z_1) + f^*(Z_1)G(Z_1)) = \int f_*(z)G(z)dz = \langle f_*, G \rangle,$$

where the second equality holds since  $\epsilon$  and  $Z$  are independent. Suppose  $\|G\|_{\mathbf{L}_2} = 1$ . Then

$$\begin{aligned} \text{Var}(\langle \hat{f}, G \rangle) &= \frac{1}{N} \text{Var}(\epsilon_1 G(Z_1) + f^*(Z_1)G(Z_1)) = \frac{1}{N} \text{Var}(\epsilon_1 G(Z_1)) + \frac{1}{N} \text{Var}(f^*(Z_1)G(Z_1)) \\ &\leq \frac{1}{N} \left( \mathbb{E}(\epsilon_1^2 G(Z_1)^2) + \mathbb{E}\{f^*(Z_1)G(Z_1)\}^2 \right) = \frac{1}{N} \mathbb{E}(\epsilon_1^2) \int_{[0,1]^d} G^2(z)dz + \frac{1}{N} \int \{f^*(z)G(z)\}^2 dz \\ &\leq \frac{1}{N} C_\epsilon \|G\|_{\mathbf{L}_2}^2 + \frac{1}{N} \|f^*\|_{\infty}^2 \|G\|_{\mathbf{L}_2}^2 = O\left(\frac{1}{N}\right). \end{aligned}$$

$\square$

**Lemma 22.** *Let  $d_1, d_2 \in \mathbb{Z}^+$  be such that  $d_1 + d_2 = d$ . Suppose  $\{\phi_k^{\mathbb{S}}\}_{k=1}^{\infty}$  be a collection of  $\mathbf{L}_2$  basis such that  $\|\phi_k^{\mathbb{S}}\|_{\infty} \leq C_{\mathbb{S}}$ . For positive integers  $m$  and  $\ell$ , denote*

$$\mathcal{M} = \text{span} \left\{ \phi_{\mu_1}^{\mathbb{S}}(z_1) \cdots \phi_{\mu_{d_1}}^{\mathbb{S}}(z_{d_1}) \right\}_{\mu_1, \dots, \mu_{d_1}=1}^m \quad \text{and} \quad \mathcal{L} = \text{span} \left\{ \phi_{\eta_1}^{\mathbb{S}}(z_{d_1+1}) \cdots \phi_{\eta_{d_2}}^{\mathbb{S}}(z_d) \right\}_{\eta_1, \dots, \eta_{d_2}=1}^{\ell}. \quad (100)$$

Then it holds that

$$\|(\hat{f} - f^*) \times_x \mathcal{P}_{\mathcal{M}} \times_y \mathcal{P}_{\mathcal{L}}\|_{\text{op}} = O_{\mathbb{P}} \left( \sqrt{\frac{m^{d_1} + \ell^{d_2}}{N}} + \frac{\sqrt{m^{3d_1} \ell^{d_2} \log(N)}}{N} + \frac{\sqrt{m^{d_1} \ell^{3d_2} \log(N)}}{N} \right).$$

*Proof.* Similar to Lemma 9, by ordering the indexes  $(\mu_1, \dots, \mu_{d_1})$  and  $(\eta_1, \dots, \eta_{d_2})$  in (100), we can also write

$$\mathcal{M} = \text{span}\{\Phi_{\mu}(x)\}_{\mu=1}^{m^{d_1}} \quad \text{and} \quad \mathcal{L} = \text{span}\{\Psi_{\eta}(y)\}_{\eta=1}^{\ell^{d_2}}. \quad (101)$$

Note that  $\widehat{f} \times_x \mathcal{P}_{\mathcal{M}} \times_y \mathcal{P}_{\mathcal{L}}$  and  $f^* \times_x \mathcal{P}_{\mathcal{M}} \times_y \mathcal{P}_{\mathcal{L}}$  are both zero in the orthogonal complement of the subspace  $\mathcal{M} \otimes \mathcal{L}$ . Let  $\widehat{B}$  and  $B^*$  be two matrices in  $\mathbb{R}^{m^{d_1} \times \ell^{d_2}}$  such that

$$\widehat{B}_{\mu,\eta} = \widehat{f}[\Phi_\mu, \Psi_\eta] = \frac{1}{N} \sum_{i=1}^N W_i \Phi_\mu(X_i) \Psi_\eta(Y_i) \quad \text{and} \quad B_{\mu,\eta}^* = f^*[\Phi_\mu, \Psi_\eta] = \mathbb{E}(\widehat{f}[\Phi_\mu, \Psi_\eta]),$$

where  $X_i = (Z_{i,1}, \dots, Z_{i,d_1}) \in \mathbb{R}^{d_1}$  and  $Y_i = (Z_{i,d_1+1}, \dots, Z_{i,d}) \in \mathbb{R}^{d_2}$ . Therefore

$$\|\widehat{B} - B^*\|_{\text{op}} = \|(\widehat{f} - f^*) \times_x \mathcal{P}_{\mathcal{M}} \times_y \mathcal{P}_{\mathcal{L}}\|_{\text{op}}. \quad (102)$$

Since  $\{\epsilon_i\}_{i=1}^N$  are subGaussian, it follows from a union bound argument that there exists a sufficiently large constant  $C_1$  such that

$$\mathbb{P}\left(\max_{1 \leq i \leq N} |\epsilon_i| \leq C_1 \sqrt{\log(N)}\right) \geq 1 - N^{-1}. \quad (103)$$

The following procedures are similar to Lemma 9, but we need to estimate the variance brought by additional random variables  $\epsilon_i$  here.

**Step 1.** Let  $v = (v_1, \dots, v_{m^{d_1}}) \in \mathbb{R}^{m^{d_1}}$  and suppose that  $\|v\|_2 = 1$ . Then by orthonormality of  $\{\Phi_\mu(x)\}_{\mu=1}^{m^{d_1}}$  in  $\mathbf{L}_2$  it follows that

$$\left\| \sum_{\mu=1}^{m^{d_1}} v_\mu \Phi_\mu \right\|_{\mathbf{L}_2([0,1]^{d_1})}^2 = 1.$$

In addition, since

$$\|\phi_{\mu_1}^{\mathbb{S}}(z_1) \cdots \phi_{\mu_{d_1}}^{\mathbb{S}}(z_{d_1})\|_{\infty} \leq \prod_{j=1}^{d_1} \|\phi_{\mu_j}^{\mathbb{S}}\|_{\infty} \leq C_{\mathbb{S}}^{d_1},$$

it follows that  $\|\Phi_\mu\|_{\infty} \leq C_{\mathbb{S}}^{d_1}$  for all  $1 \leq \mu \leq m^{d_1}$  and

$$\left\| \sum_{\mu=1}^{m^{d_1}} v_\mu \Phi_\mu \right\|_{\infty} \leq \sqrt{\sum_{\mu=1}^{m^{d_1}} v_\mu^2} \sqrt{\sum_{\mu=1}^{m^{d_1}} \|\Phi_\mu\|_{\infty}^2} = O(\sqrt{m^{d_1}}).$$

**Step 2.** Let  $w = (w_1, \dots, w_{\ell^{d_2}}) \in \mathbb{R}^{\ell^{d_2}}$  and suppose that  $\|w\|_2 = 1$ . Then by orthonormality of  $\{\Psi_\eta(y)\}_{\eta=1}^{\ell^{d_2}}$  in  $\mathbf{L}_2([0,1]^{d_2})$ ,

$$\left\| \sum_{\eta=1}^{\ell^{d_2}} w_\eta \Psi_\eta \right\|_{\mathbf{L}_2([0,1]^{d_2})}^2 = 1.$$

In addition, since

$$\|\phi_{\eta_1}^{\mathbb{S}}(z_{d_1+1}) \cdots \phi_{\eta_{d_2}}^{\mathbb{S}}(z_d)\|_{\infty} \leq \prod_{j=1}^{d_2} \|\phi_{\eta_j}^{\mathbb{S}}\|_{\infty} \leq C_{\mathbb{S}}^{d_2},$$

it follows that  $\|\Psi_\eta\|_{\infty} \leq C_{\mathbb{S}}^{d_2}$ . Therefore

$$\left\| \sum_{\eta=1}^{\ell^{d_2}} w_\eta \Psi_\eta \right\|_{\infty} \leq \sqrt{\sum_{\eta=1}^{\ell^{d_2}} w_\eta^2} \sqrt{\sum_{\eta=1}^{\ell^{d_2}} \|\Psi_\eta\|_{\infty}^2} = O(\sqrt{\ell^{d_2}}).$$

**Step 3.** For fixed  $v = (v_1, \dots, v_{m^{d_1}})$  and  $w = (w_1, \dots, w_{\ell^{d_2}})$ , we bound  $v^\top (A^* - \widehat{A})w$ . Let  $\Delta_i = \sum_{\mu=1}^{m^{d_1}} v_\mu \Phi_\mu(X_i) \sum_{\eta=1}^{\ell^{d_2}} w_\eta \Psi_\eta(Y_i) (f(X_i, Y_i) + \epsilon_i)$ . Since the measurement errors  $\{\epsilon_i\}_{i=1}^N$  and the random designs  $\{X_i, Y_i\}_{i=1}^N$  are independent, it follows that

$$\begin{aligned} \text{Var}(\Delta_i) &\leq \mathbb{E}(\Delta_i^2) = \iint \left\{ \sum_{\mu=1}^{m^{d_1}} v_\mu \Phi_\mu(x) \right\}^2 \left\{ \sum_{\eta=1}^{\ell^{d_2}} w_\eta \Psi_\eta(y) \right\}^2 (f^*(x, y) + \mathbb{E}(\epsilon_i)^2) dx dy \\ &\leq 2 \left( \|f^*\|_\infty^2 + C_\epsilon \right) \int \left\{ \sum_{\mu=1}^{m^{d_1}} v_\mu \Phi_\mu(x) \right\}^2 dx \int \left\{ \sum_{\eta=1}^{\ell^{d_2}} w_\eta \Psi_\eta(y) \right\}^2 dy \\ &= 2 \left( \|f^*\|_\infty^2 + C_\epsilon \right) \left\| \sum_{\mu=1}^{m^{d_1}} v_\mu \Phi_\mu(x) \right\|_{\mathbf{L}_2([0,1]^{d_1})}^2 \left\| \sum_{\eta=1}^{\ell^{d_2}} w_\eta \Psi_\eta(y) \right\|_{\mathbf{L}_2([0,1]^{d_2})}^2 = 2 \left( \|f^*\|_\infty^2 + C_\epsilon \right). \end{aligned}$$

where the last equality follows from **Step 1** and **Step 2**. In addition, suppose the good event in (103) holds. Then uniformly for all  $1 \leq i \leq N$ ,

$$|\Delta_i| \leq \left\| \sum_{\mu=1}^{m^{d_1}} v_\mu \Phi_\mu(X_i) \right\|_\infty \left\| \sum_{\eta=1}^{\ell^{d_2}} w_\eta \Psi_\eta(Y_i) \right\|_\infty (\|f^*\|_\infty + |\epsilon_i|) = O(\sqrt{m^{d_1} \ell^{d_2}} |\epsilon_i|) = O(\sqrt{m^{d_1} \ell^{d_2}} \sqrt{\log(N)}).$$

So for given  $v, w$ , by Bernstein's inequality

$$\begin{aligned} \mathbb{P}_{Z|\epsilon} \left( \left| v^\top (B^* - \widehat{B})w \right| \geq t \right) &= \mathbb{P}_{Z|\epsilon} \left( \left| \frac{1}{N} \sum_{i=1}^N \Delta_i - \mathbb{E}(\Delta_i) \right| \geq t \right) \\ &\leq 2 \exp \left( \frac{-cNt^2}{\|f^*\|_\infty^2 + C_\epsilon + t\sqrt{m^{d_1} \ell^{d_2} \log(N)}} \right). \end{aligned}$$

**Step 4.** Let  $\mathcal{N}(\frac{1}{4}, m^{d_1})$  be a  $1/4$  covering net of unit ball in  $\mathbb{R}^{m^{d_1}}$  and  $\mathcal{N}(\frac{1}{4}, \ell^{d_2})$  be a  $1/4$  covering net of unit ball in  $\mathbb{R}^{\ell^{d_2}}$ , then by 4.4.3 on page 90 of Vershynin (2018)

$$\|B^* - \widehat{B}\|_{\text{op}} \leq 2 \sup_{v \in \mathcal{N}(\frac{1}{4}, m^{d_1}), w \in \mathcal{N}(\frac{1}{4}, \ell^{d_2})} v^\top (B^* - \widehat{B})w.$$

So by union bound and the fact that the size of  $\mathcal{N}(\frac{1}{4}, m^{d_1})$  is bounded by  $9^{m^{d_1}}$  and the size of  $\mathcal{N}(\frac{1}{4}, \ell^{d_2})$  is bounded by  $9^{\ell^{d_2}}$ ,

$$\begin{aligned} \mathbb{P} \left( \|B^* - \widehat{B}\|_{\text{op}} \geq t \right) &\leq \mathbb{P} \left( \sup_{v \in \mathcal{N}(\frac{1}{4}, m^{d_1}), w \in \mathcal{N}(\frac{1}{4}, \ell^{d_2})} v^\top (B^* - \widehat{B})w \geq \frac{t}{2} \right) \\ &\leq 9^{m^{d_1} + \ell^{d_2}} 2 \exp \left( \frac{-cNt^2}{\|f^*\|_\infty^2 + C_\epsilon + t\sqrt{m^{d_1} \ell^{d_2} \log(N)}} \right). \end{aligned} \tag{104}$$

Therefore

$$\|B^* - \widehat{B}\|_{\text{op}} = O_{\mathbb{P}} \left( \sqrt{\frac{m^{d_1} + \ell^{d_2}}{N}} + \frac{\sqrt{m^{3d_1} \ell^{d_2} \log(N)}}{N} + \frac{\sqrt{m^{d_1} \ell^{3d_2} \log(N)}}{N} \right)$$

as desired.  $\square$

**Corollary 7.** Suppose  $\{\phi_k^{\mathbb{S}}\}_{k=1}^{\infty}$  be a collection of  $\mathbf{L}_2$  basis such that  $\|\phi_k^{\mathbb{S}}\|_{\infty} \leq C_{\mathbb{S}}$ . Let

$$\mathcal{M} = \text{span} \left\{ \phi_{\mu_1}^{\mathbb{S}}(z_1) \right\}_{\mu_1=1}^m \quad \text{and} \quad \mathcal{L} = \text{span} \left\{ \phi_{\eta_1}^{\mathbb{S}}(z_2) \cdots \phi_{\eta_{d-1}}^{\mathbb{S}}(z_d) \right\}_{\eta_1, \dots, \eta_{d-1}=1}^{\ell}.$$

If in addition that  $m \asymp N^{1/(2\alpha+1)}$  and that  $\ell^{d-1} = O(N^{\frac{2\alpha-1}{2(2\alpha+1)}} / \log(N))$ , then

$$\|(\widehat{f} - f^*) \times_x \mathcal{P}_{\mathcal{M}} \times_y \mathcal{P}_{\mathcal{L}}\|_{\text{op}} = O_{\mathbb{P}} \left( \sqrt{\frac{\dim(\mathcal{M}) + \dim(\mathcal{L})}{N}} \right). \quad (105)$$

*Proof.* The proof is almost the same as the proof in Corollary 3 with above choice of  $m$  and  $\ell$ .  $\square$

## H.2 Simulations and real data

We analyze the numerical performance of our VRS, Nadaraya–Watson kernel regression (NWKR) estimators, and neural networks (NN) in various nonparametric regression problems. The implementation of VRS is provided in Algorithm 2 and the inputs of VRS in the regression setting are detailed in Corollary 6. For neural network estimators, we use the feedforward architecture that are either wide and deep. We measure the estimation accuracy by relative  $\mathbf{L}_2$ -error defined as

$$\frac{\|f^* - \widetilde{f}\|_{\mathbf{L}_2(\Omega)}}{\|f^*\|_{\mathbf{L}_2(\Omega)}},$$

where  $\widetilde{f}$  is the regression function estimator of a given method. The subsequent simulations and real data examples consistently demonstrate that VRS outperforms both NN and NWKR in a range of nonparametric regression problems.

• **Simulation V.** We sample data  $\{W_i, Z_i\}_{i=1}^N \subset \mathbb{R} \times [-1, 1]^d$  from the regression model

$$W_i = f^*(Z_i) + \epsilon_i,$$

where  $\{\epsilon_i\}_{i=1}^N$  are independently sampled from standard normal distribution,  $\{Z_i\}_{i=1}^N$  are sampled from the uniform distribution on  $[-1, 1]^d$ , and

$$f^*(x_1, \dots, x_d) = \sin \left( \sum_{j=1}^d x_j \right) \quad \text{for } (x_1, \dots, x_d) \in [-1, 1]^d.$$

In the first set of experiments, we set  $d = 5$  and vary sample size  $N$  from 0.1 million to 1 million. In the second set of experiments, the sample size  $N$  is fixed at 1 million, while the dimensionality  $d$  varies from 2 to 10. Each experimental setup is replicated 100 times to ensure robustness, and we present the average relative  $l_2$ -error for each method in Figure 10.

• **Simulation VI.** We sample data  $\{W_i, Z_i\}_{i=1}^N \subset \mathbb{R} \times [-1, 1]^d$  from the regression model

$$W_i = f^*(Z_i) + \epsilon_i,$$

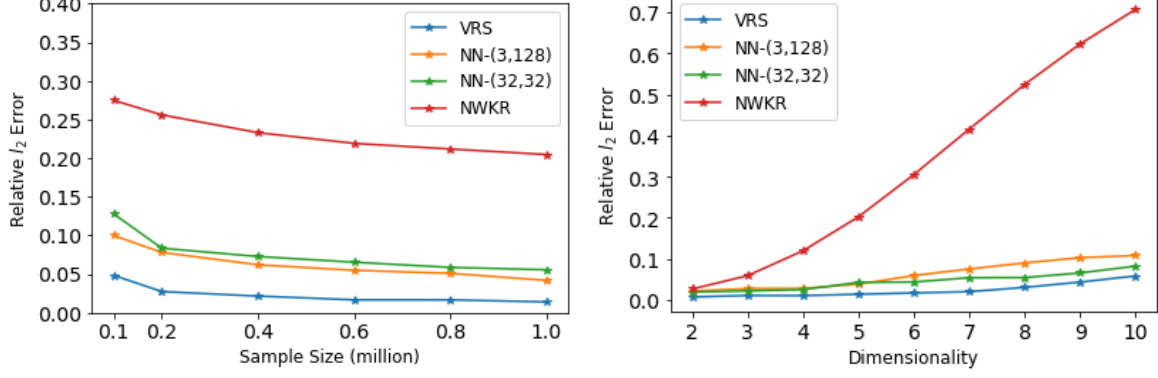


Figure 10: The plot on the left corresponds to **Simulation V** with  $d = 5$  and  $N$  varying from 0.1 million to 1 million; the plot on the right corresponds to **Simulation V** with  $N$  being 1 million and  $d$  varying from 2 to 10.

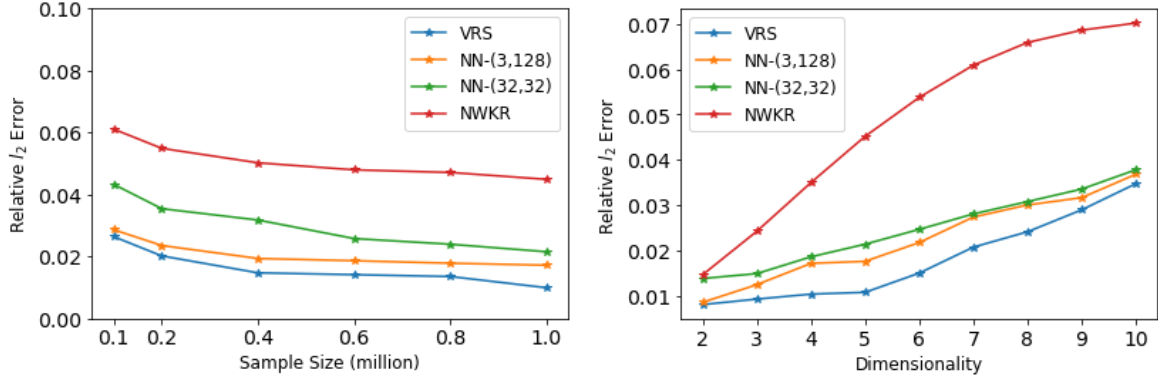


Figure 11: The plot on the left corresponds to **Simulation VI** with  $d = 5$  and  $N$  varying from 0.1 million to 1 million; the plot on the right corresponds to **Simulation VI** with  $N$  being 1 million and  $d$  varying from 2 to 10.

where  $\{\epsilon_i\}_{i=1}^N$  are independently sampled from standard normal distribution, and  $\{Z_i\}_{i=1}^N$  are independently sampled in  $[-1, 1]^d$  from a  $d$ -dimensional truncated Gaussian distribution with mean vector 0 and covariance matrix  $4I_d$ . Here  $I_d$  is the identity matrix in  $d$ -dimensions. In addition,

$$f^*(x_1, \dots, x_d) = \frac{1}{2} \exp\left(-\frac{1}{d} \sum_{i=1}^d \frac{3x_i^2 + 1}{4}\right) + \frac{1}{2} \exp\left(-\frac{1}{d} \sum_{i=1}^d \frac{7x_i^2 + 1}{8}\right)$$

for  $(x_1, \dots, x_d) \in [-1, 1]^d$ . In the first set of experiments, we fix  $d = 5$  and vary  $N$  vary from 0.1 million to 1 million. In the second set of experiments, we fix the sample size  $N$  at 1 million and let  $d$  vary from 2 to 10. We repeat each experiment setting 100 times and report the averaged relative  $L_2$ -error for each method in Figure 11.

• **Real data II.** We study the problem of predicting the house price in California using the [California housing](#) dataset. This dataset contains 20640 house price data from the 1990 California census, along with 8 continuous features such as locations, median house age, and total number bedrooms for house price prediction. Since the true regression function is unknown, we randomly split the dataset into 90% training and 10% test data and evaluate the performance of various approaches by relative test error. Let  $\tilde{f}$  be any

regression estimator computed based on the training data. The relative test error of this estimator is defined as

$$\sqrt{\frac{1}{N_{\text{test}}} \sum_{i=1}^{N_{\text{test}}} \frac{(\tilde{f}(Z_i) - W_i)^2}{W_i^2}},$$

where  $\{Z_i, W_i\}_{i=1}^{N_{\text{test}}}$  are the test data. The relative test errors for VRS, NWKR, and NN are 0.0275, 0.0367, and 0.0285, respectively, showing that VRS numerical surpasses other methods in this real data example.

## I Additional numerical results and details

### I.1 Kernel methods

In our simulated experiments and real data examples, we choose Gaussian kernel for the kernel density estimators and Nadaraya–Watson kernel regression (NWKR) estimators. The bandwidths in all the numerical examples are chosen using cross-validations. We refer interested readers to [Wasserman \(2006\)](#) for an introduction to nonparametric statistics.

### I.2 Sample generation in VRS

Following Algorithm 3, we obtain the tensor represented density  $\tilde{p}$ . To generate the samples, we follow Gibbs samplers and rewrite the joint density into the product of marginal densities:

$$\tilde{p}(x_1, x_2, \dots, x_d) = \tilde{p}(x_1)\tilde{p}(x_2|x_1) \cdots \tilde{p}(x_d|x_1, \dots, x_{d-1})$$

where  $\tilde{p}(x_1)$  is the one marginal density, which requires the integration over other  $d - 1$  variables. In our setting, we use some orthogonal basis functions and the first basis is commonly a constant. Based on orthogonality, we only need to choose the first slices of coefficient tensor to compute the one marginal density and this only requires  $O(1)$  complexity. Then we follow Markov Chain Monte Carlo (MCMC) to generate sample  $\tilde{x}_1$  from this one marginal density. Next, we need to compute the next one marginal  $\tilde{p}(x_2|x_1)$ . We fix  $x_1$  as  $\tilde{x}_1$  and choose the first slices of coefficient tensor to represent the integration over other  $d - 2$  variables. After that, we successfully compute one marginal density  $\tilde{p}(x_2|x_1)$  and follow MCMC to generate sample  $\tilde{x}_2$ . We repeat the procedure for all conditional probability and we could generate sample  $(\tilde{x}_1, \tilde{x}_2, \dots, \tilde{x}_d)$  in  $O(d)$  complexity.

The density given by tensor-sketching based method may not always be positive. There are some postprocessing techniques to deal with the issue. For example, [Han et al. \(2018\)](#) proposes a method to do minimization between the output density with a square of testing density, where the testing density shares the same tensor architecture. After that, we could use the square of testing density to implement MCMC sampling. Besides, based on our observation towards our method, the negative part of output density is quick small and we could choose a small threshold such as  $10^{-7}$  to avoid the negative component.

### I.3 Neural network density estimator

For neural network estimators, we use two popular density estimation architectures: Masked Autoregressive Flow (MAF) ([Papamakarios et al. \(2017\)](#)) and Neural Autore-

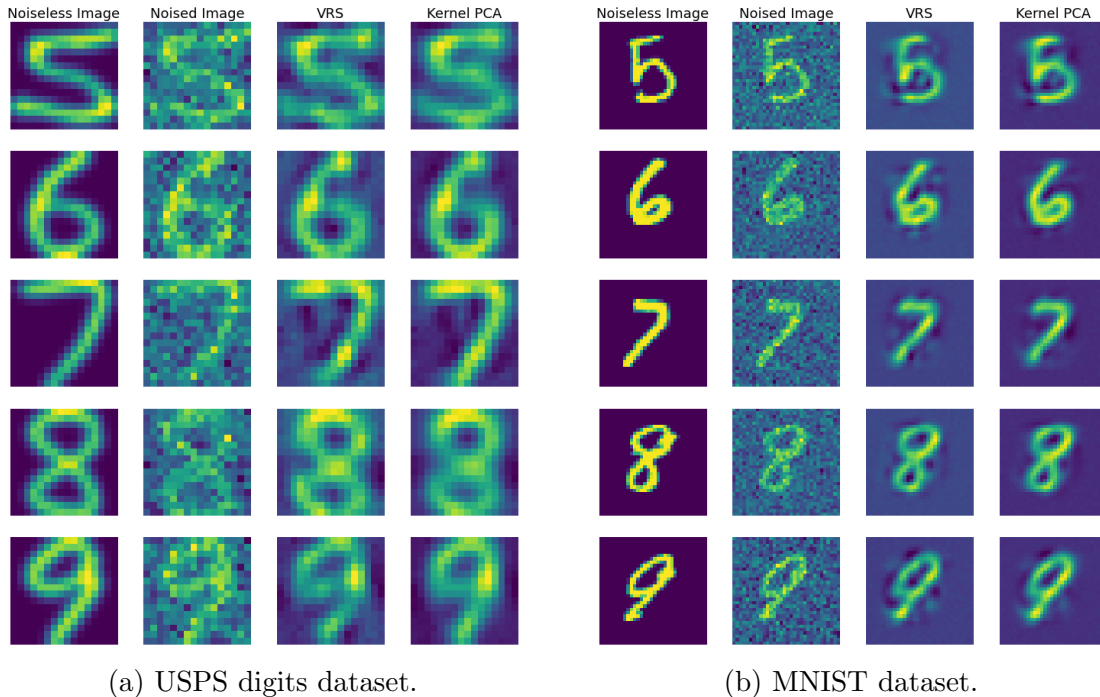


Figure 12: Denoising images from (a) USPS digits dataset and (b) MNIST dataset. In both (a) and (b), the first column shows the ground truth images from the test data, the second column shows the images polluted by Gaussian noise, the third column shows the images denoised using VRS, and the last column shows the images denoised using kernel PCA.

gressive Flows (NAF) (Huang et al. (2018)) for comparisons. Both neural networks are trained using the Adam optimizer (Kingma and Ba (2014)). For MAF, we use 5 transforms and each transform is a 3-hidden layer neural network with width 128. For NAF, we choose 3 transforms and each transform is a 3-hidden layer neural network with width 128.

#### I.4 Additional image denoising result

We provide additional image denoising results in this subsection. In Figure 12, we have randomly selected another five images from the test set of the USPS digits dataset and MNIST dataset to illustrate the denoised results using VRS and kernel PCA.